Towards a seamless Integration of CAD and Simulation

Partition of Unity Enrichment

Multi-scale fracture and model order reduction Pierre Kerfriden, Lars Beex, Jack Hale, Olivier Goury, Daniel Alves Paladim, Elisa Schenone, Davide Baroli, Thanh Tung Nguyen

Advanced discretisation techniques Danas Sutula, Xuan Peng, Haojie Lian, Peng Yu, Qingyuan Hu, Sundararajan Natarajan, Nguyen-Vinh Phu

Error estimation Pierre Kerfriden, Satyendra Tomar, Daniel Alves Paladim, Andrés Gonzalez Estrada

Biomechanics applications Alexandre Bilger, Hadrien Courtecuisse, Bui Huu Phuoc

and all the others!

CISM Course, Udine, Italy, 2017 June 5-9

Stéphane P.A. Bordas stephane.bordas@alum.northwestern.edu http://legato-team.eu

Organised by Gernot Beer & Stéphane Bordas

Part 0. Enrichment of the finite element method

Enrichment

- When the standard finite element method is unable to efficiently reproduce certain features of the sought solution:

1. Discontinuities	-	cracks, *material interfaces*
2. Large gradients	-	*yield lines, shock waves*
3. Singularities	-	*notches, cracks, corners*
4. Boundary layers	-	*fluid-fluid, fluid-solid*
5. Oscillatory behavior	-	*vibrations, impact*

- The approximation space can be extended by introducing of an *a priori* knowledge about the sought solution, and thereby:

1. Rendering the mesh independent of any phenomena
2. reducing error of the approximation locally and globally
3. improving convergence rates

Classification of discontinuities

Strong discontinuities

- The primal field of the solution is discontinuous, e.g. cracks lead to strong discontinuities in the displacement field.

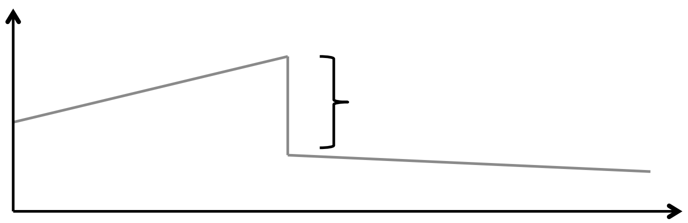

Weak discontinuities

- The first derivative of the solution is discontinuous, e.g. discontinuities in the strain field through a material interface.

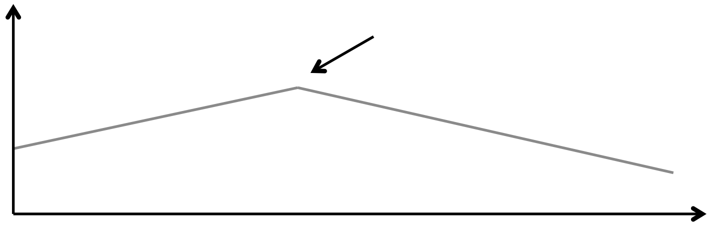

Classification of enrichments

Global enrichment

- The enrichment is employed on the global level, over the **entire domain**.
- Useful for problems that can be considered as **globally non-smooth** e.g. high-frequency solutions (Helmholtz equation)

Local enrichment

- This enrichment scheme is adopted locally, over a **local subdomain**.
- Useful for problems that only involve **locally non-smooth** phenomena, e.g. solutions with discontinuities.

Classification of enrichments

Extrinsic enrichment

- Associated with additional degrees of freedom and additional shape functions to augment the standard approximation basis.

1. Extended finite element method (XFEM) - Moës et al. (1999)
2. Generalised finite element method (GFEM) - Strouboulis et al. (2000a)
3. Enriched element free Galerkin - Ventura et al. (2002)
4. *hp* – clouds (Meshless/Hybrid) - Duarte and Oden (1996)

Intrinsic enrichment

- Not accompanied by additional degrees of freedom. Instead, some standard functions are replaced with special (problem specific) functions.

1. Enriched moving least squares (Meshless) - Fleming et al. (1997)
2. Enriched weight function (Meshless) - Duflot et al. (2004b)
3. Intrinsic partition of unity methods - Fries, Belytschko (2006)
4. Elements with embedded discontinuities

Singular elements (Barsoum, 1974)

For simulating the crack tip singular field in LEFM

- A simple way how to introduce a singularity of $1/\sqrt{r}$ in isoperimetric finite elements is by displacing the mid-side nodes of two adjacent edges to one quarter of the element edge length from the node where the singularity is desired.

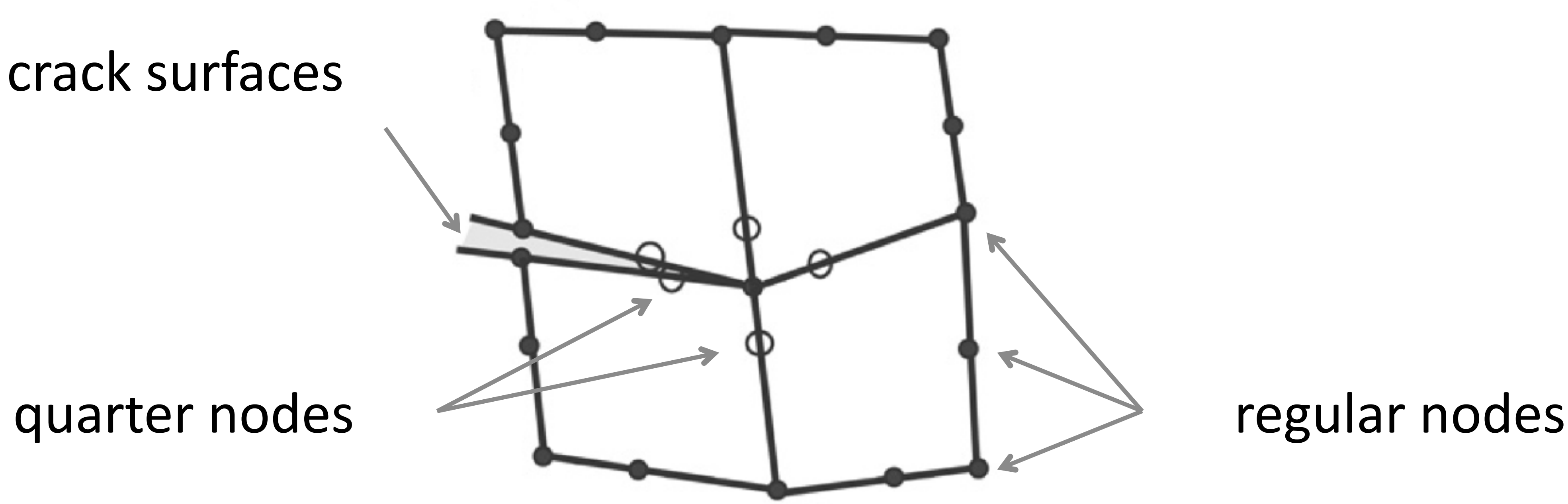

Partition of unity finite element method (PUFEM)

Partition of unity (PU)

- A set of functions ϕ_i whose sum at any point $\boldsymbol{x}$ inside a domain Ω is equal to unity:

$$\forall \mathbf{x} \in \Omega, \mathbf{x} : \sum_{I=1} \phi_I(\mathbf{x}) = 1$$

- Example PU functions are the finite element "hat" functions:

$$N_1(x) = \frac{x_2 - x}{x_2 - x_1}, x \in [x_1, x_2] \qquad N_2(x) = \frac{x - x_1}{x_2 - x_1}, x \in [x_1, x_2]$$

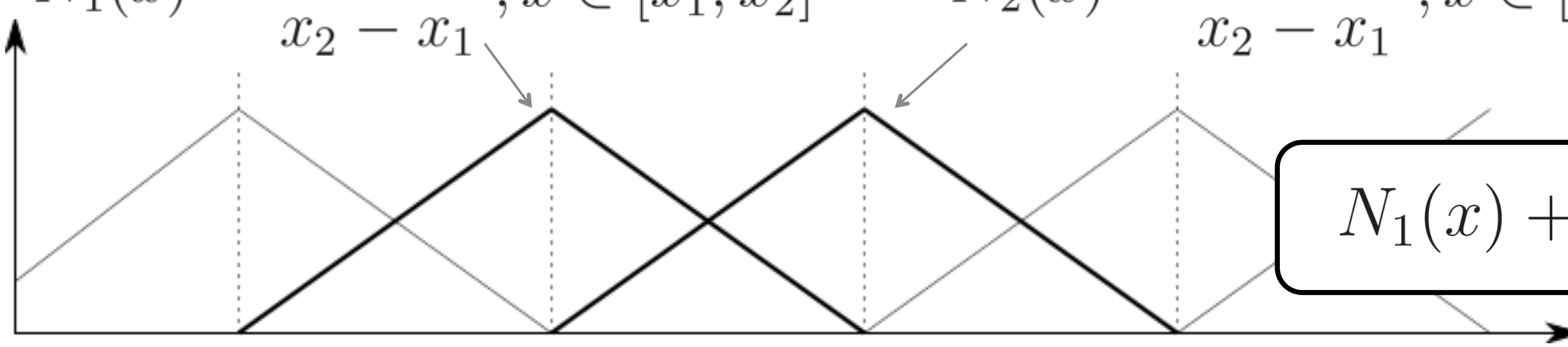

$$\boxed{N_1(x) + N_2(x) = 1}$$

Partition of unity finite element method (PUFEM)

Reproducibility of PU

- Any function $\boldsymbol{p(x)}$ can be reproduced by a product of that function and the partition of unity functions:

$$\sum_{I=1} \phi_I(\mathbf{x}) p(\mathbf{x}) = p(\mathbf{x})$$

- The function can be adjusted if the sum is modified by introducing parameters $\boldsymbol{q_I}$:

$$\sum_{I=1} \phi_I(\mathbf{x}) p(\mathbf{x}) q_I = \bar{p}(\mathbf{x})$$

- Reproducibility of $\boldsymbol{p(x)}$ can be controlled and localised to arbitrary regions where $\boldsymbol{q_I \neq 0}$

Formulation of PUFEM (example)

- Find the solution to the following 1D boundary value problem (BVP):

$$\forall x \in [0, l] : \frac{\mathrm{d}^2 u}{\mathrm{d}x^2} + f = 0$$

$$\text{with BC} : u(0) = 0,\ u(l) = u_l$$

- If we define two bilinear forms:

$$a(w, u) = \int_0^l \frac{\mathrm{d}w}{\mathrm{d}x}\frac{\mathrm{d}u}{\mathrm{d}x}\,\mathrm{d}x \qquad (w, f) = \int_0^l wf\,\mathrm{d}x$$

- The discrete variational problem can be stated as:

find $u^h \in U^h$ satisfying the BC such that for all $w^h \in W^h$:

$$a(w^h, u^h) = (w^h, f)$$

Formulation of PUFEM (example)

- The approximation/trial function in PUFEM:

$$u^h(x) = \underbrace{\sum_{I=1} N_I(x) u_I}_{\text{standard FE}} + \underbrace{\sum_{J=1} \phi_J(x)\psi(x) q_J}_{\text{PU enriched}}$$

- By choosing $w^h = \delta u^h$, leads to the discrete system of equations:

$$a(\delta u^h, u^h) = (\delta u^h, f)$$

$$\Downarrow$$

$$\mathbf{K}_{ij}^{se} = \int_0^l \frac{\mathrm{d}N_i}{\mathrm{d}x}\frac{\mathrm{d}(\phi_j\psi)}{\mathrm{d}x}\,\mathrm{d}x$$

$$\mathbf{K}_{ij}^{ss} = \int_0^l \frac{\mathrm{d}N_i}{\mathrm{d}x}\frac{\mathrm{d}N_j}{\mathrm{d}x}\,\mathrm{d}x$$

$$\mathbf{K}_{ij}^{es} = \int_0^l \frac{\mathrm{d}(\phi_i\psi)}{\mathrm{d}x}\frac{\mathrm{d}N_j}{\mathrm{d}x}\,\mathrm{d}x$$

$$\mathbf{K}_{ij}^{ee} = \int_0^l \frac{\mathrm{d}(\phi_i\psi)}{\mathrm{d}x}\frac{\mathrm{d}(\phi_j\psi)}{\mathrm{d}x}\,\mathrm{d}x$$

$$\begin{bmatrix} \mathbf{K}^{ss} & \mathbf{K}^{se} \\ \mathbf{K}^{es} & \mathbf{K}^{ee} \end{bmatrix} \begin{Bmatrix} \mathbf{u}^s \\ \mathbf{q}^e \end{Bmatrix} = \begin{Bmatrix} \mathbf{f}^s \\ \mathbf{f}^e \end{Bmatrix}$$

$$f_i^s = \int_0^l N_i f_x\,\mathrm{d}x$$

$$f_i^e = \int_0^l (\phi_i\psi) f_x\,\mathrm{d}x$$

Partition of unity finite element method (PUFEM)

Remarks

- Allows to introduce an arbitrary function $\boldsymbol{\psi}(\boldsymbol{x})$ in the approximation space by splitting the approximation into a **standard** and **enriched** parts.
- Enrichment can be **localised** to a small region around the features of interest – computationally advantageous.
- Provides a systematic means of introducing multiple enrichments.

References:

- Melenk and Babuska (1996)
- Duarte and Oden (1996)

The Generalised Finite Element Method (GFEM)

GFEM

- Originally associated with global PU enrichment
- Shape functions in the enriched part are usually different from the shape functions in the standard part i.e. $\phi_I(x) \neq N_I(x)$
- Introduced numerically generated enrichment functions, e.g. a solution in the vicinity of a bifurcated crack as enrichment

References:

- Melenk (1995)
- Melenk and Babuška (1996)
- Strouboulis et al. (2000)

The Extended Finite Element Method (XFEM)

XFEM

- Associated with local discontinuous PU enrichment e.g.:

  a. propagation of cracks
  b. evolution of dislocations
  c. phase boundaries

- Both GFEM and XFEM are essentially identical in their application, i.e. extrinsic PU enrichment

References:

- Belytschko and Black (1999)
- Moës et. al. (1999)
- Dolbow (1999)

Formulation for crack growth:

$$\mathbf{u}^h(\mathbf{x}) = \underbrace{\sum_{I \in \mathcal{N}_I} N_I(\mathbf{x})\mathbf{u}^I}_{\text{standard part}} + \underbrace{\sum_{J \in \mathcal{N}_J} N_J(\mathbf{x}) H(\mathbf{x}) \mathbf{a}^J}_{\text{discontinuous enrichment}} + \underbrace{\sum_{K \in \mathcal{N}_K} N_K(\mathbf{x}) \sum_{\alpha=1}^{4} f_\alpha(\mathbf{x}) \mathbf{b}^{K\alpha}}_{\text{singular tip enrichment}}$$

$$H(\mathbf{x}) = \begin{cases} +1 & \text{if } \mathbf{x} \text{ above crack} \\ -1 & \text{if } \mathbf{x} \text{ below crack} \end{cases}$$

$$\{f_\alpha(r,\theta), \alpha = 1,4\} = \left\{ \sqrt{r}\sin\frac{\theta}{2}, \sqrt{r}\cos\frac{\theta}{2}, \sqrt{r}\sin\frac{\theta}{2}\sin\theta, \sqrt{r}\cos\frac{\theta}{2}\sin\theta \right\}$$

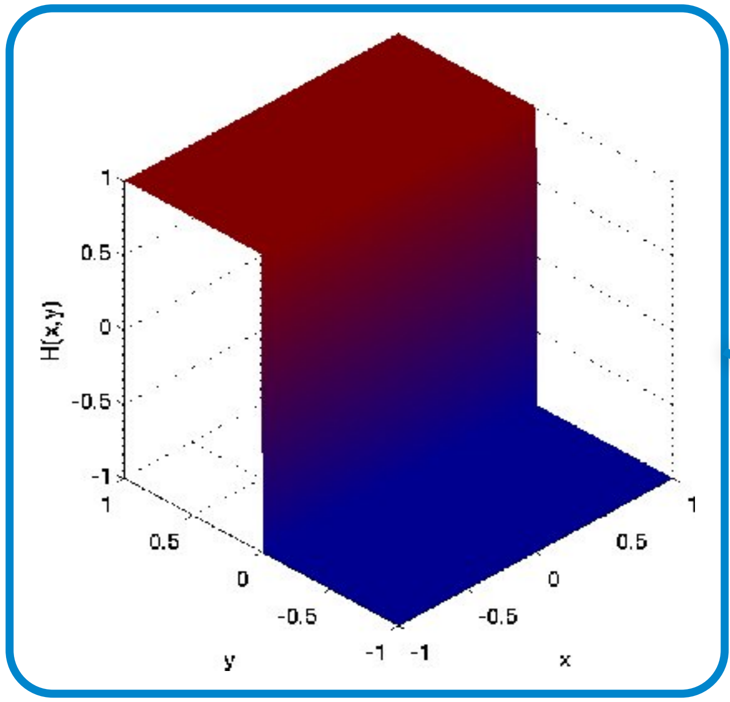

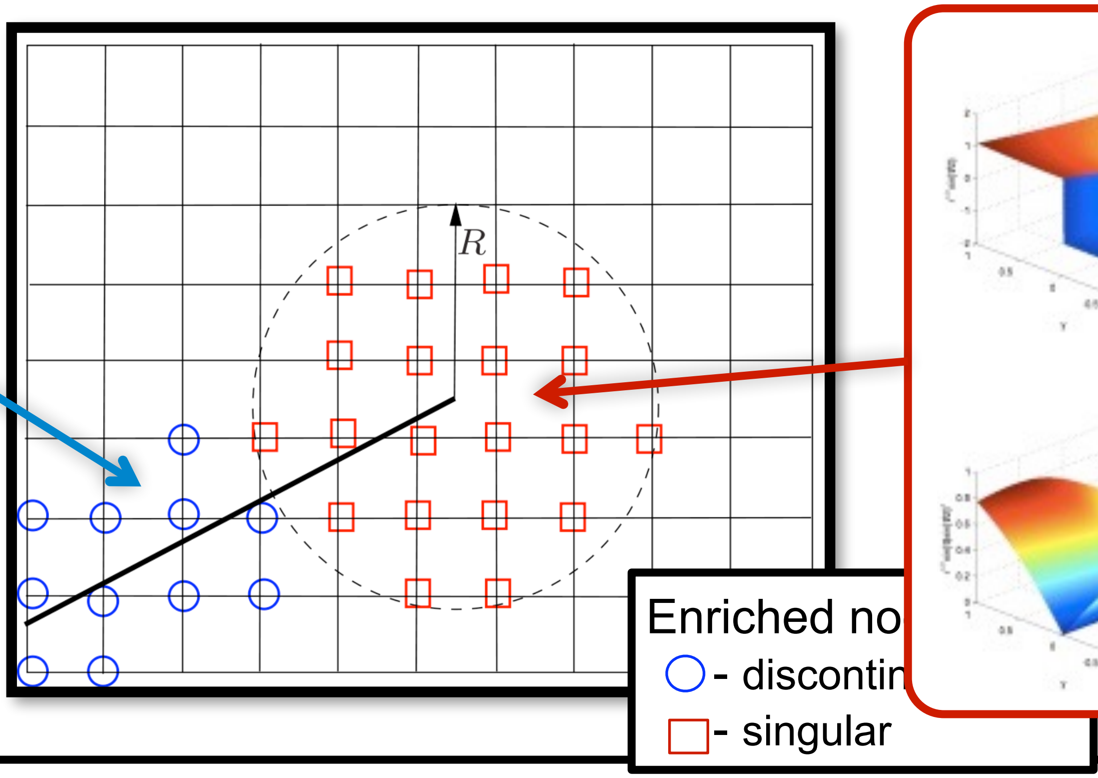

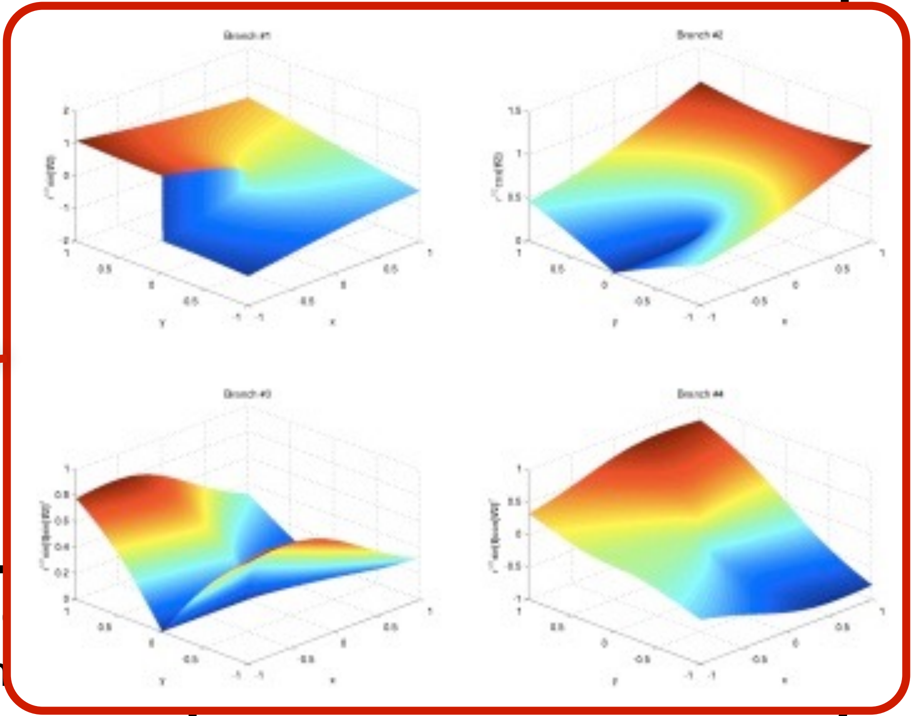

$$u_i^h(\mathrm{x}) = \sum_{\substack{I \\ n_I \subset \mathrm{N}}} N_I(\mathrm{x}) u_{iI} + \sum_{\substack{J \\ n_J \subset \mathrm{N}^c}} N_J(\mathrm{x}) a_{iJ} H(\mathrm{x}) + \sum_{\substack{K \\ n_K \subset \mathrm{N}^f}} \phi_K(\mathrm{x}) b_{iK} \Psi(\mathrm{x})$$

classical

enriched

Heaviside function

Asymptotic fields

$$H(\mathbf{x}) = \begin{cases} +1 & \text{if } \mathbf{x} \text{ above} \\ -1 & \text{if } \mathbf{x} \text{ below} \end{cases}$$

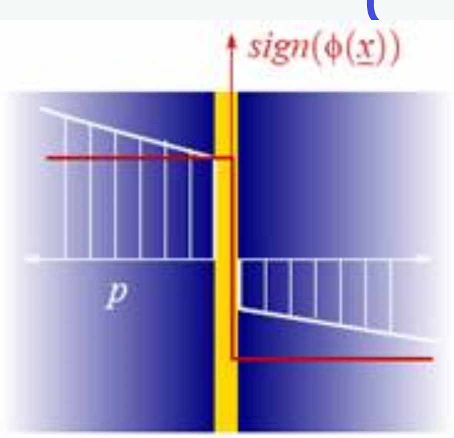

$$\psi(r,\theta) = \sqrt{r}\cos\frac{\theta}{2}, \sqrt{r}\sin\frac{\theta}{2}, \sqrt{r}\sin\theta\sin\frac{\theta}{2}, \sqrt{r}\sin\theta\cos\frac{\theta}{2}$$

Selection of enriched nodes

$$u_i^h(\mathrm{x}) = \sum_{\substack{I \\ n_I \subset \mathrm{N}}} N_I(\mathrm{x}) u_{iI} + \sum_{\substack{J \\ n_J \subset \mathrm{N}^c}} N_J(\mathrm{x}) a_{iJ} H(\mathrm{x}) + \sum_{\substack{K \\ n_K \subset \mathrm{N}^f}} \phi_K(\mathrm{x}) b_{iK} \Psi(\mathrm{x})$$

enriched

Asymptotic fields

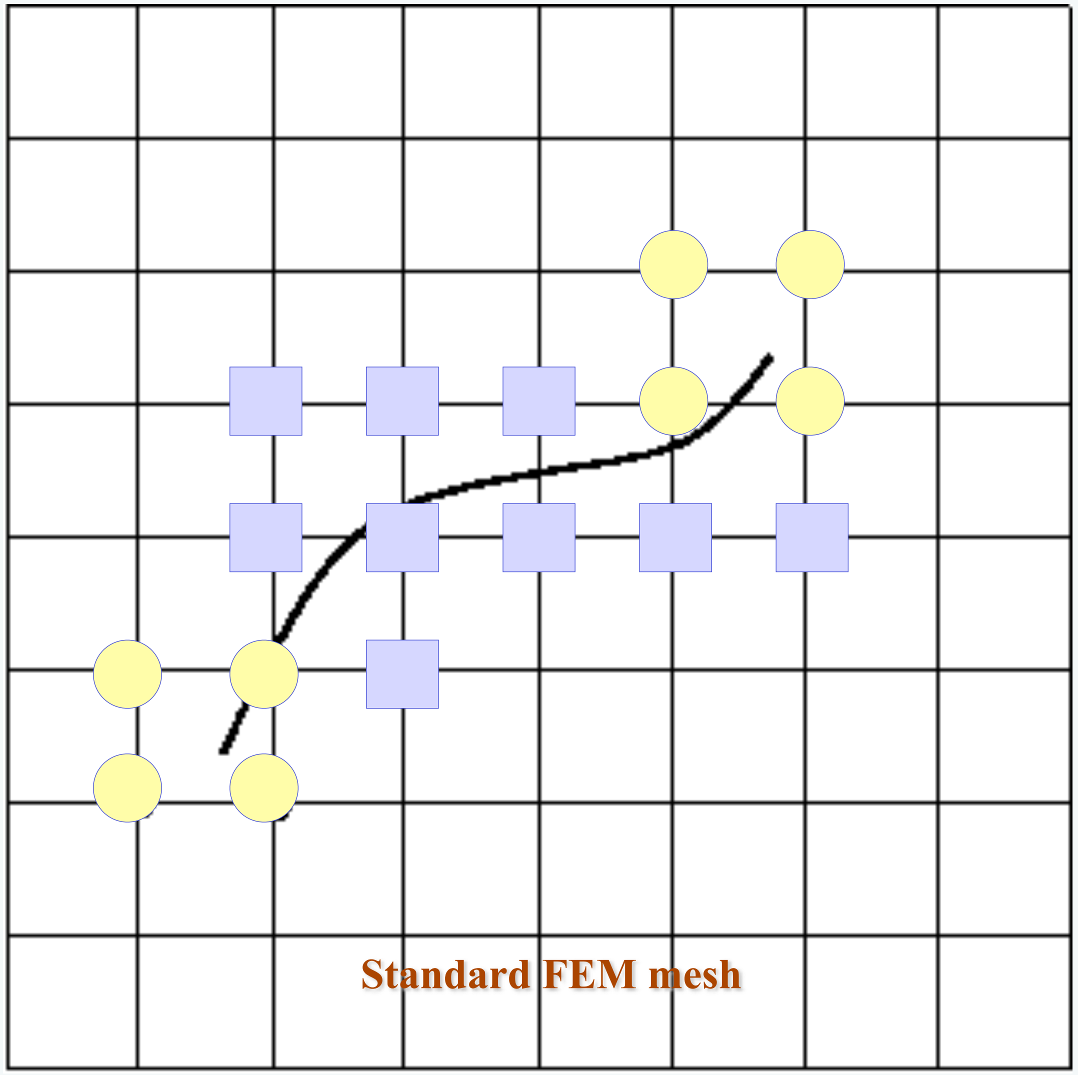

Heaviside function

Standard FEM mesh

ENRICHED NODES

Tip

Interior

Part I. Some recent advances in enriched FEM

Handling discontinuities in isogeometric formulations

with Nguyen Vinh Phu, Marie Curie Fellow

Discontinuities modeling

PUM enriched methods

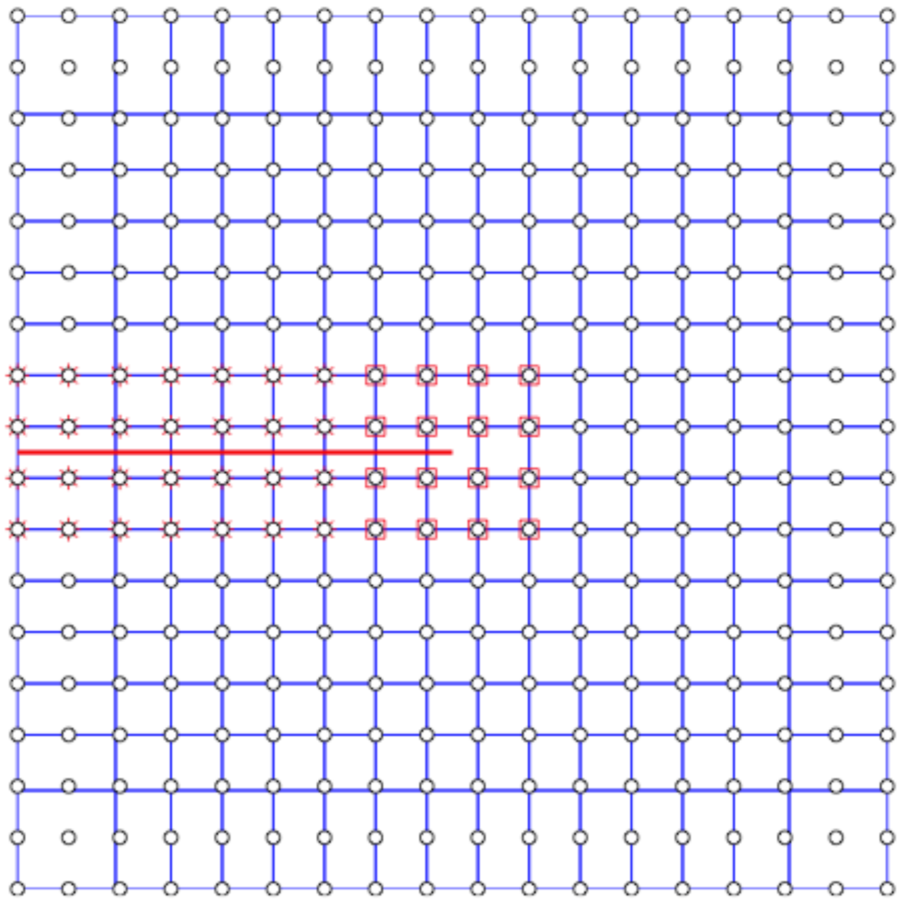

- IGA: link to CAD and accurate stress fields
- XFEM: no remeshing

Mesh conforming methods

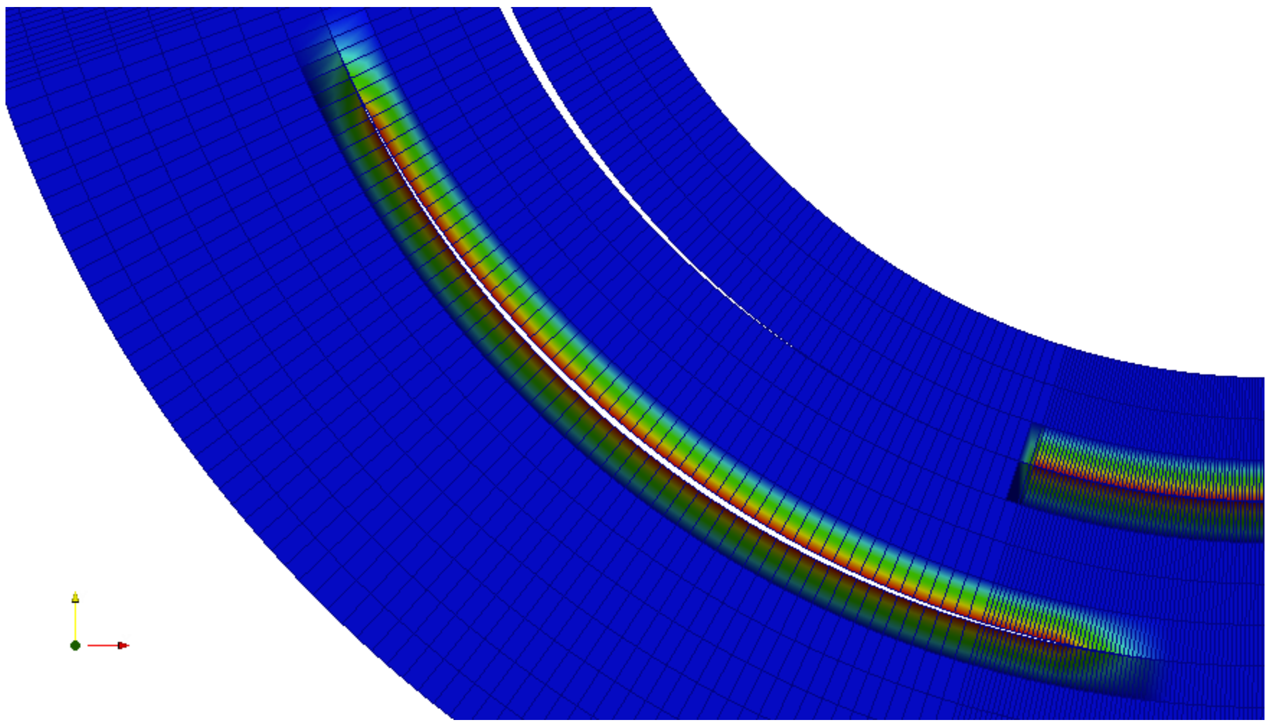

- IGA: link to CAD and accurate stress fields
- Apps: delamination

PUM enriched methods (XIGA)

$$\mathbf{u}^h(\mathbf{x}) = \sum_{I \in \mathcal{S}} R_I(\mathbf{x})\mathbf{u}_I + \sum_{J \in \mathcal{S}^c} R_J(\mathbf{x})\Phi(\mathbf{x})\mathbf{a}_J$$

NURBS basis functions

enrichment functions

1. E. De Luycker, D. J. Benson, T. Belytschko, Y. Bazilevs, and M. C. Hsu. X-FEM in isogeometric analysis for linear fracture mechanics. IJNME, 87(6):541–565, 2011.
2. S. S. Ghorashi, N. Valizadeh, and S. Mohammadi. Extended isogeometric analysis for simulation of stationary and propagating cracks. IJNME, 89(9): 1069–1101, 2012.
3. D. J. Benson, Y. Bazilevs, E. De Luycker, M.-C. Hsu, M. Scott, T. J. R. Hughes, and T. Belytschko. A generalized finite element formulation for arbitrary basis functions: From isogeometric analysis to XFEM. IJNME, 83(6):765–785, 2010.
4. A. Tambat and G. Subbarayan. Isogeometric enriched field approximations. CMAME, 245–246:1 – 21, 2012.

Delamination analysis with cohesive elements (standard approach)

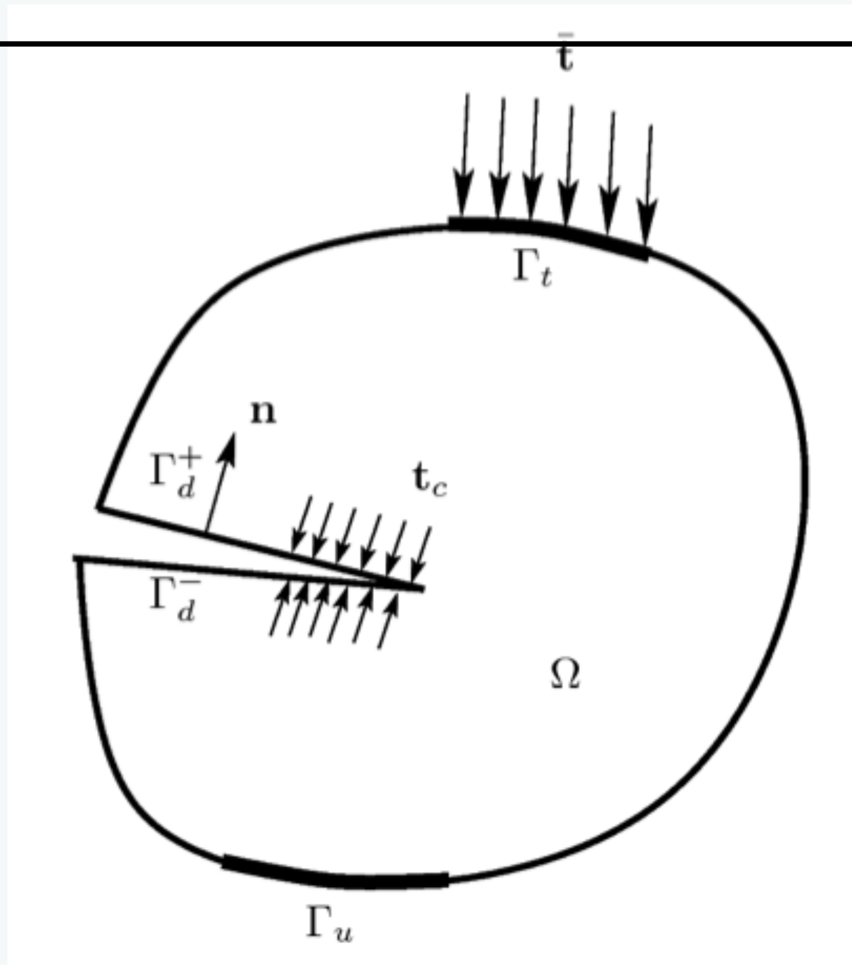

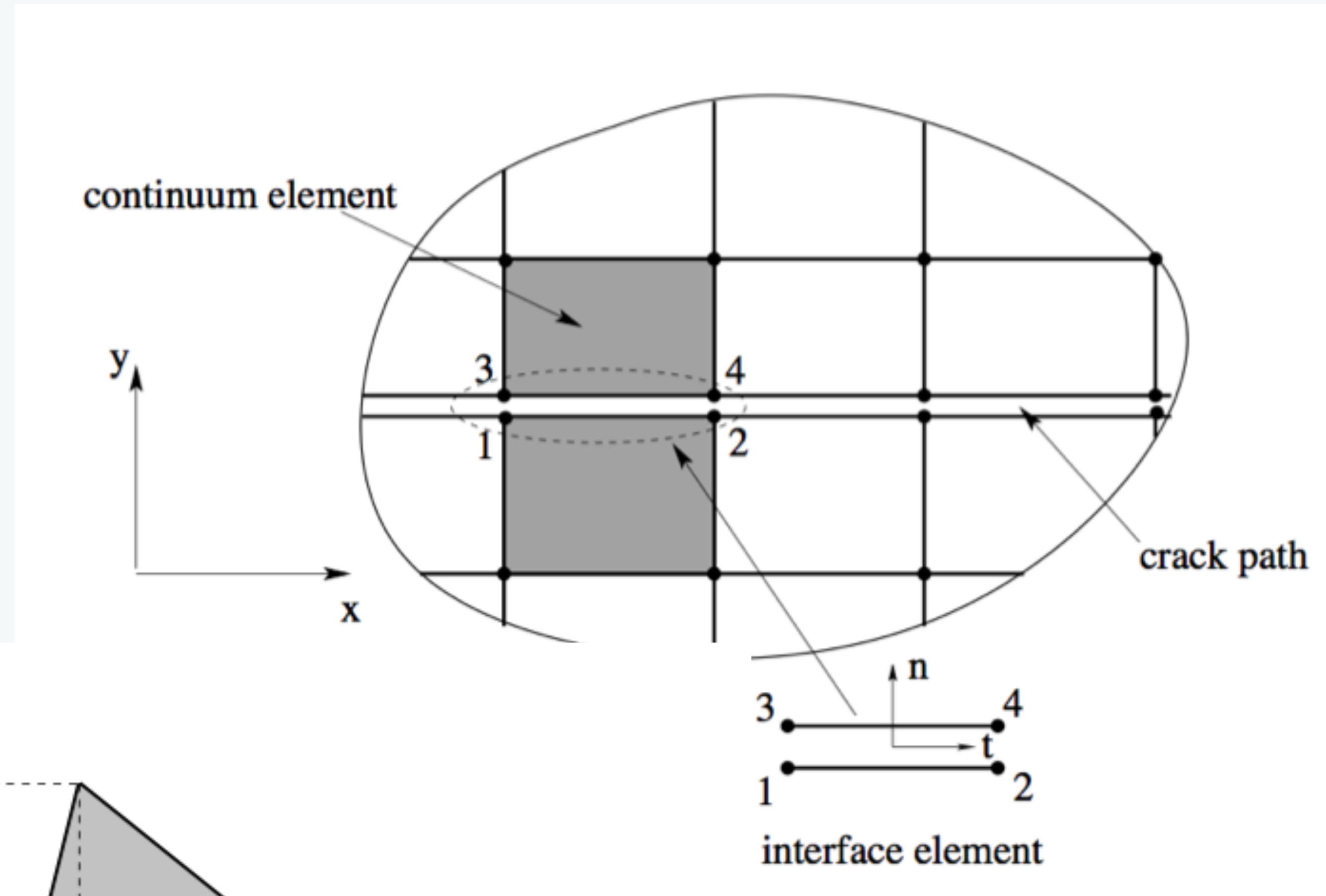

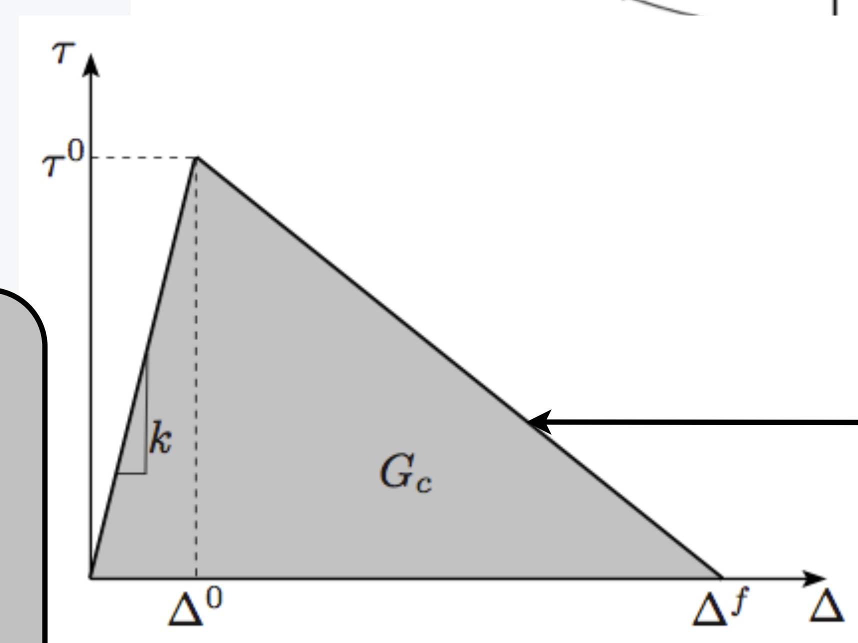

- No link to CAD
- Long preprocessing
- Refined meshes

$$\int_{\Omega} \delta \mathbf{u} \cdot \mathbf{b} \mathrm{d}\Omega + \int_{\Gamma_t} \delta \mathbf{u} \cdot \bar{\mathbf{t}} \mathrm{d}\Gamma_t = \int_{\Omega} \delta \boldsymbol{\epsilon} : \boldsymbol{\sigma}(\mathbf{u}) \mathrm{d}\Omega + \int_{\Gamma_d} \delta [\![\mathbf{u}]\!] \cdot \mathbf{t}^c([\![\mathbf{u}]\!]) \mathrm{d}\Gamma_d$$

Isogeometric cohesive elements

quadratic basis

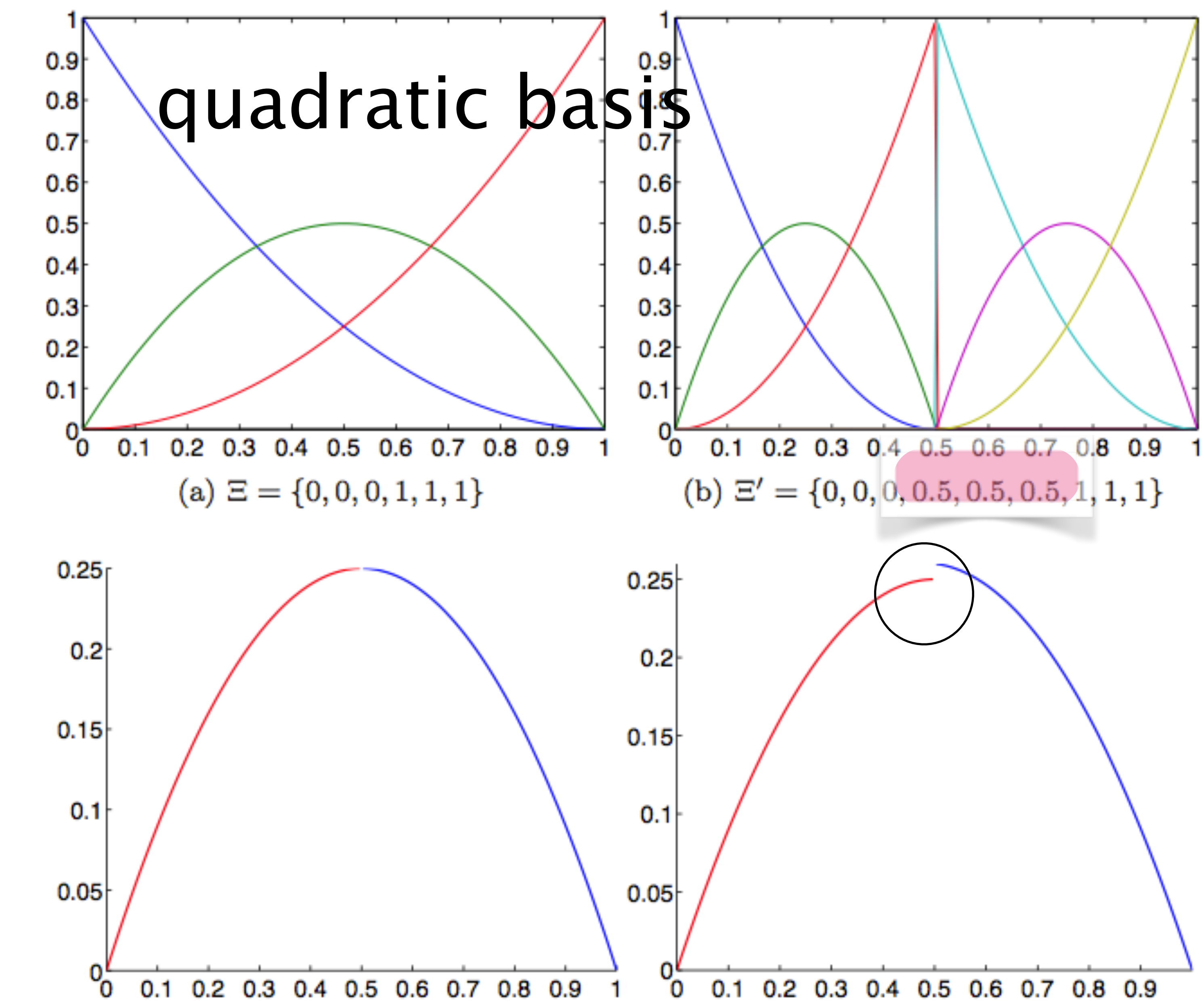

(a) $\Xi = \{0,0,0,1,1,1\}$ (b) $\Xi' = \{0,0,0,0.5,0.5,0.5,1,1,1\}$

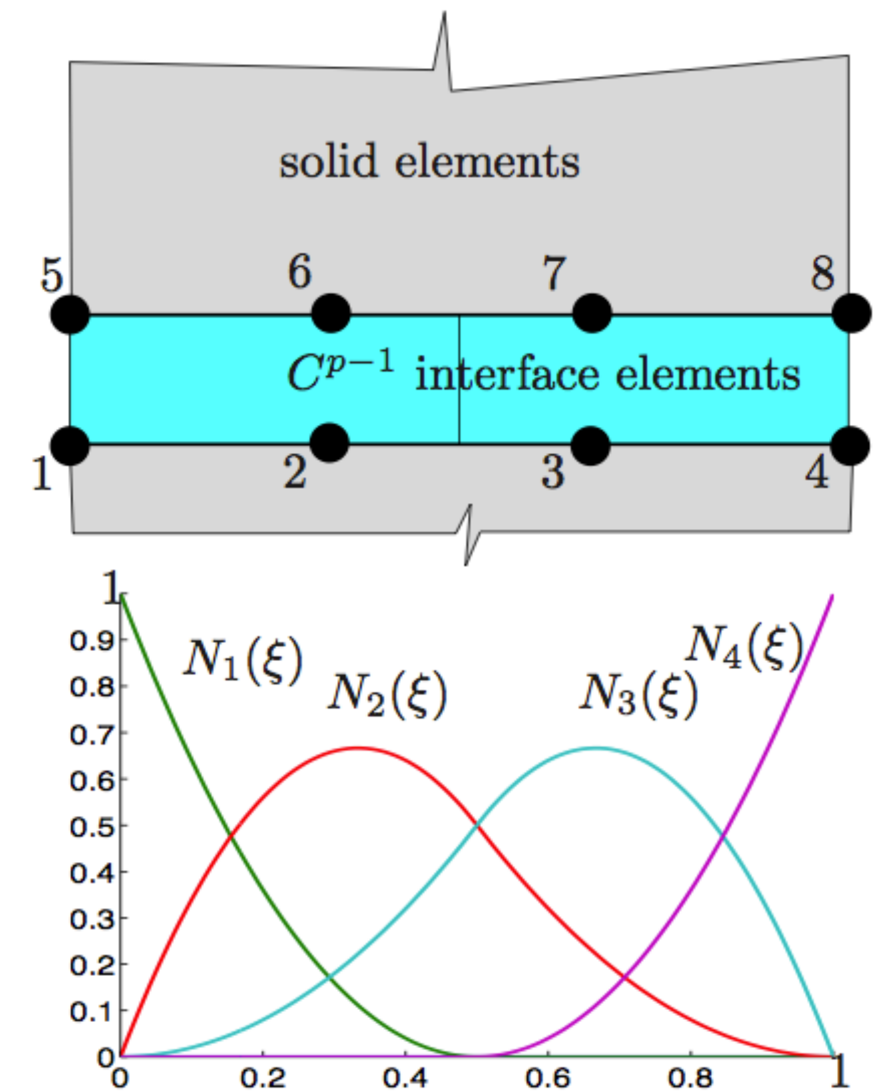

Knot insertion

1. C. V. Verhoosel, M. A. Scott, R. de Borst, and T. J. R. Hughes. An isogeometric approach to cohesive zone modeling. IJNME, 87(15):336–360, 2011.
2. V.P. Nguyen, P. Kerfriden, S. Bordas. Isogeometric cohesive elements for two and three dimensional composite delamination analysis, 2013, Arxiv.

Isogeometric cohesive elements: advantages

- Direct link to CAD
- Exact geometry
- Fast/straightforward generation of interface elements
- Accurate stress field
- Computationally cheaper

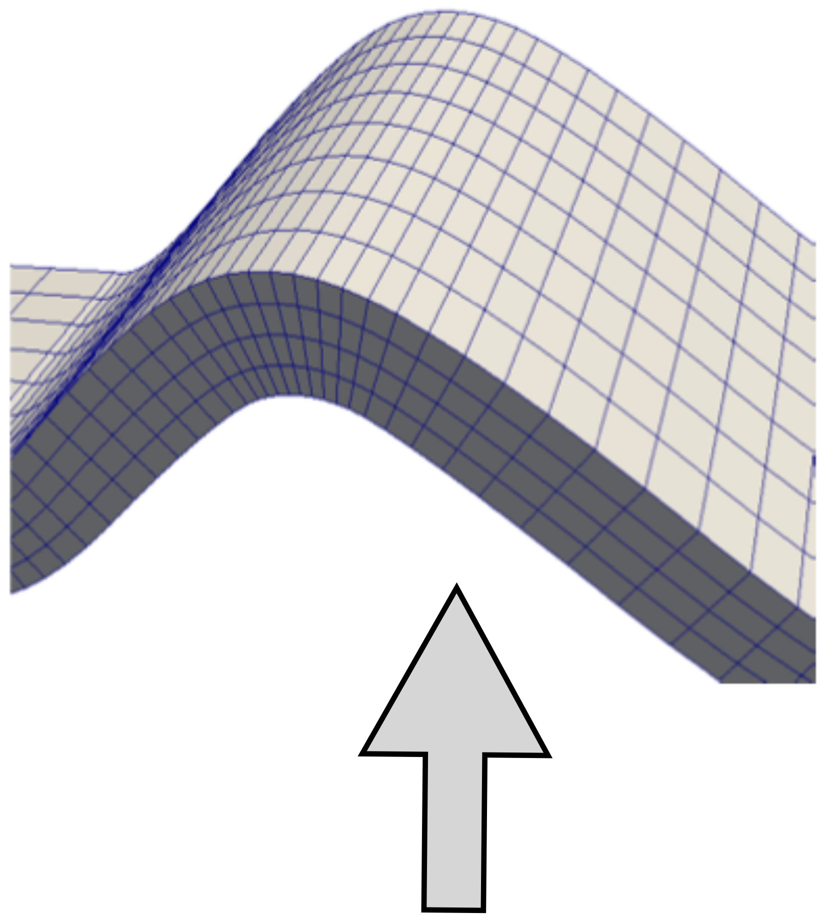

- 2D Mixed mode bending test (MMB)
- 2 x 70 quartic-linear B-spline elements
- Run time on a laptop 4GBi7: 6 s
- Energy arc-length control

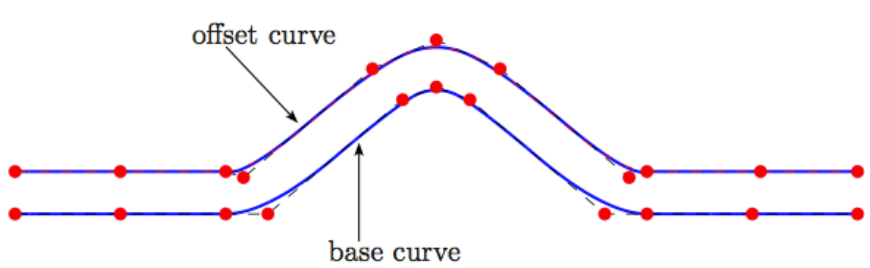

V. P. Nguyen and H. Nguyen-Xuan. High-order B-splines based finite elements for delamination analysis of laminated composites. Composite Structures, 102:261–275, 2013.

Isogeometric cohesive elements: 2D example

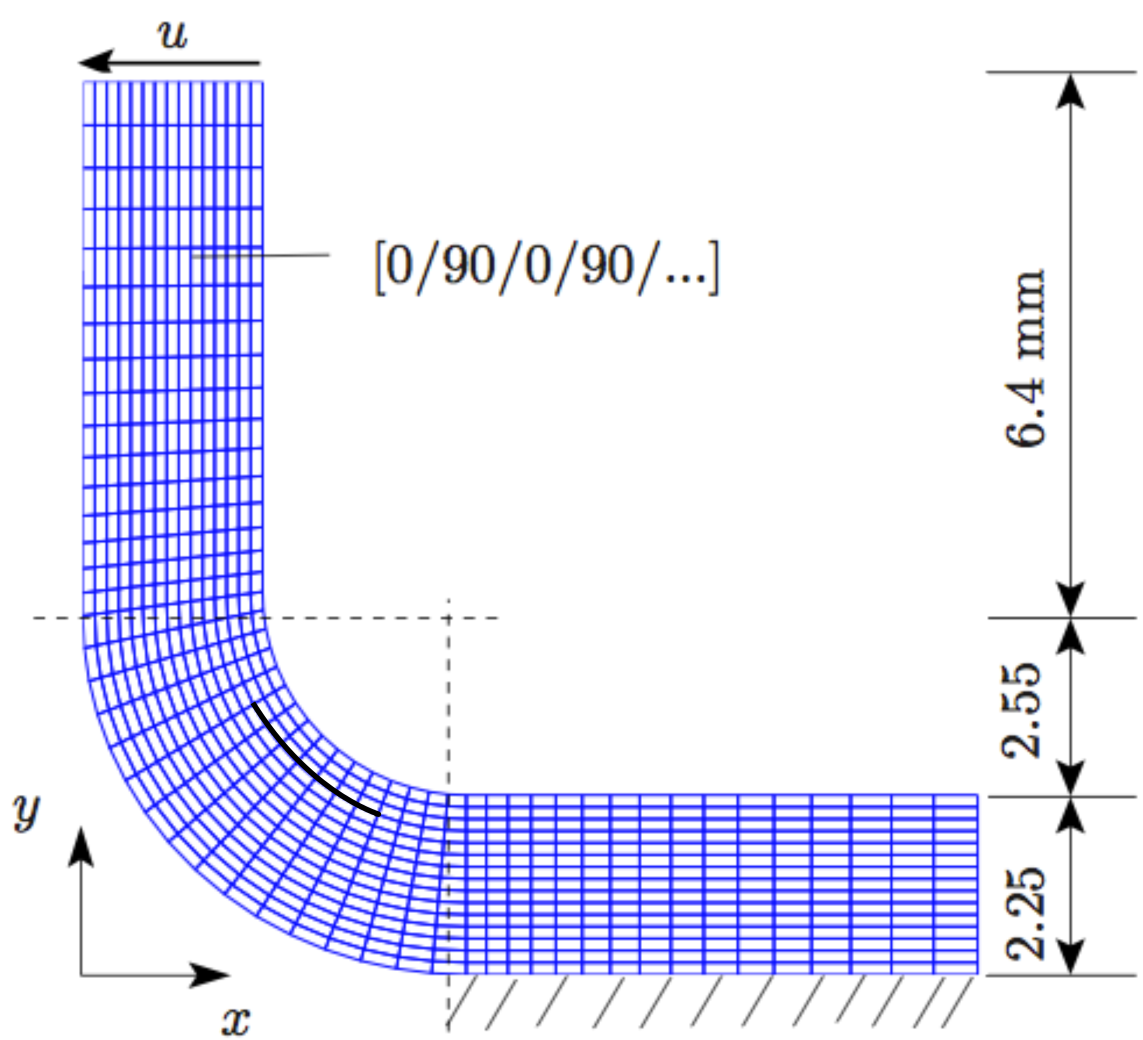

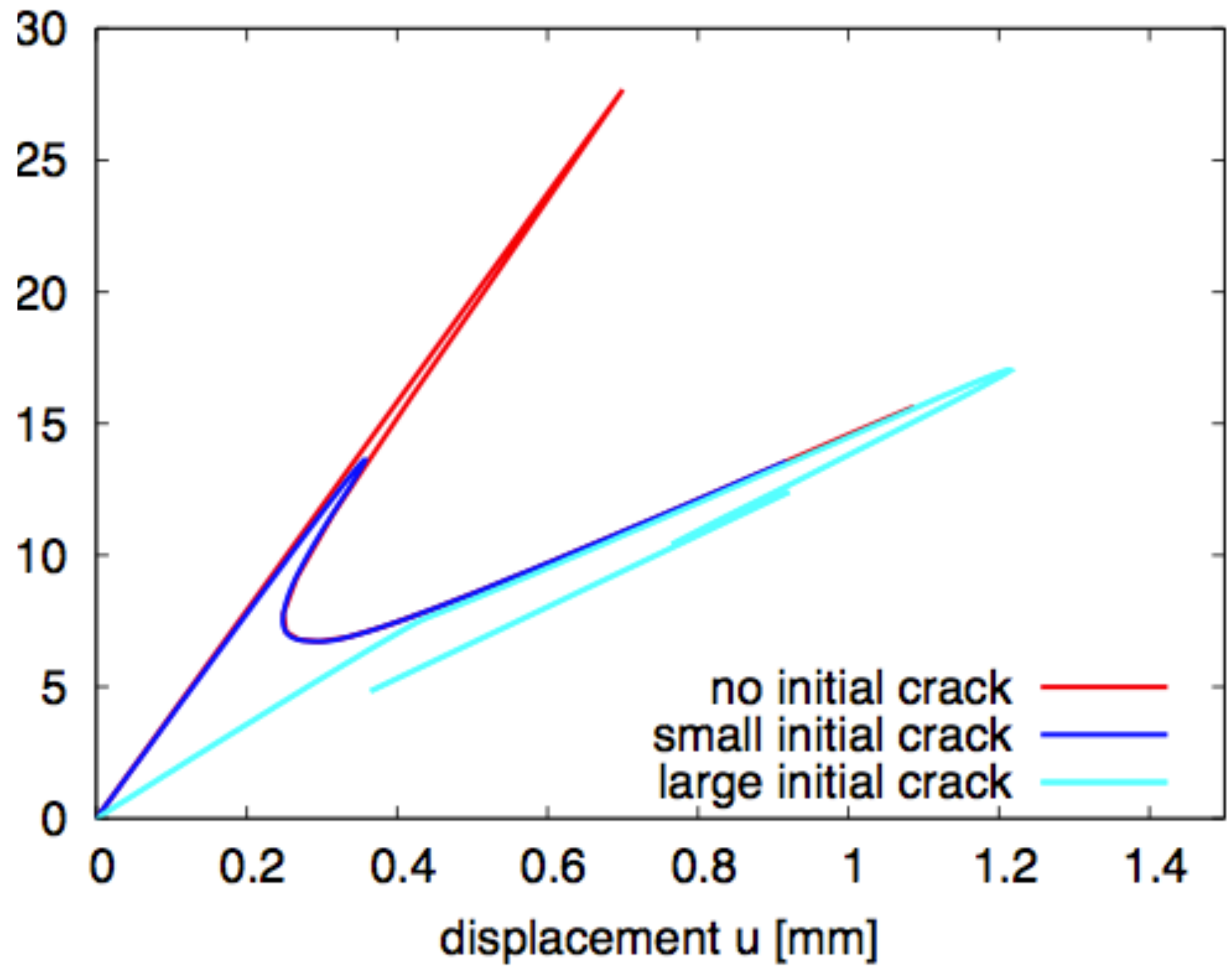

- Exact geometry by NURBS + direct link to CAD
- It is straightforward to vary
  (1) the number of plies and
  (2) # of interface elements:
- Suitable for parameter studies/design
- Solver: energy-based arc-length method (Gutierrez, 2007)

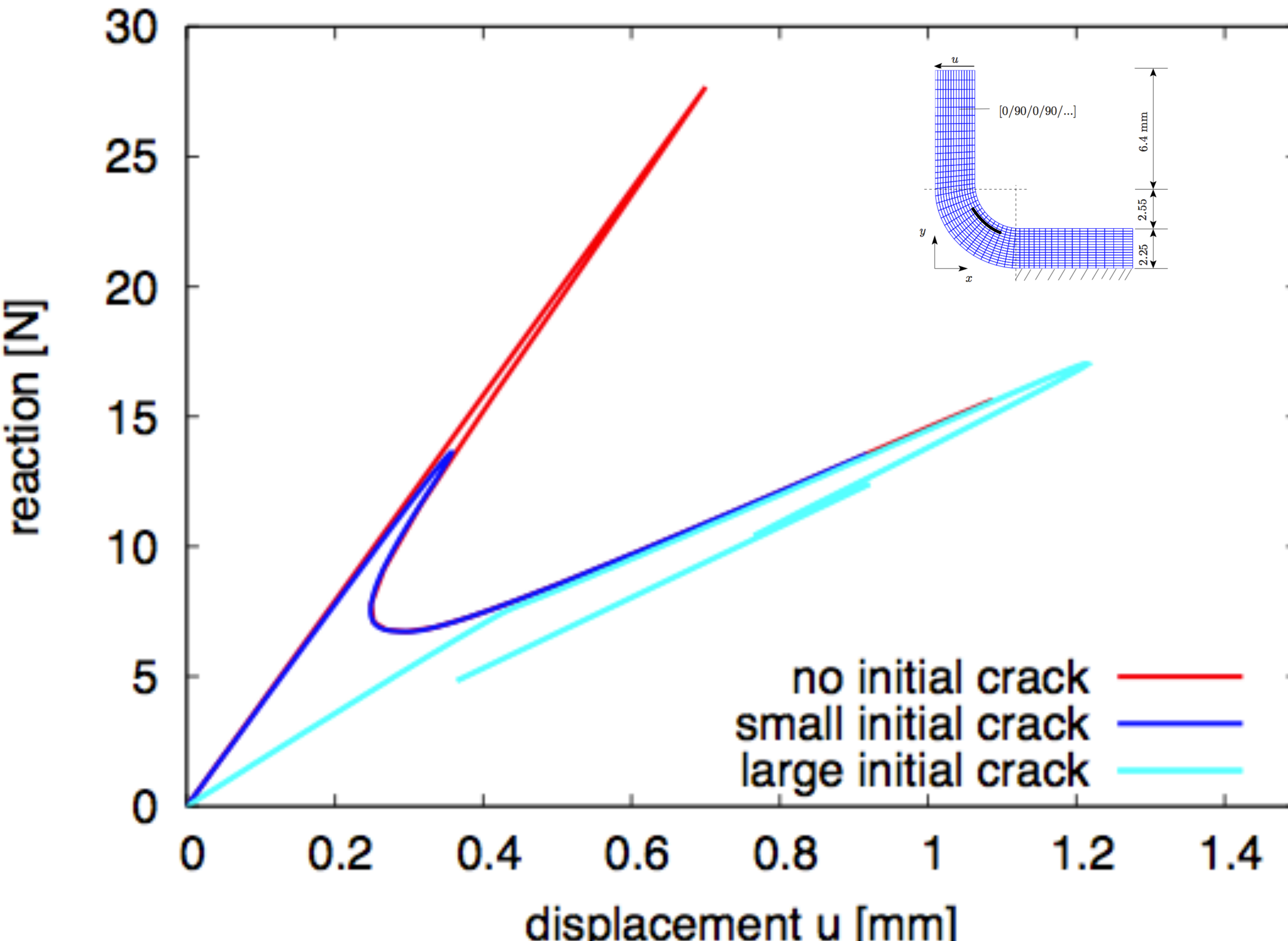

30
25
20
15
10
5
0
0
0.2
0.4
0.6
0.8
1
1.2
1.4
reaction [N]
displacement u [mm]
no initial crack
small initial crack
large initial crack
u
[0/90/0/90/...]
6.4 mm
2.55
2.25
y
x

Isogeometric cohesive elements: 2D example

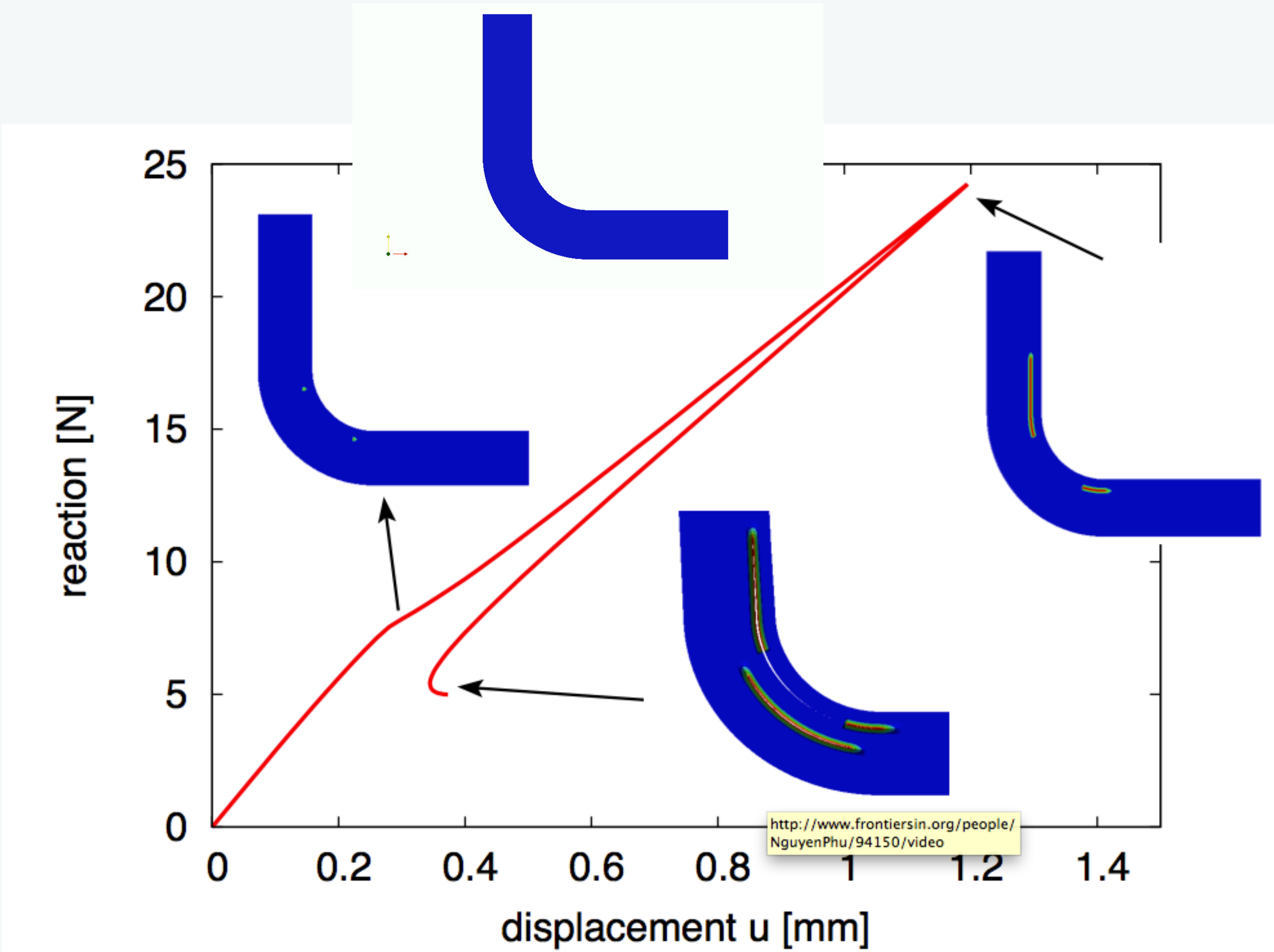

Isogeometric cohesive elements: 3D example with shells

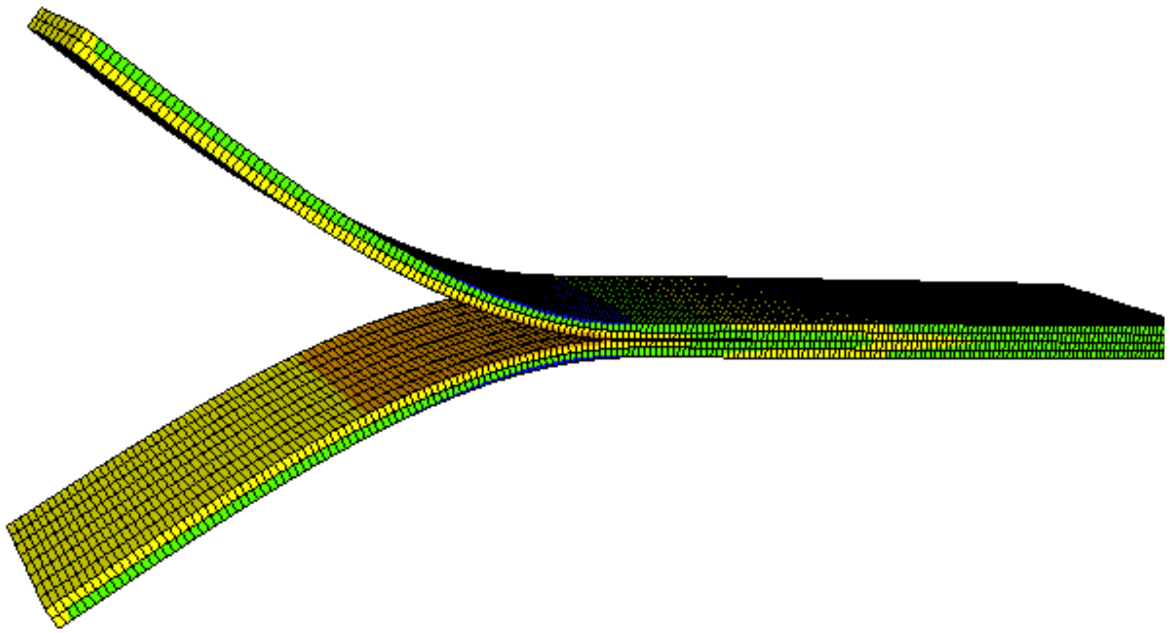

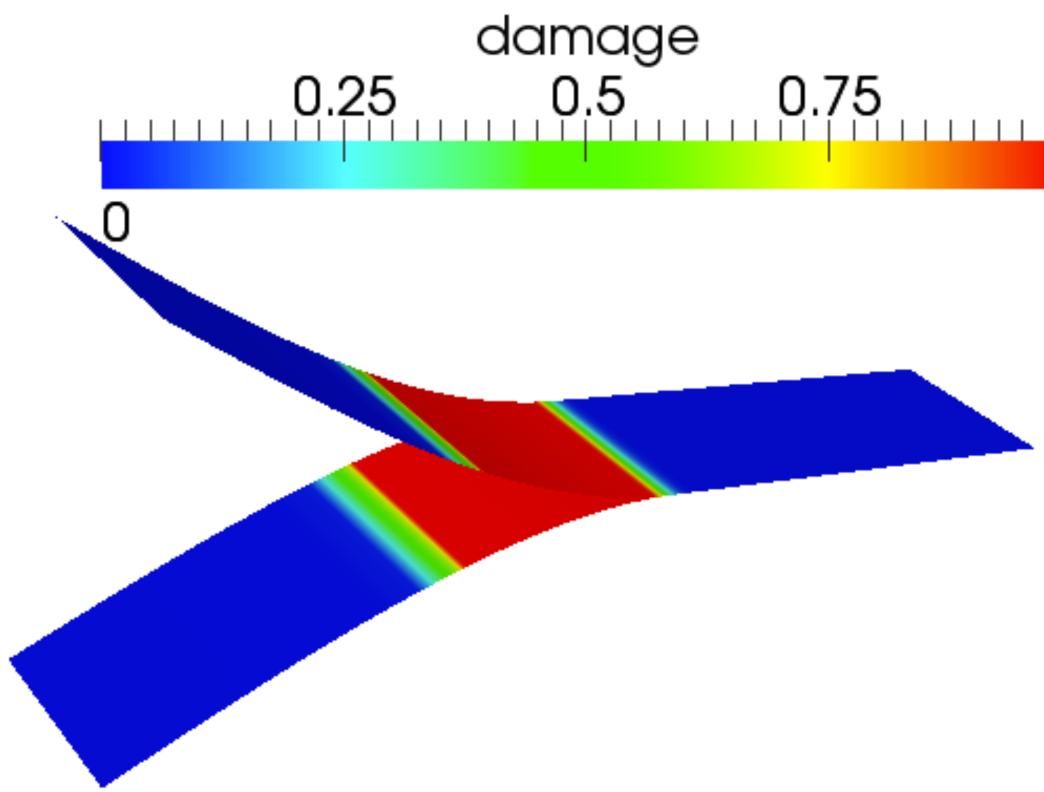

- Rotation free B-splines shell elements (Kiendl et al. CMAME)
- Two shells, one for each lamina
- Bivariate B-splines cohesive interface elements in between

Isogeometric cohesive elements: 3D examples

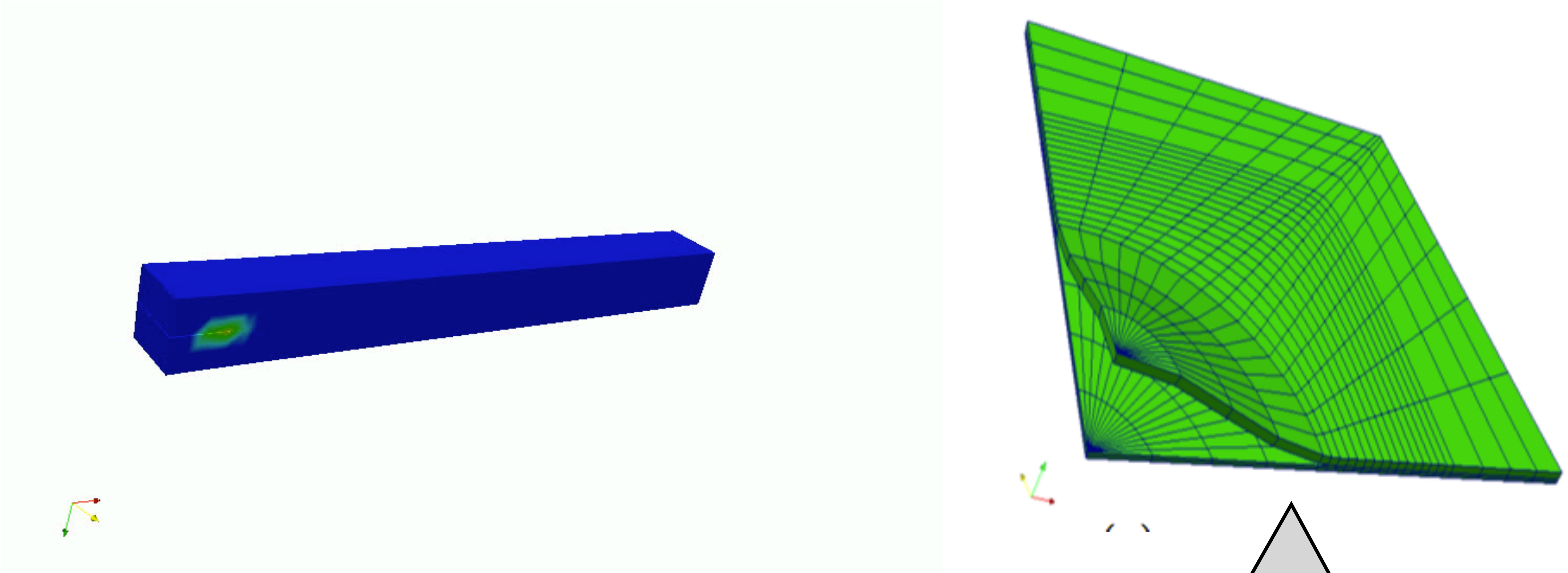

- cohesive elements for 3D meshes the same as 2D
- large deformations

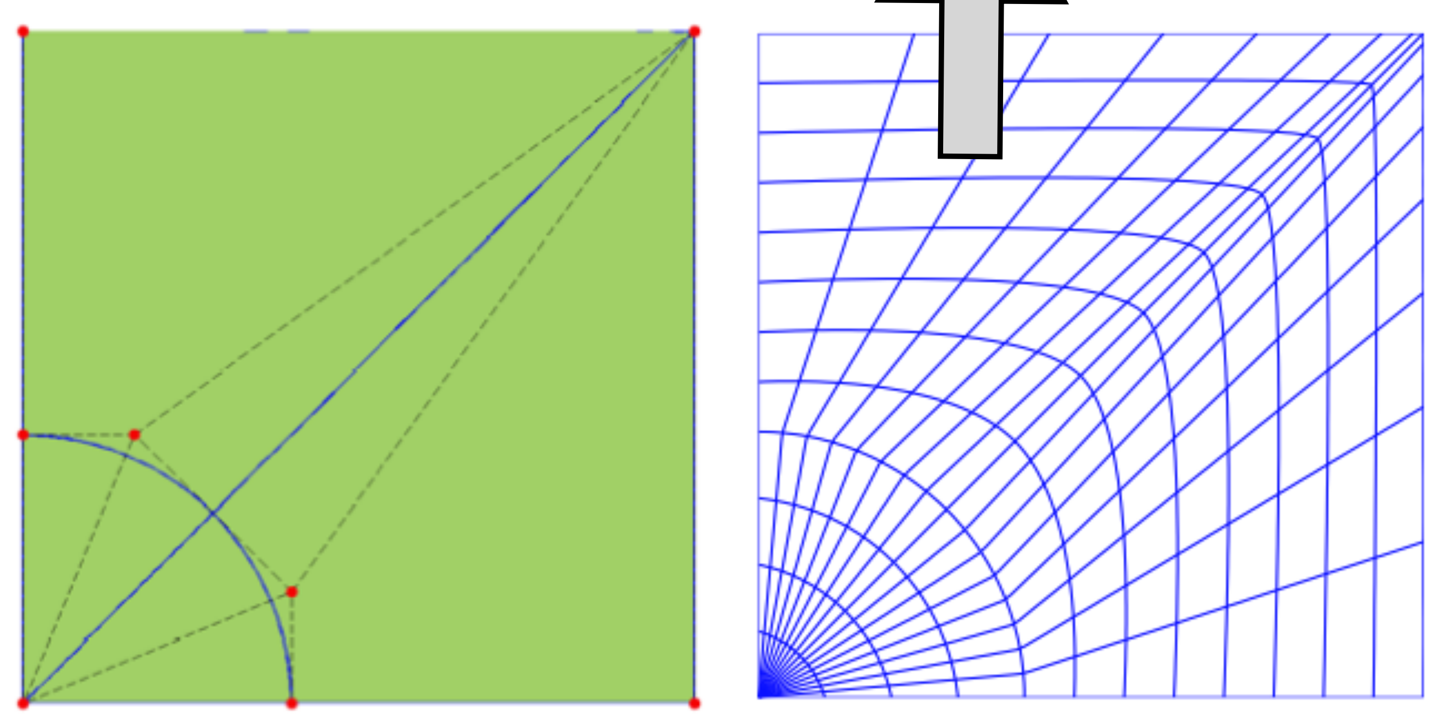

Isogeometric cohesive elements

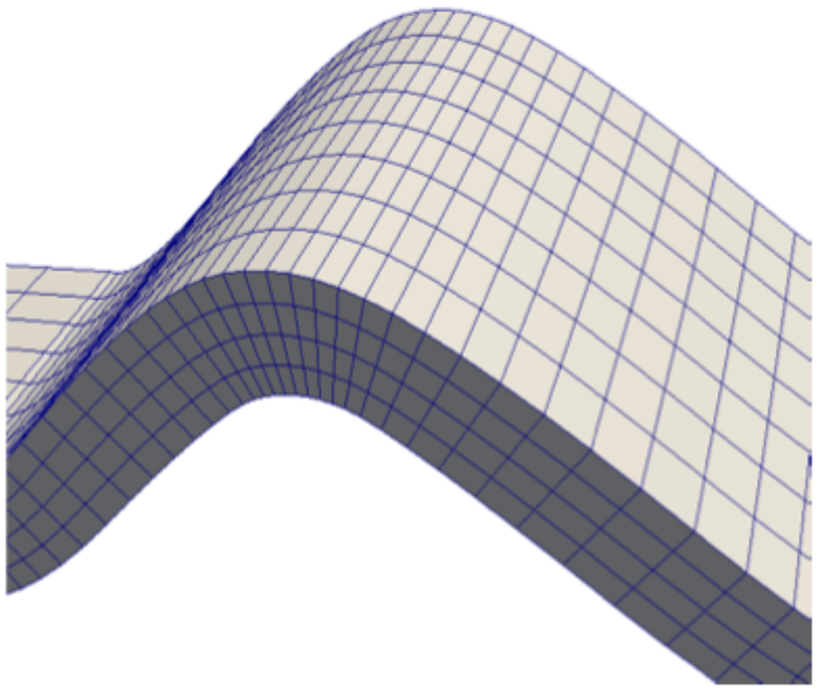

- singly curved thick-wall laminates
- geometry/displacements: NURBS
- trivariate NURBS from NURBS surface(*)
- cohesive surface interface elements

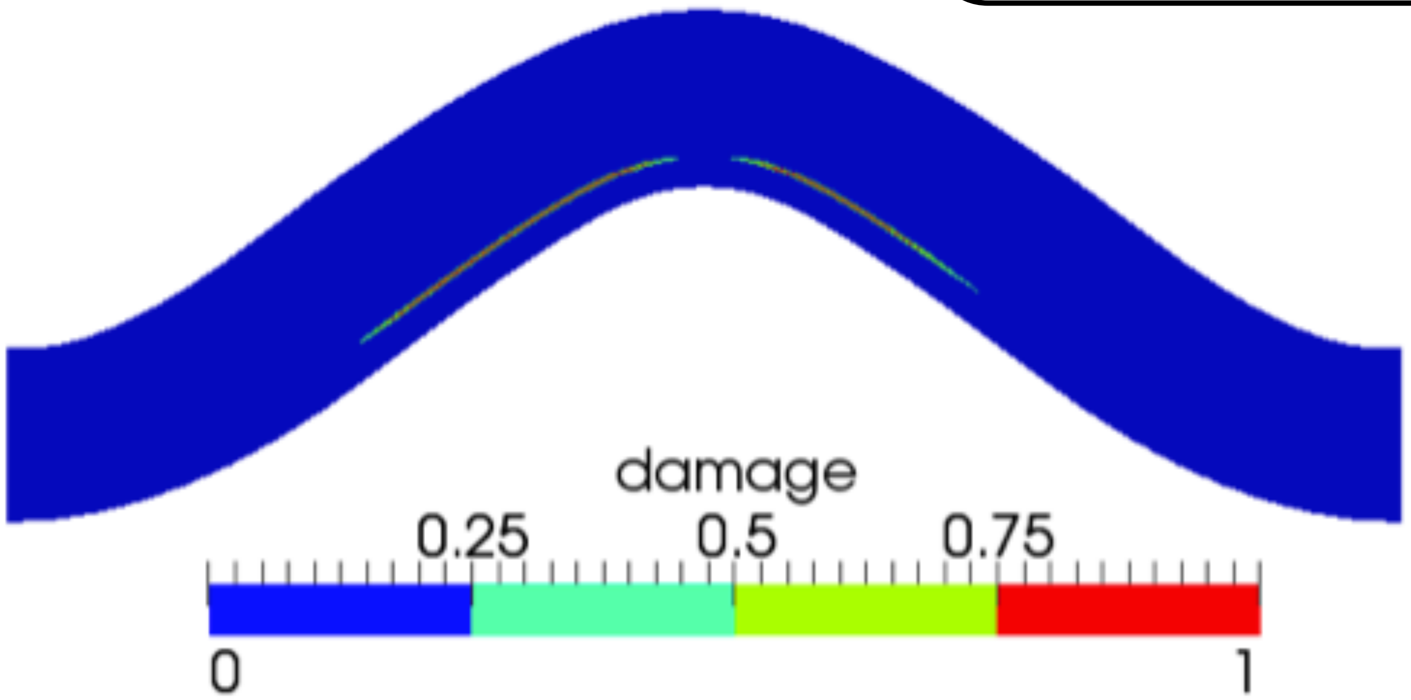

(*)V. P. Nguyen, P. Kerfriden, S.P.A. Bordas, and T. Rabczuk. An integrated design-analysis framework for three dimensional composite panels. Computer Aided Design, 2013. submitted.

Non-matching interface elements for delamination and contact

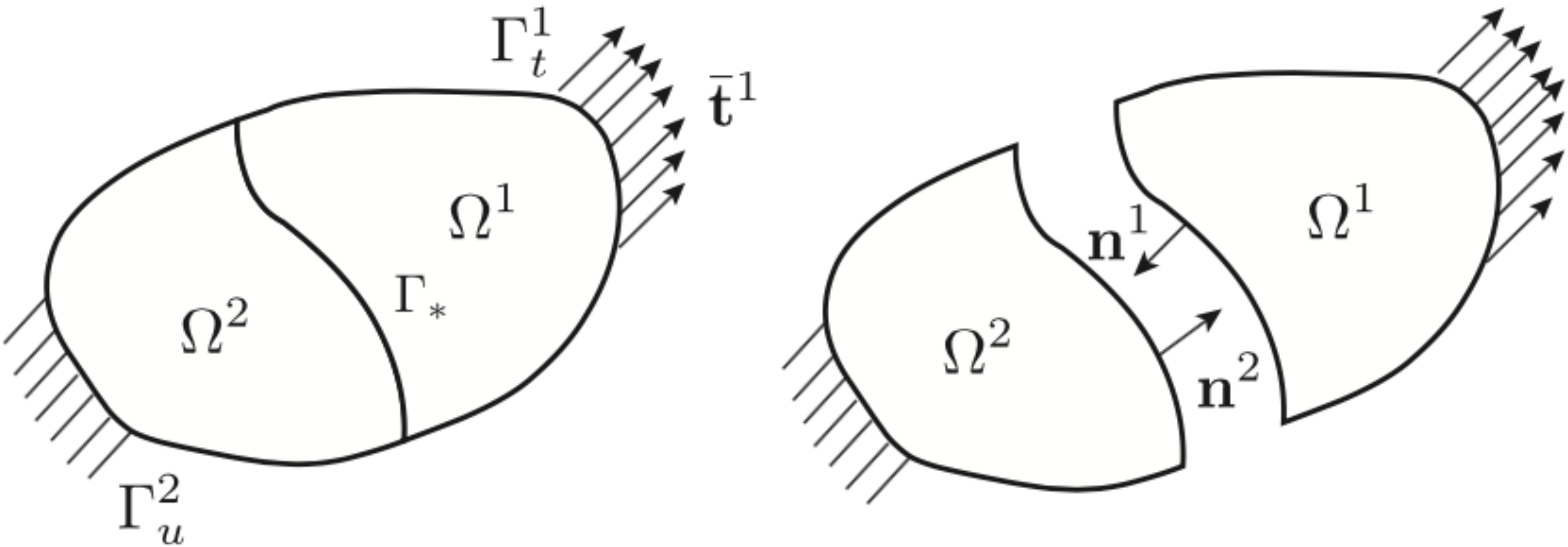

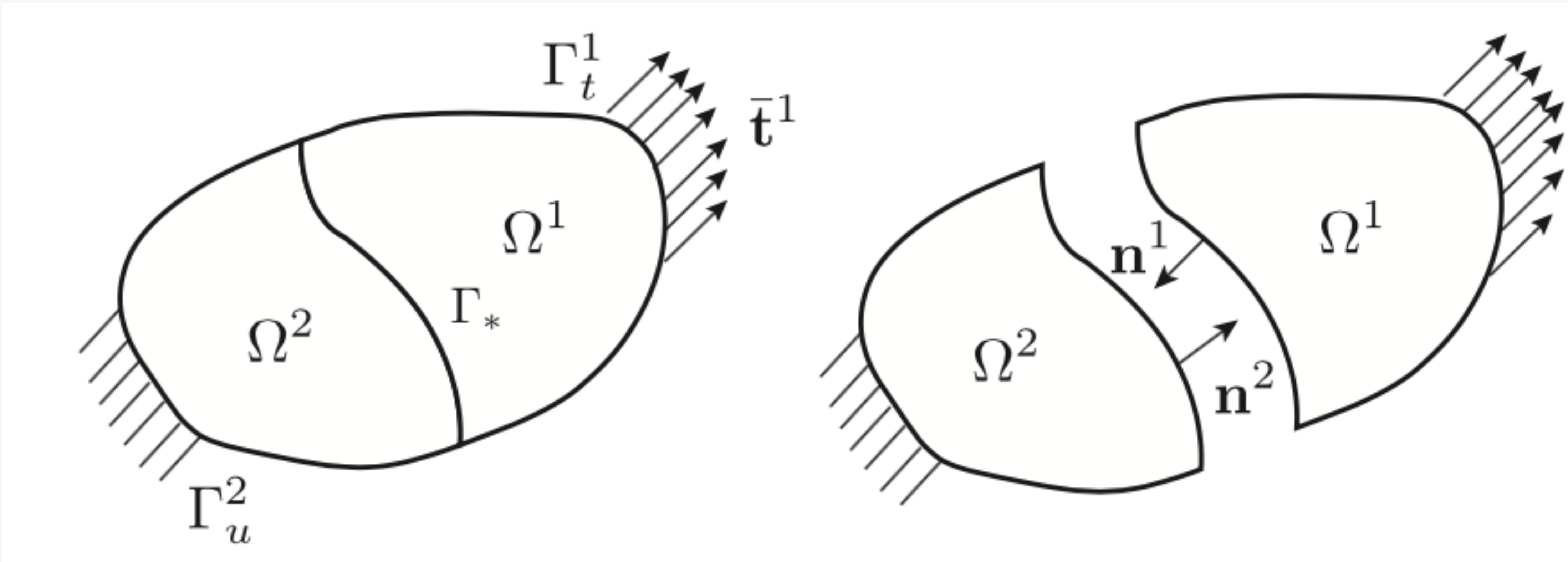

$$
\begin{aligned}
-\nabla \cdot \boldsymbol{\sigma}^m &= \mathbf{b}^m && \text{on} \quad \Omega^m \\
\mathbf{u}^m &= \bar{\mathbf{u}}^m && \text{on} \quad \Gamma_u^m \\
\boldsymbol{\sigma}^m \cdot \mathbf{n}^m &= \bar{\mathbf{t}}^m && \text{on} \quad \Gamma_t^m \\
\mathbf{u}^1 &= \mathbf{u}^2 && \text{on} \quad \Gamma_* \\
\boldsymbol{\sigma}^1 \cdot \mathbf{n}^1 &= -\boldsymbol{\sigma}^2 \cdot \mathbf{n}^2 && \text{on} \quad \Gamma_*
\end{aligned}
$$

$$
\begin{aligned}
-\nabla\, \boldsymbol{\sigma}^m &= \mathbf{b}^m && \text{on} \quad \Omega^m \\
\mathbf{u}^m &= \bar{\mathbf{u}}^m && \text{on} \quad \Gamma_u^m \\
\boldsymbol{\sigma}^m \cdot \mathbf{n}^m &= \bar{\mathbf{t}}^m && \text{on} \quad \Gamma_t^m \\
-\boldsymbol{\sigma}^1 \cdot \mathbf{n}^1 = \boldsymbol{\sigma}^2 \cdot \mathbf{n}^2 &= \mathbf{t} && \text{on} \quad \Gamma_* \\
\mathbf{t} &= \mathbf{t}([\![\mathbf{u}]\!], \zeta) && \text{on} \quad \Gamma_*
\end{aligned}
$$

Non-matching interface elements for delamination and contact

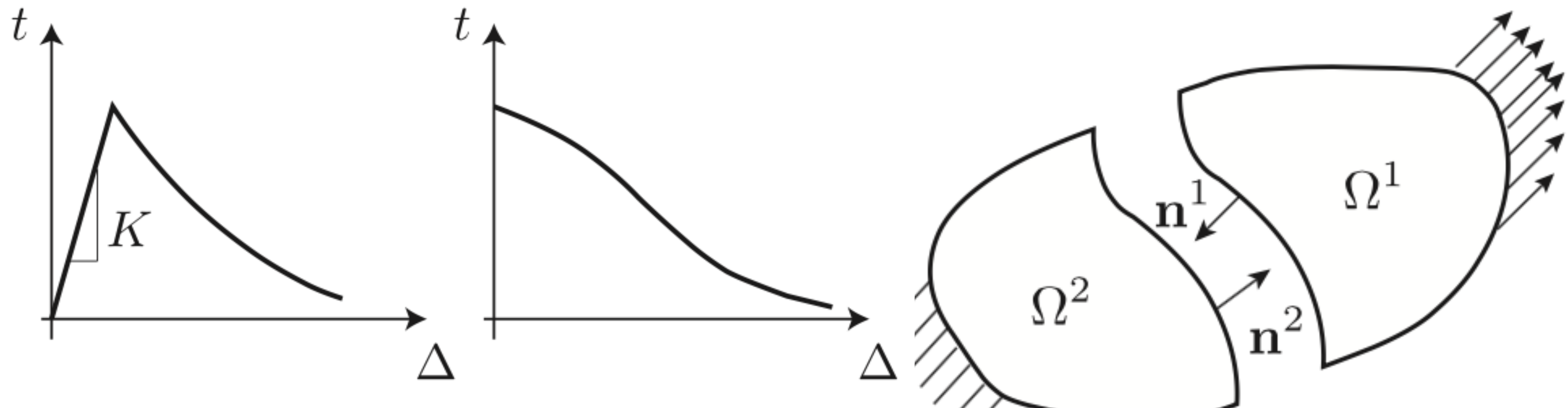

(a) intrinsic TSL (b) extrinsic TSL

$$
\begin{aligned}
-\nabla\cdot\boldsymbol{\sigma}^m &= \mathbf{b}^m && \text{on} \quad \Omega^m \\
\mathbf{u}^m &= \bar{\mathbf{u}}^m && \text{on} \quad \Gamma_u^m \\
\boldsymbol{\sigma}^m\cdot\mathbf{n}^m &= \bar{\mathbf{t}}^m && \text{on} \quad \Gamma_t^m \\
\mathbf{u}^1 &= \mathbf{u}^2 && \text{on} \quad \Gamma_* \\
\boldsymbol{\sigma}^1\cdot\mathbf{n}^1 &= -\boldsymbol{\sigma}^2\cdot\mathbf{n}^2 && \text{on} \quad \Gamma_*
\end{aligned}
$$

$$
\begin{aligned}
-\nabla\,\boldsymbol{\sigma}^m &= \mathbf{b}^m && \text{on} \quad \Omega^m \\
\mathbf{u}^m &= \bar{\mathbf{u}}^m && \text{on} \quad \Gamma_u^m \\
\boldsymbol{\sigma}^m\cdot\mathbf{n}^m &= \bar{\mathbf{t}}^m && \text{on} \quad \Gamma_t^m \\
-\boldsymbol{\sigma}^1\cdot\mathbf{n}^1 = \boldsymbol{\sigma}^2\cdot\mathbf{n}^2 &= \mathbf{t} && \text{on} \quad \Gamma_* \\
\mathbf{t} &= \mathbf{t}([\![\mathbf{u}]\!],\boldsymbol{\zeta}) && \text{on} \quad \Gamma_*
\end{aligned}
$$

Weak form

$$\boldsymbol{S}^m = \{\mathbf{u}^m(\mathbf{x}) | \mathbf{u}^m(\mathbf{x}) \in \boldsymbol{H}^1(\Omega^m), \mathbf{u}^m = \bar{\mathbf{u}}^m \ \text{ on } \Gamma_u^m\}$$

$$\boldsymbol{V}^m = \{\mathbf{w}^m(\mathbf{x}) | \mathbf{w}^m(\mathbf{x}) \in \boldsymbol{H}^1(\Omega^m), \mathbf{w}^m = \mathbf{0} \ \text{ on } \Gamma_u^m\}$$

Find $(\mathbf{u}^1, \mathbf{u}^2) \in \boldsymbol{S}^1 \times \boldsymbol{S}^2$ such that

$$\sum_{m=1}^{2} \int_{\Omega^m} (\boldsymbol{\epsilon}(\mathbf{w}^m))^{\mathrm{T}} \boldsymbol{\sigma}^m \mathrm{d}\Omega + (1-\beta) \left[-\int_{\Gamma_*} [\![\mathbf{w}]\!]^{\mathrm{T}} \mathbf{n} \{\boldsymbol{\sigma}\} \mathrm{d}\Gamma - \int_{\Gamma_*} \{\boldsymbol{\sigma}(\mathbf{w})\}^{\mathrm{T}} \mathbf{n}^{\mathrm{T}} [\![\mathbf{u}]\!] \mathrm{d}\Gamma + \int_{\Gamma_*} \alpha [\![\mathbf{w}]\!]^{\mathrm{T}} [\![\mathbf{u}]\!] \mathrm{d}\Gamma \right]$$

$$+\beta \int_{\Gamma_*} [\![\mathbf{w}]\!]^{\mathrm{T}} \mathbf{t}([\![\mathbf{u}]\!]) \mathrm{d}\Gamma = \sum_{m=1}^{2} \int_{\Gamma_t^m} (\mathbf{w}^m)^{\mathrm{T}} \bar{\mathbf{t}}^m \mathrm{d}\Gamma + \sum_{m=1}^{2} \int_{\Omega^m} (\mathbf{w}^m)^{\mathrm{T}} \mathbf{b}^m \mathrm{d}\Omega \quad \text{for all } (\mathbf{w}^1, \mathbf{w}^2) \in \boldsymbol{V}^1 \times \boldsymbol{V}^2$$

$$[\![\mathbf{u}]\!] = \mathbf{u}^1 - \mathbf{u}^2, \qquad \{\boldsymbol{\sigma}\} = \gamma \boldsymbol{\sigma}^1 + (1-\gamma) \boldsymbol{\sigma}^2$$

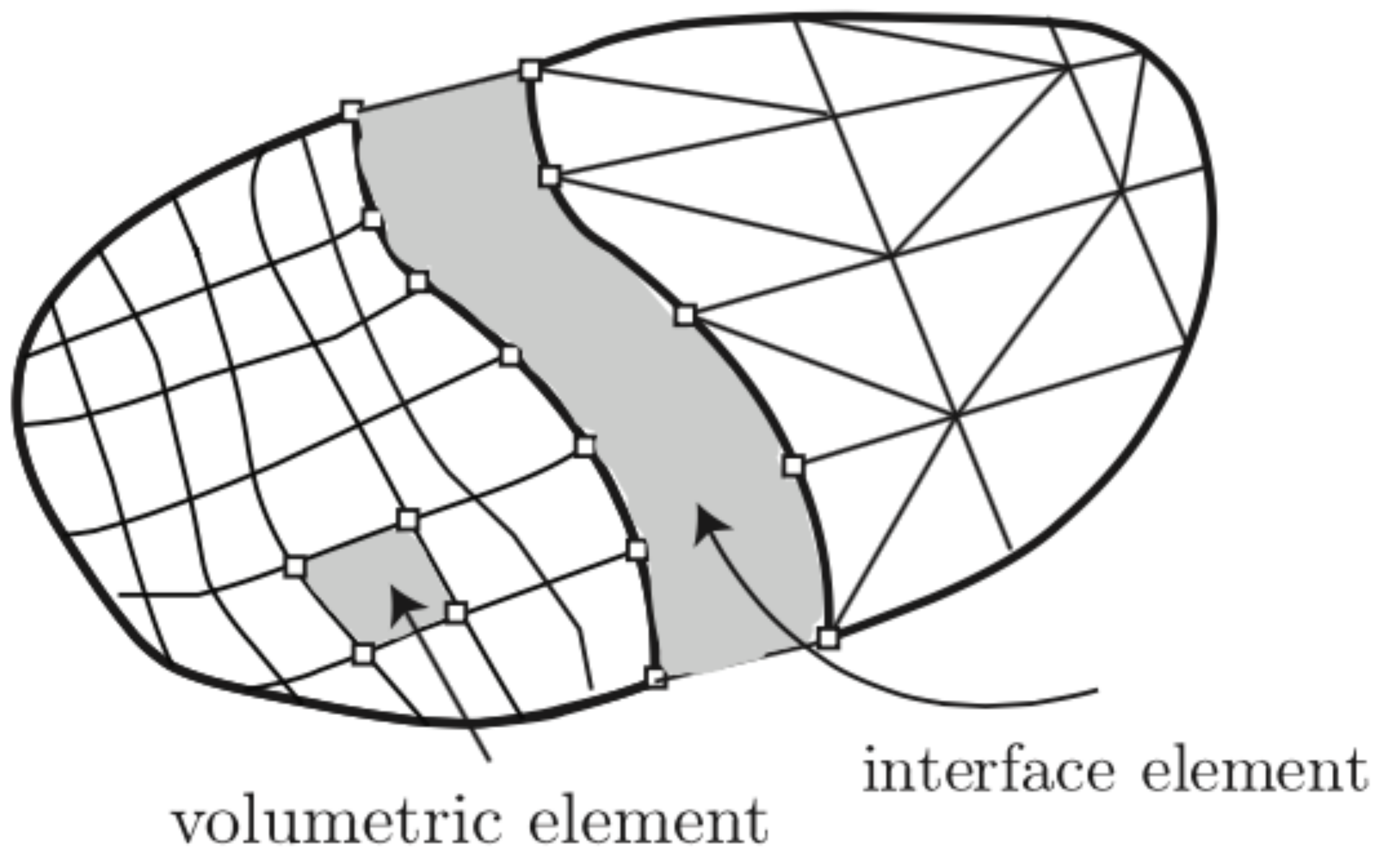

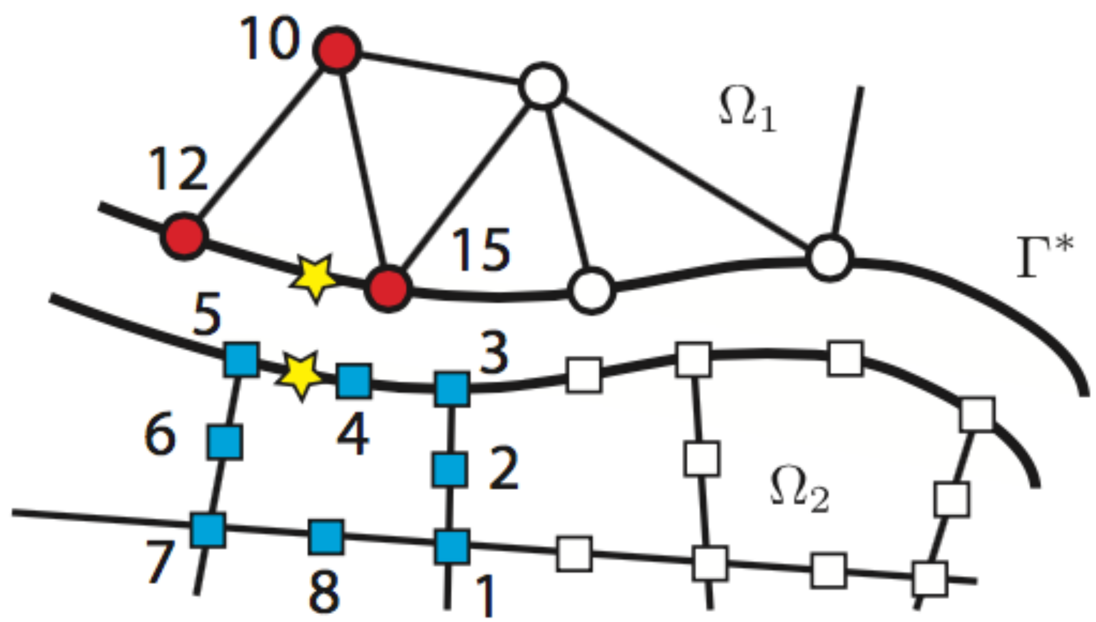

The interface elements are of zero thickness.

2D uniaxial tension test

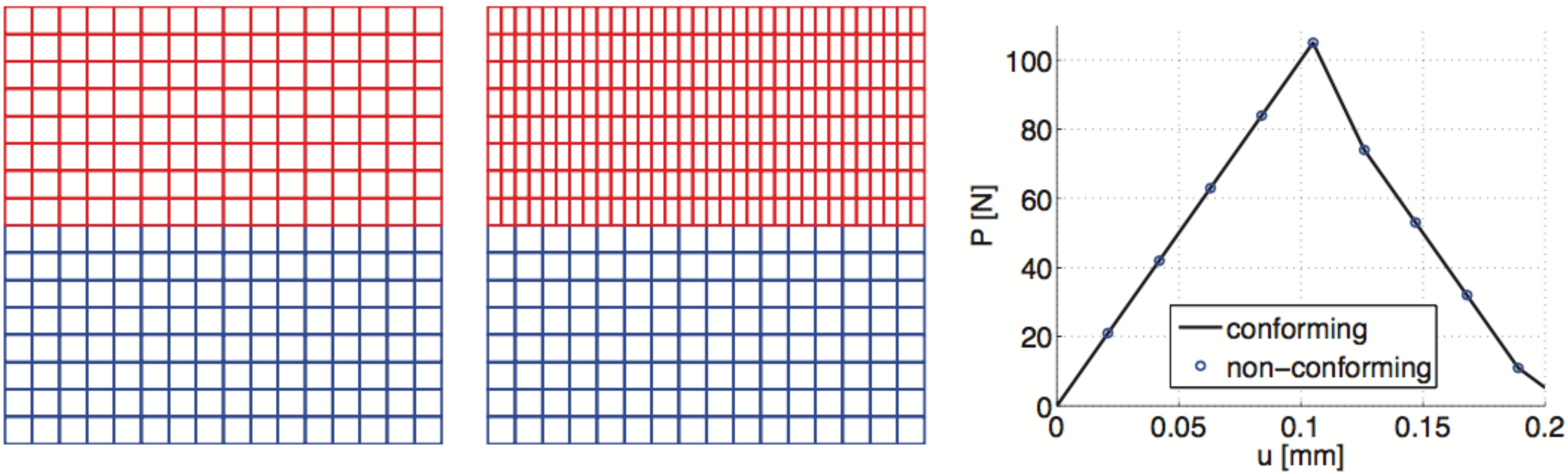

(a) conforming mesh (b) nonconforming mesh (c) load-displacement

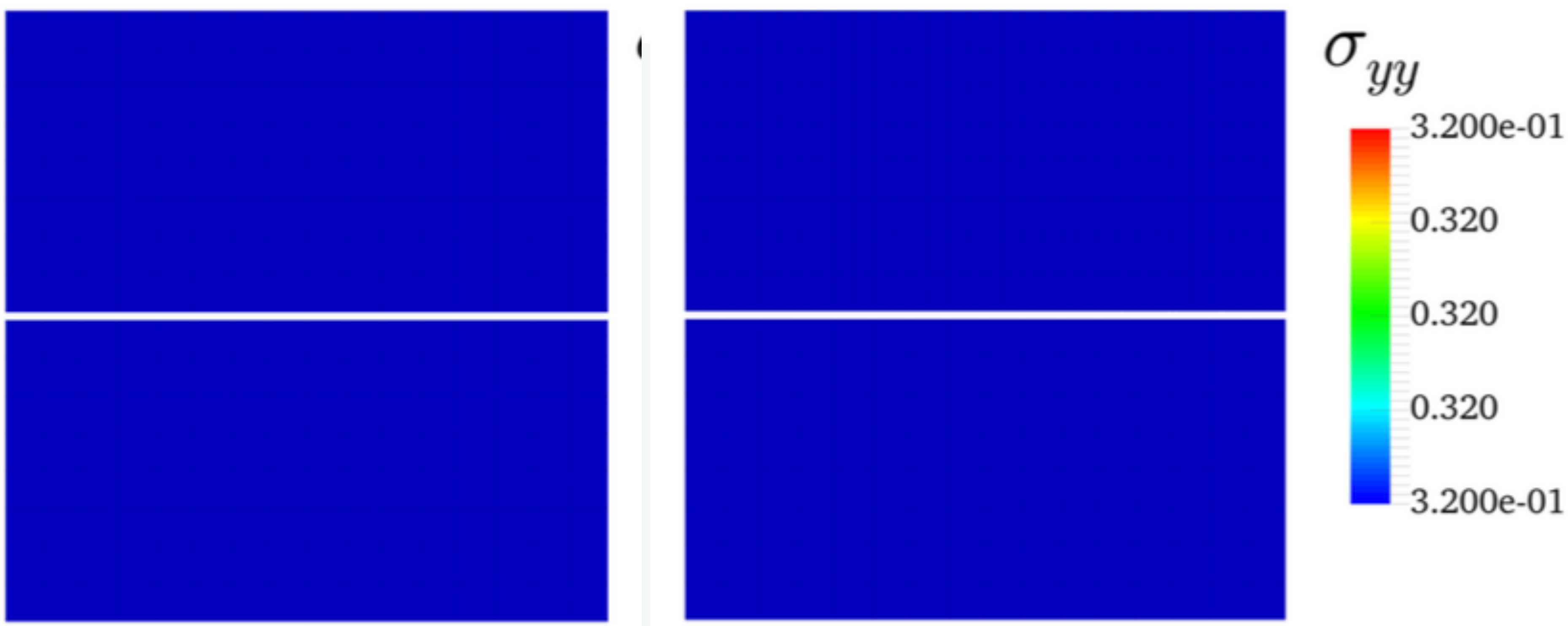

(a) matching mesh (b) non-matching mesh

3D uniaxial tension

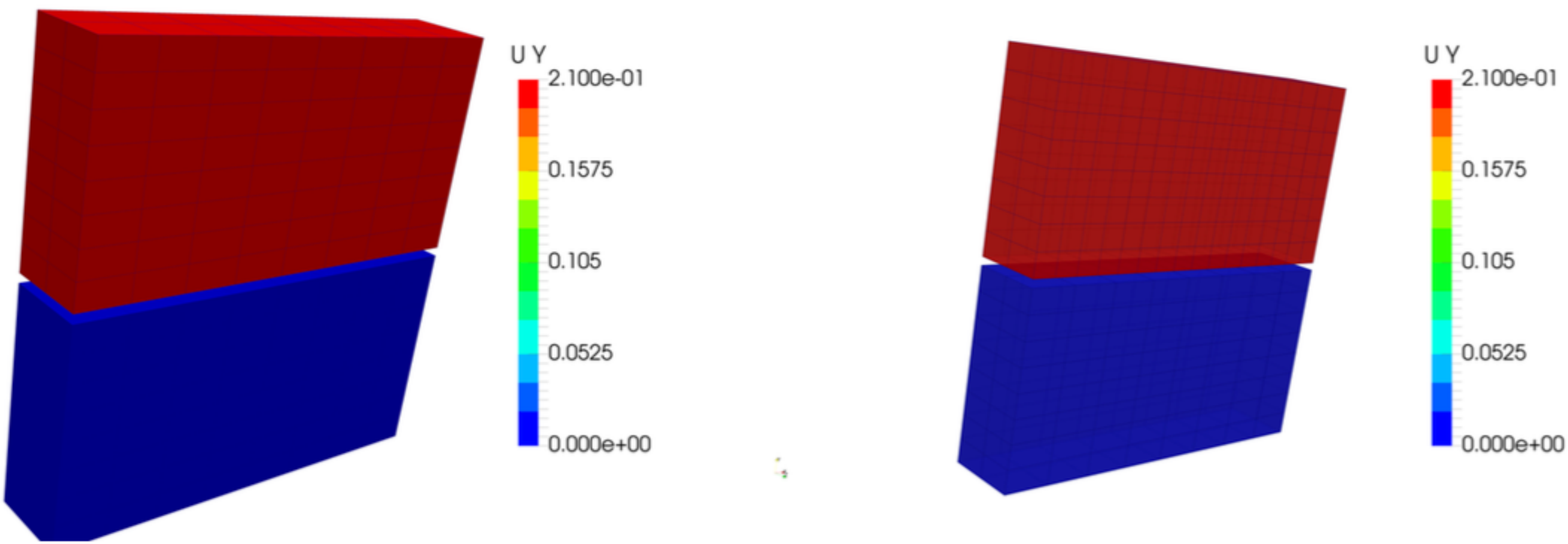

(a) matching mesh

(b) non-matching mesh

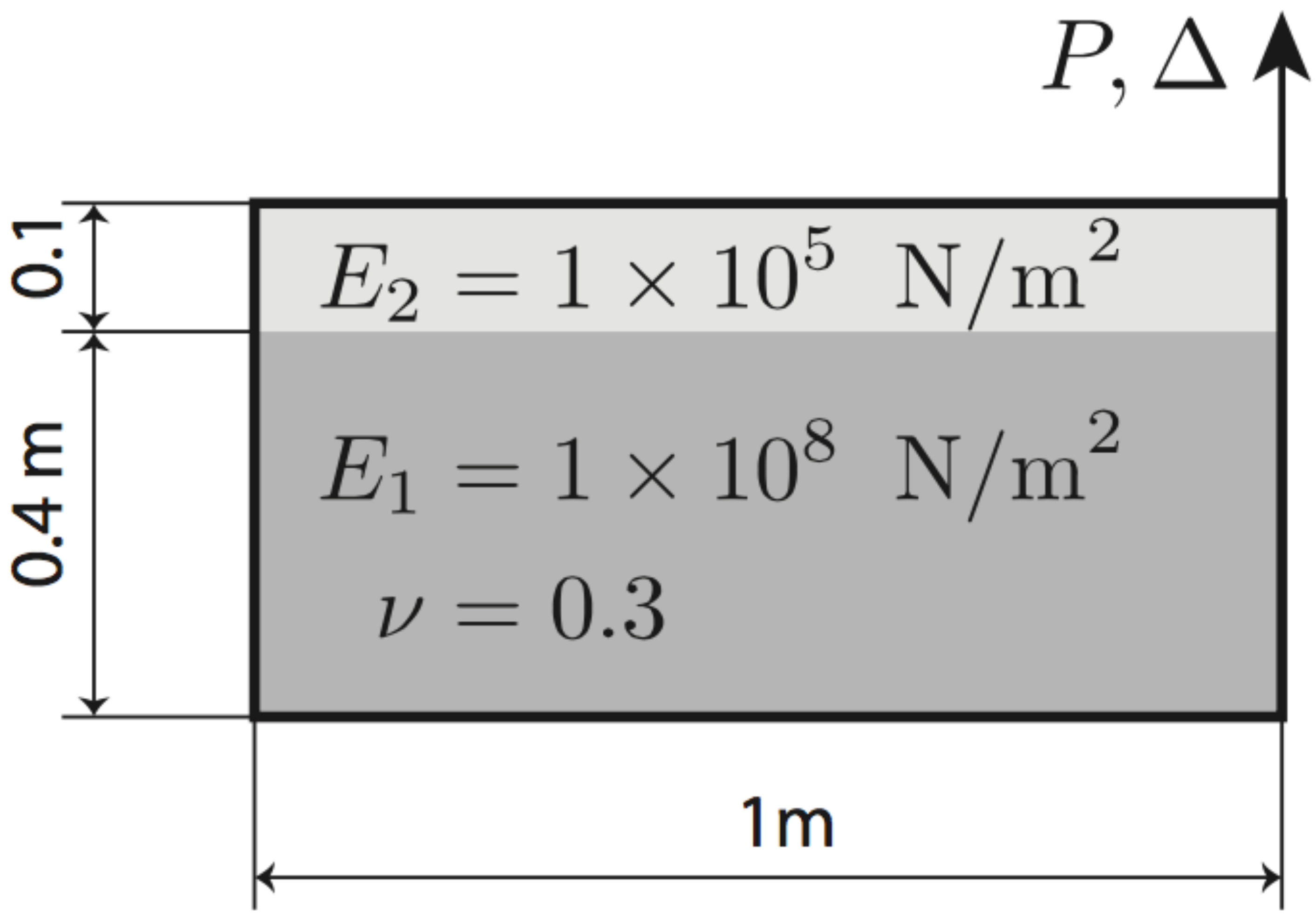

Figure 12: Peeling test: problem configuration.

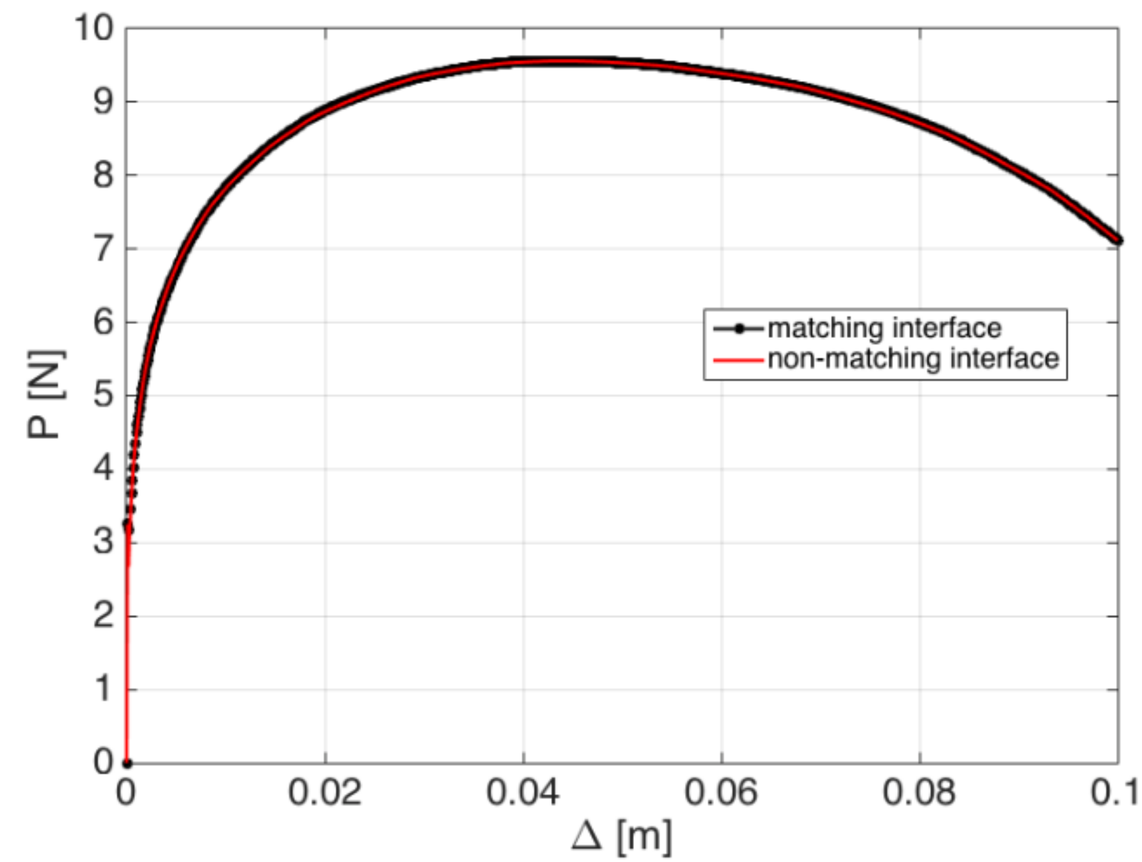

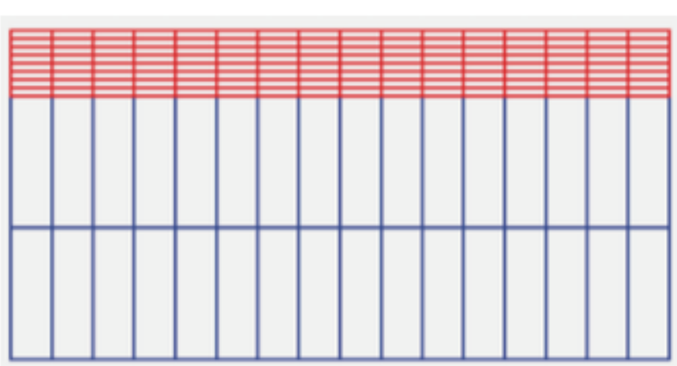

(a) matching mesh

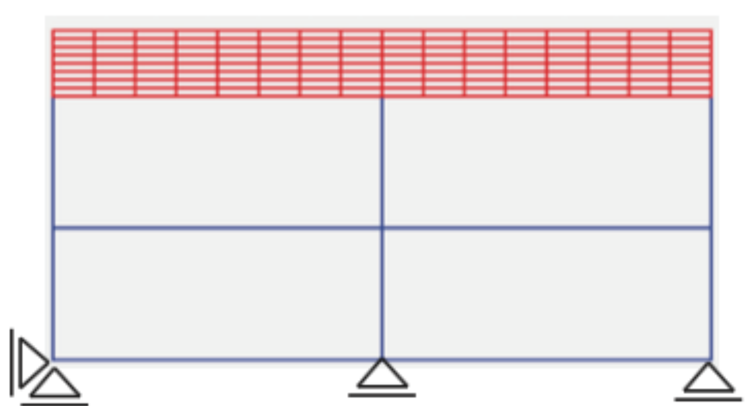

(b) non-matching mesh

2D peeling test

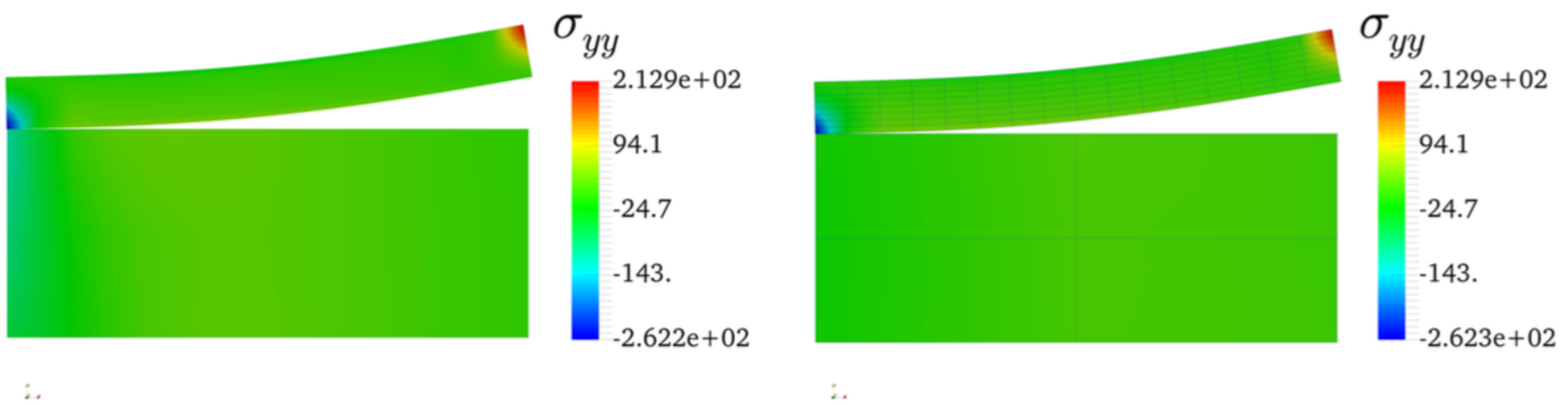

(a) matching mesh (b) non-matching mesh

2D peeling test

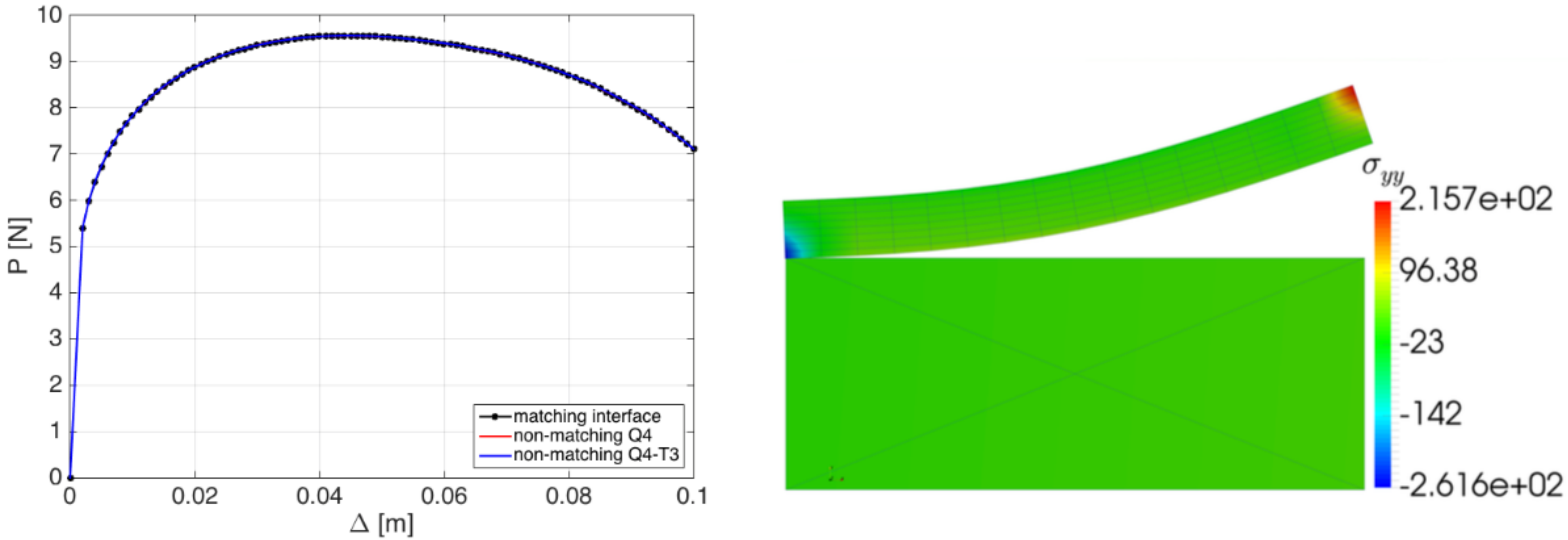

(a) load-displacement (b) stress contour

Figure 17: Peeling test: substrate discretised by three-node triangular elements whereas layer is meshed by Q4 elements. Note that there is a slight difference with the $P - \Delta$ curves in Fig. 14 as displacement increments that are ten times larger were used.

2D peeling test F(D) curves

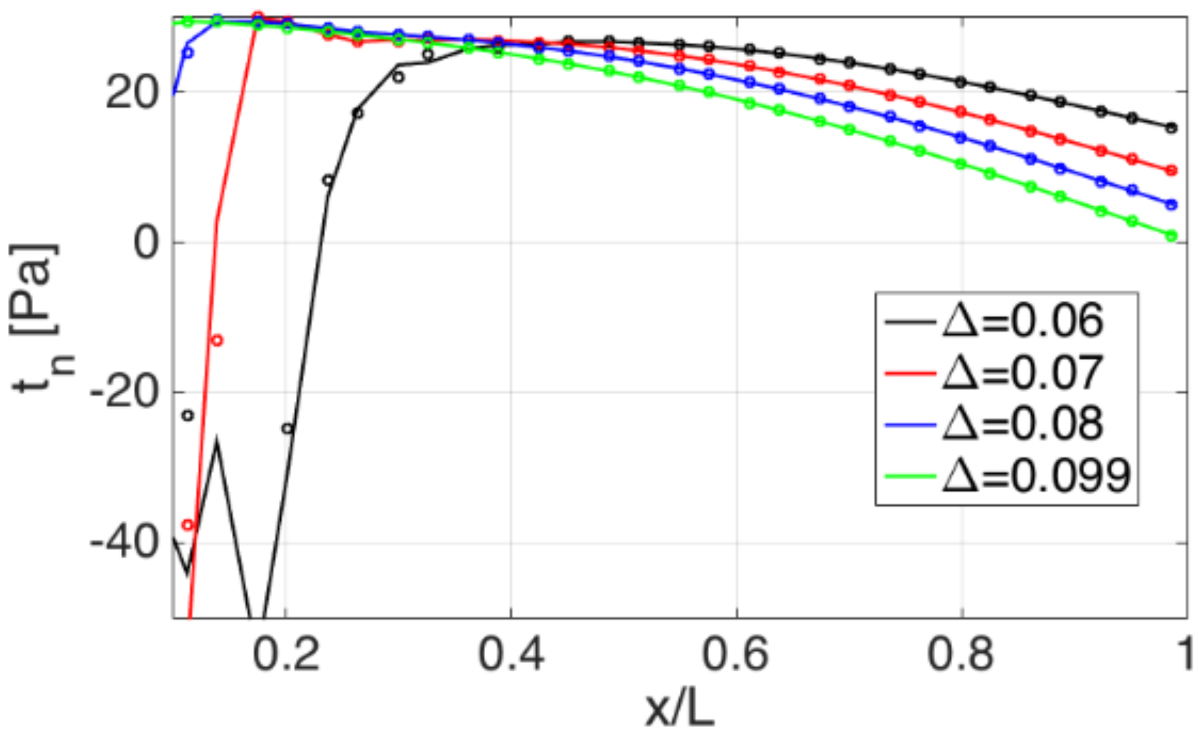

(a) normal cohesive traction

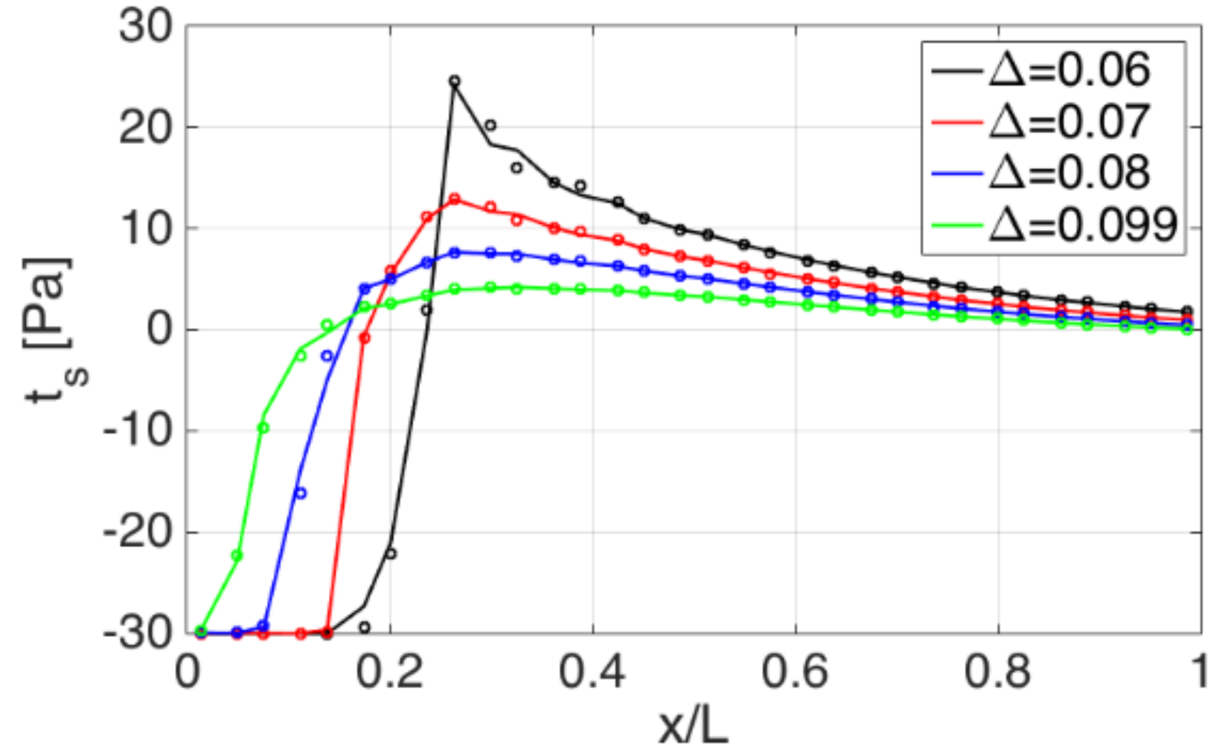

(b) tangential cohesive traction

Figure 18: Peeling test: local response of the proposed interface element (solid lines) vs. standard interface element (circles) for different imposed displacements Δ.

2D peeling test - role of integration

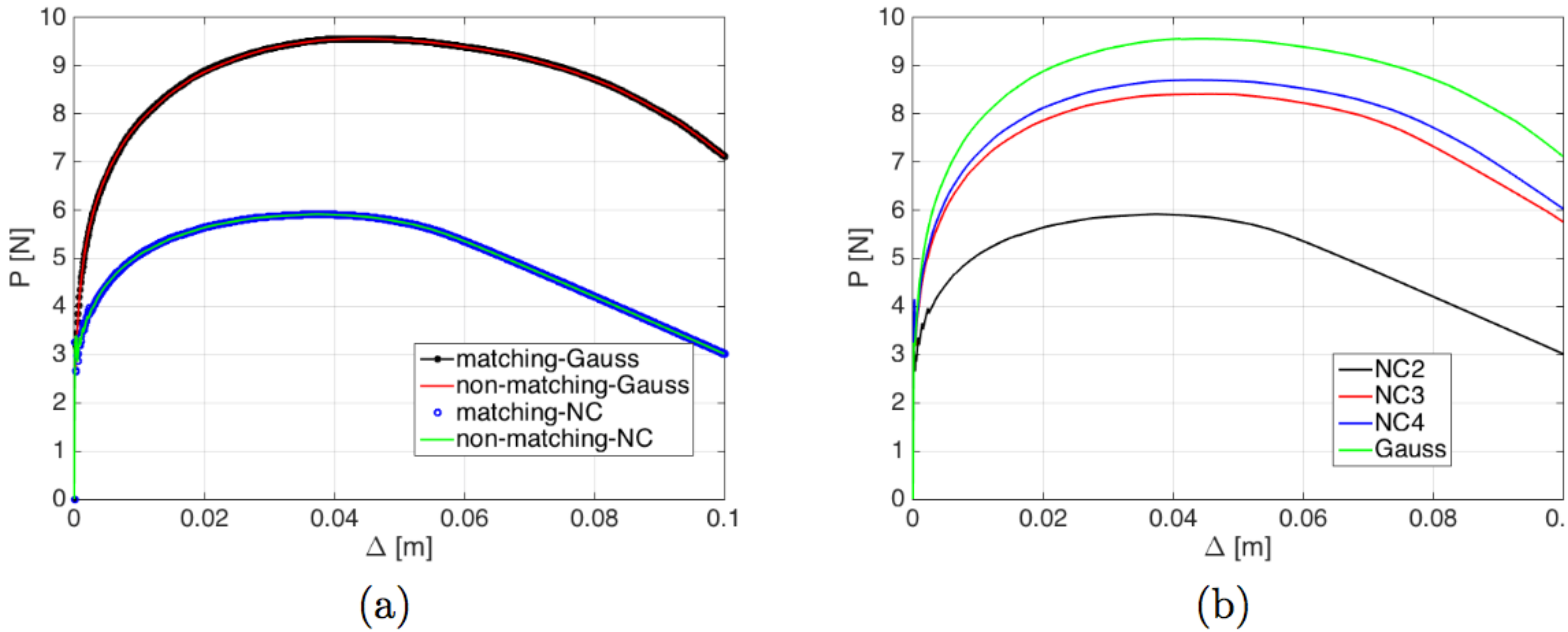

Figure 19: Peeling test: $P - \Delta$ curves obtained with matching and non-matching FE meshes with Gausss and Newton-Cotes (NC) quadrature rules. Increasing the number of NC integration points shift the $P - \Delta$ curves to the Gauss-based curve (right).

3D peeling test

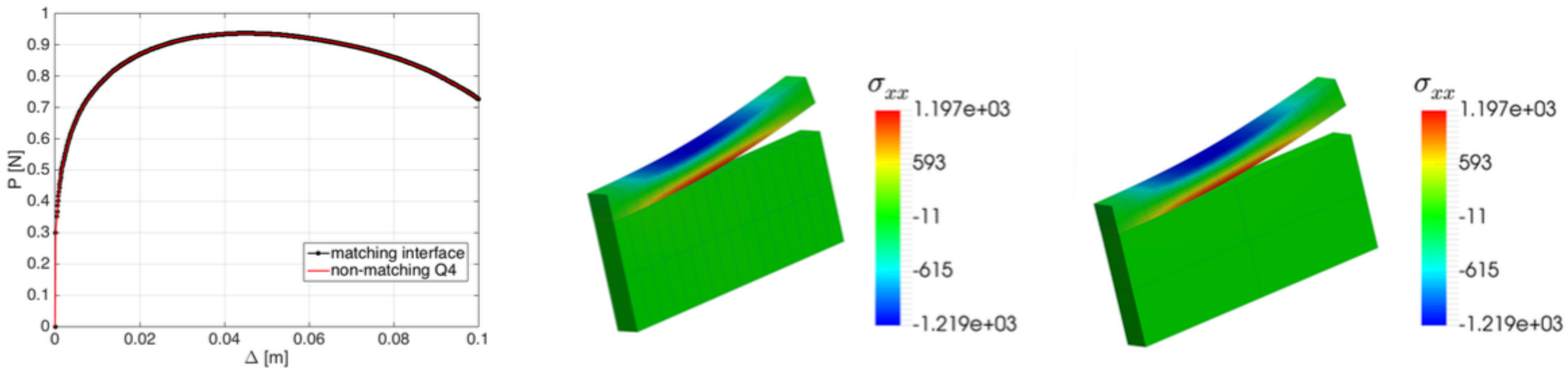

(a) load-displacement (b) matching mesh (c) non-matching

Figure 20: Three dimensional peeling test: $P - \Delta$ curves and stress distribution.

Fibre-reinforced composite - debonding

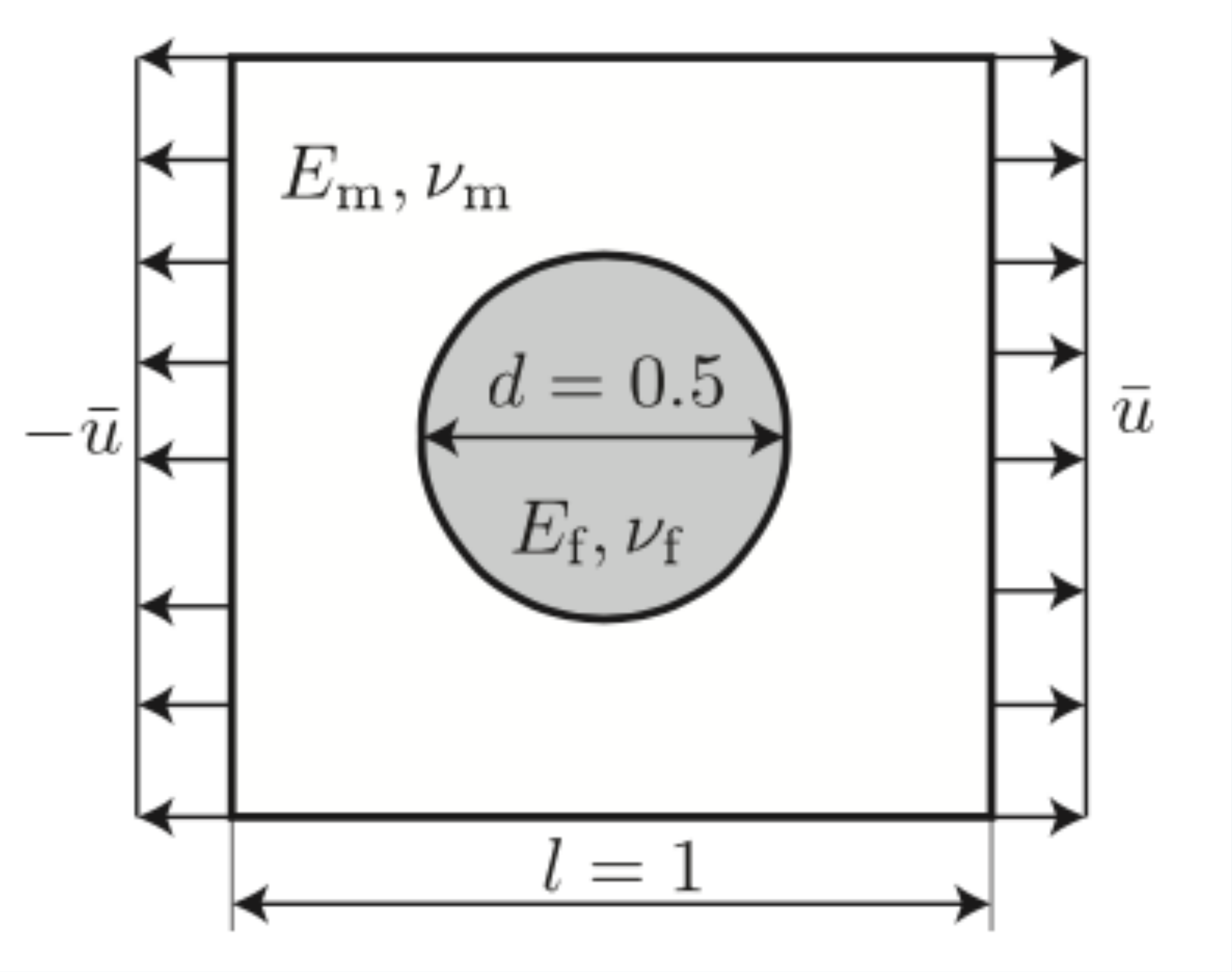

Non-matching interfaces

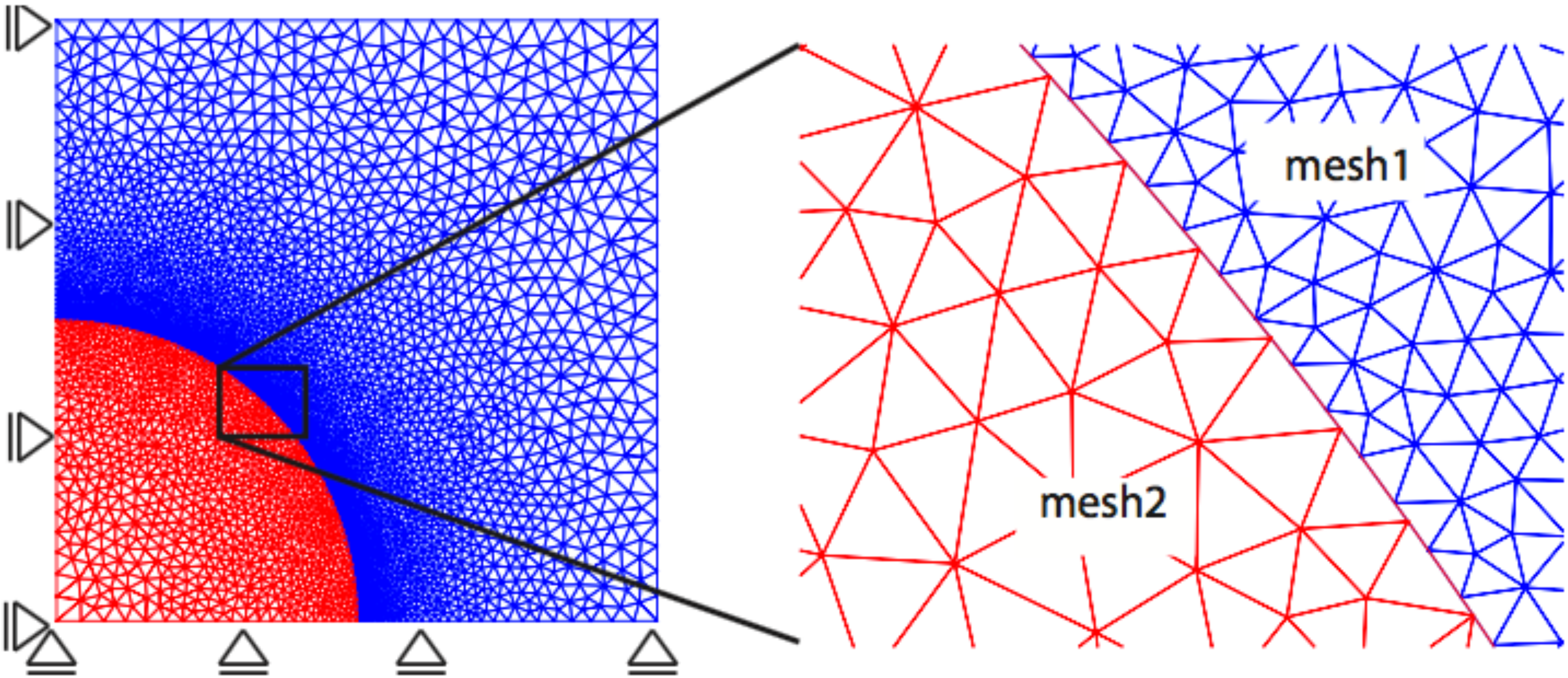

Fibre-debonding

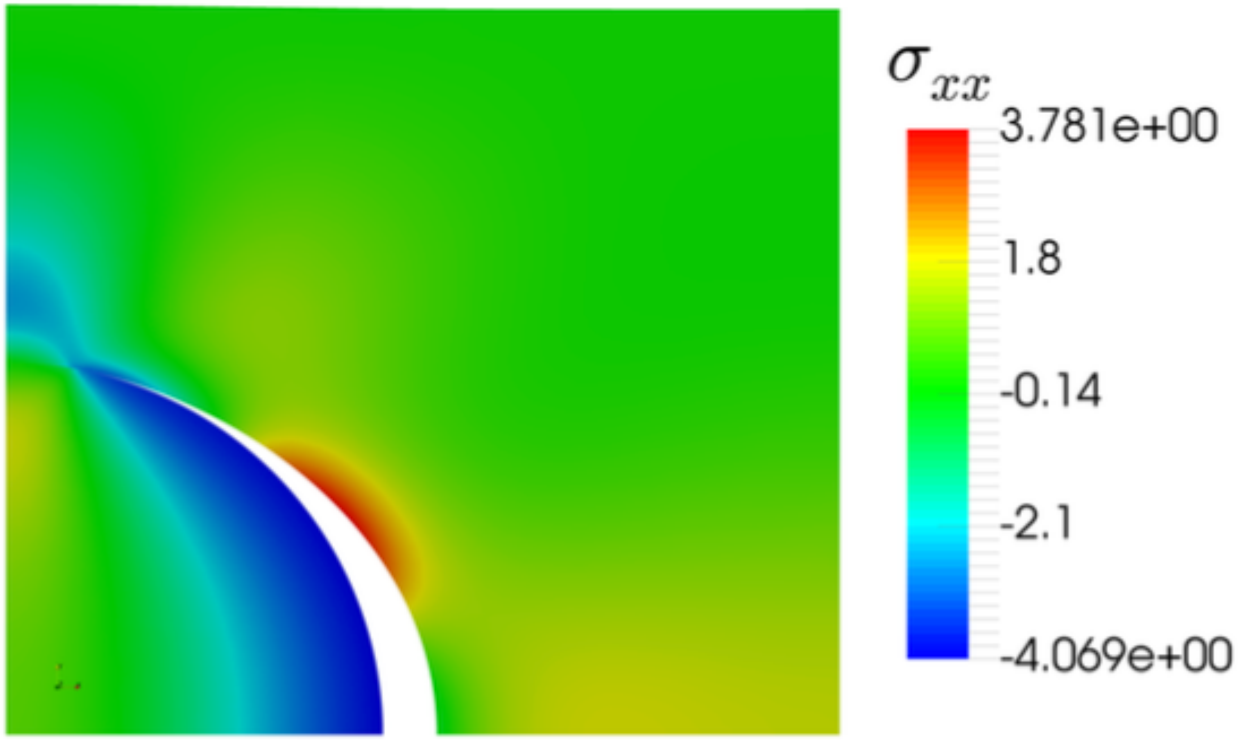

(a) matching mesh

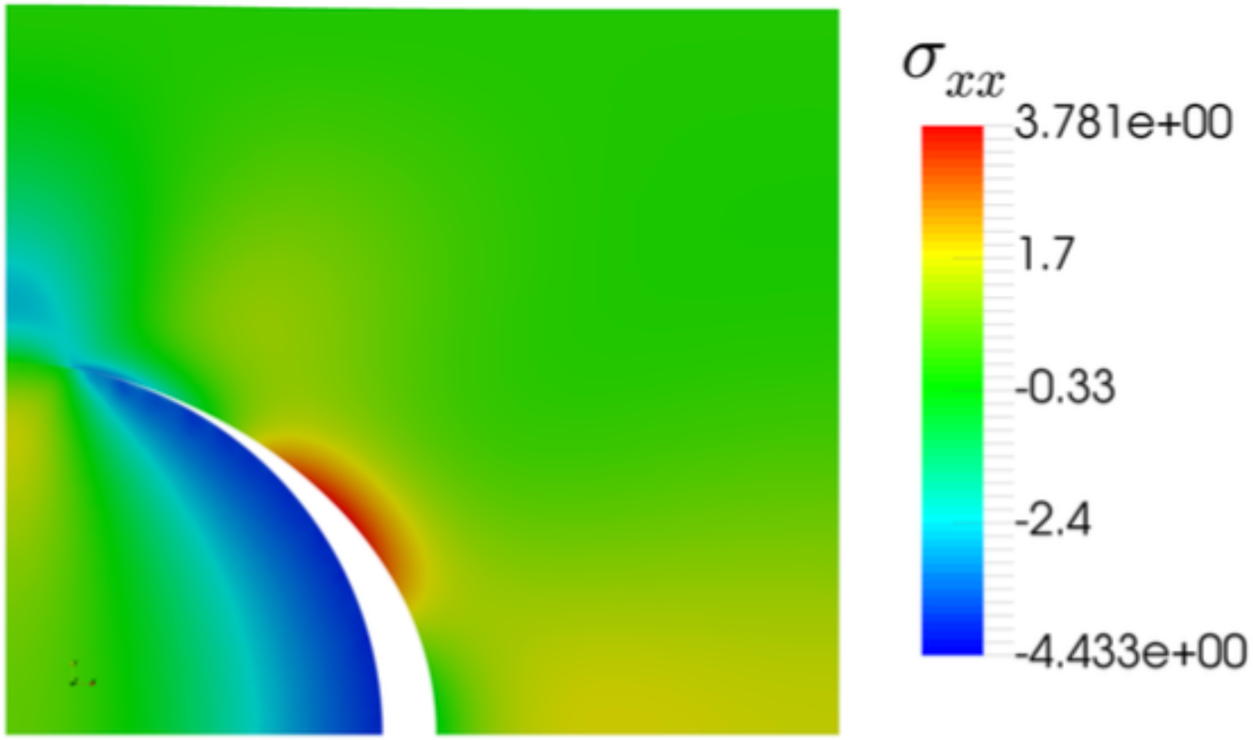

(b) non-matching mesh

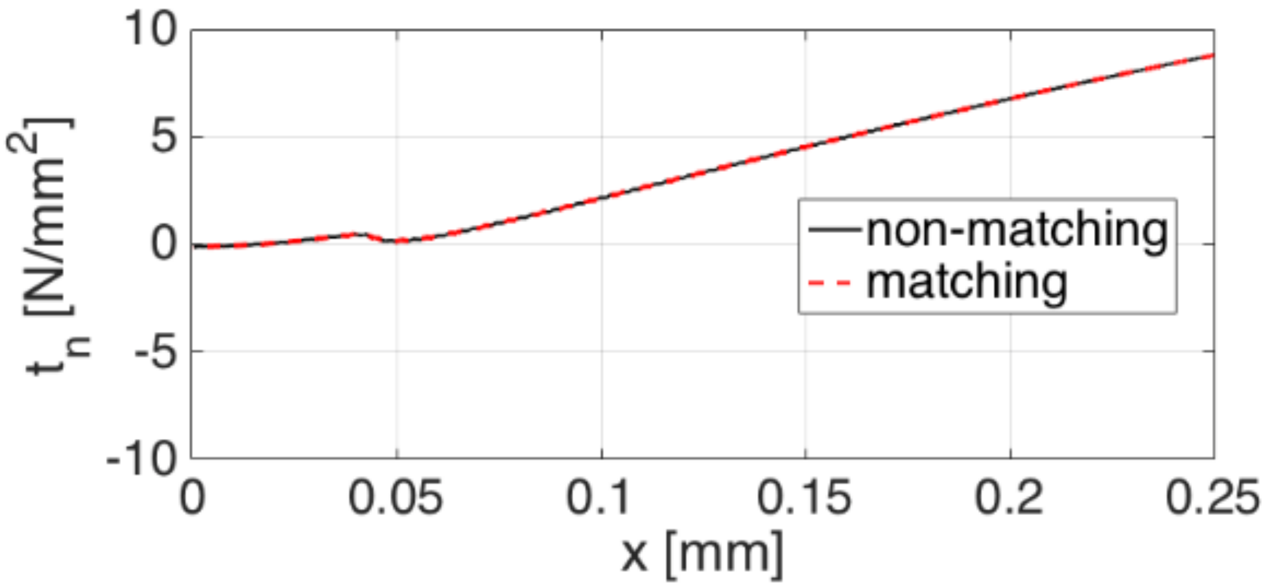

(a) normal stress

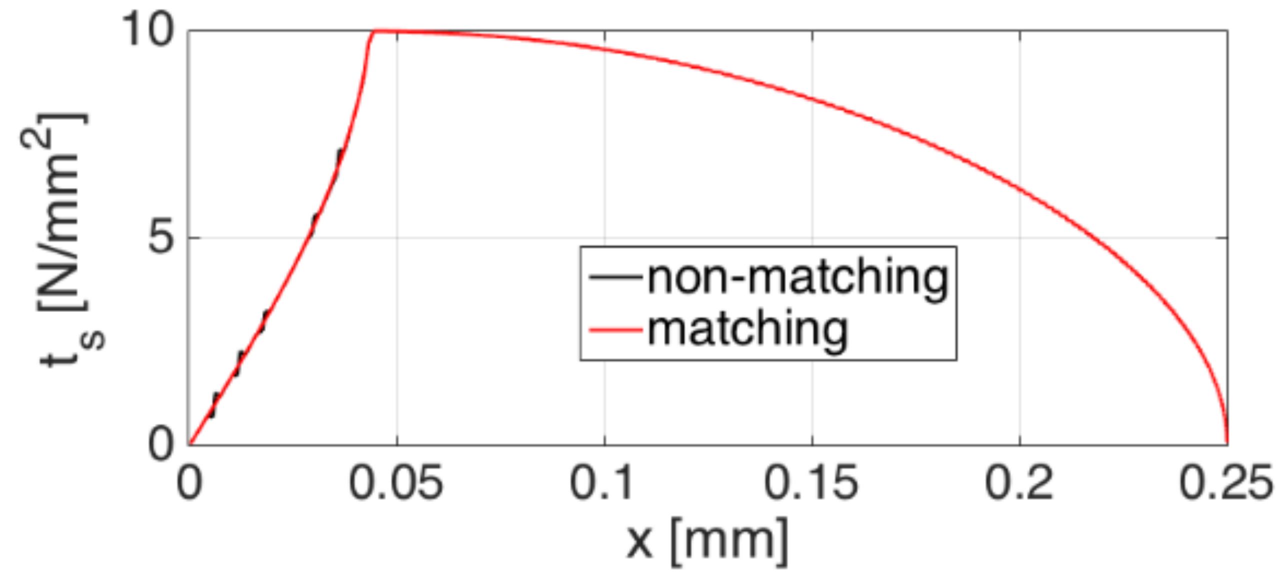

(b) tangential stress

Conclusions

- Incompatible/non-matching elements
- Small strain interfacial fracture
  - No need for conforming meshes along the interface
  - non-matching interface
  - no high-dummy stiffness
  - fewer elements (up to twice as fast)
  - Newton-Cotes integration leads to premature failure

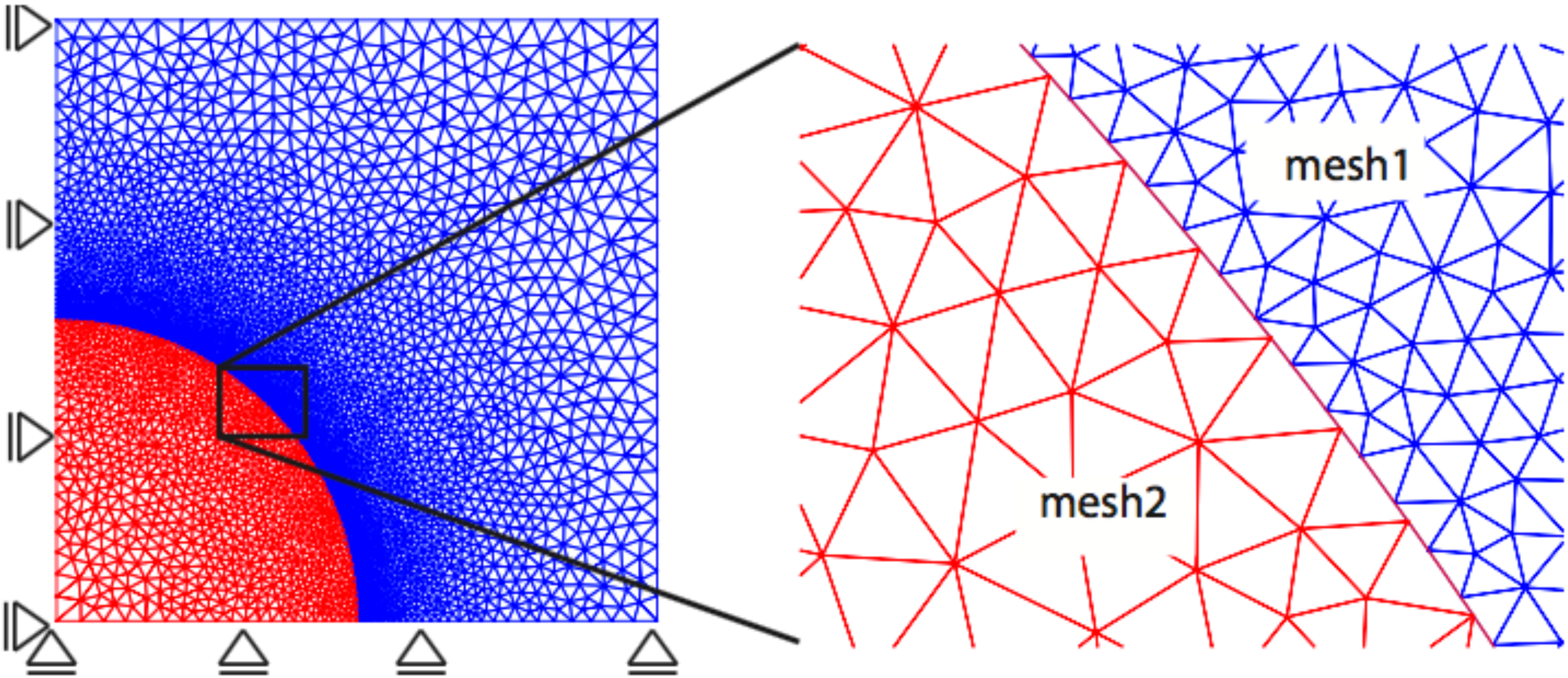

Third medium contact formulation, Wriggers

A finite element method for contact using a third medium P. Wriggers · J. Schröder · A. Schwarz Comput Mech (2013) 52:837–847

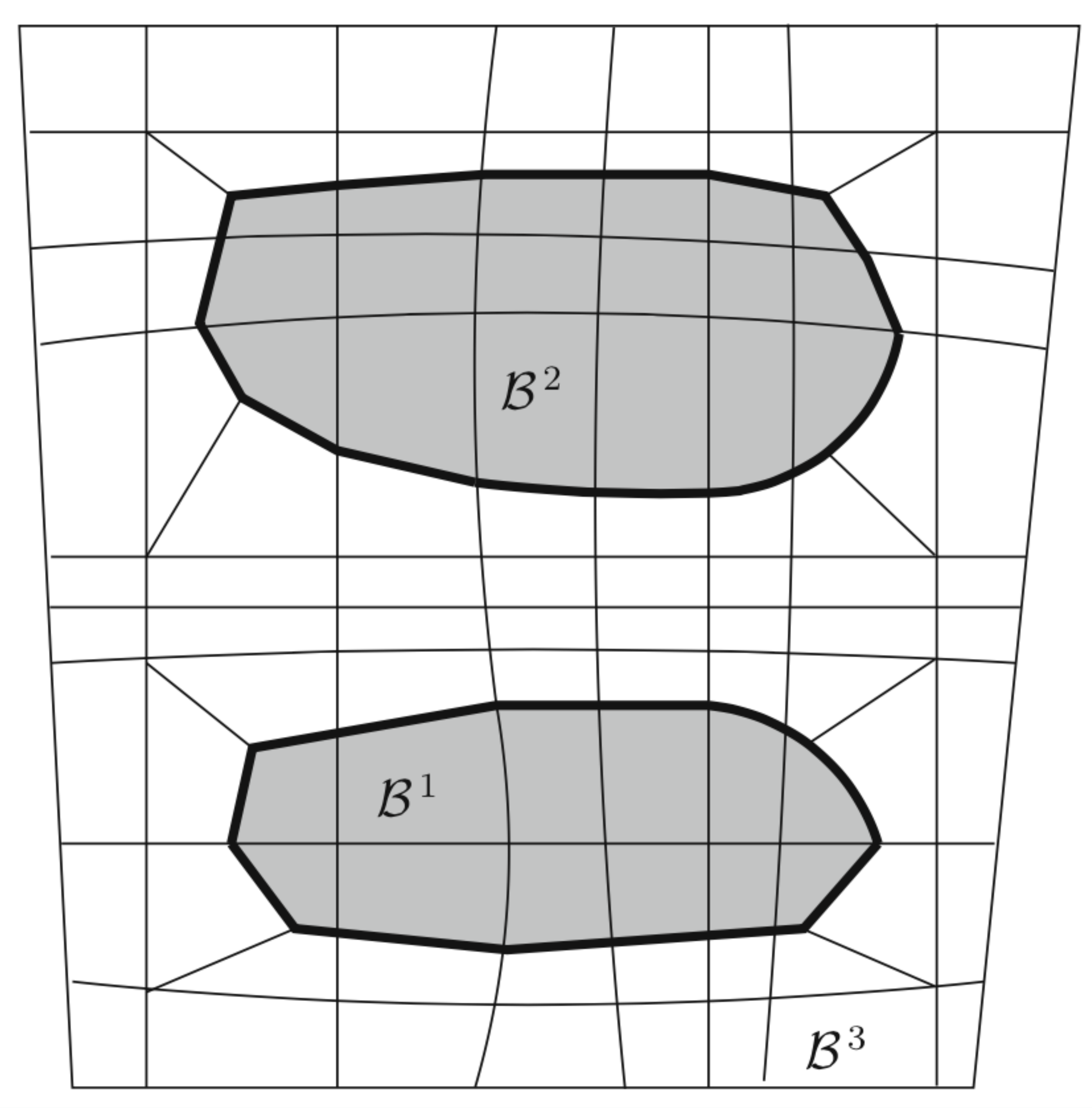

Gap function

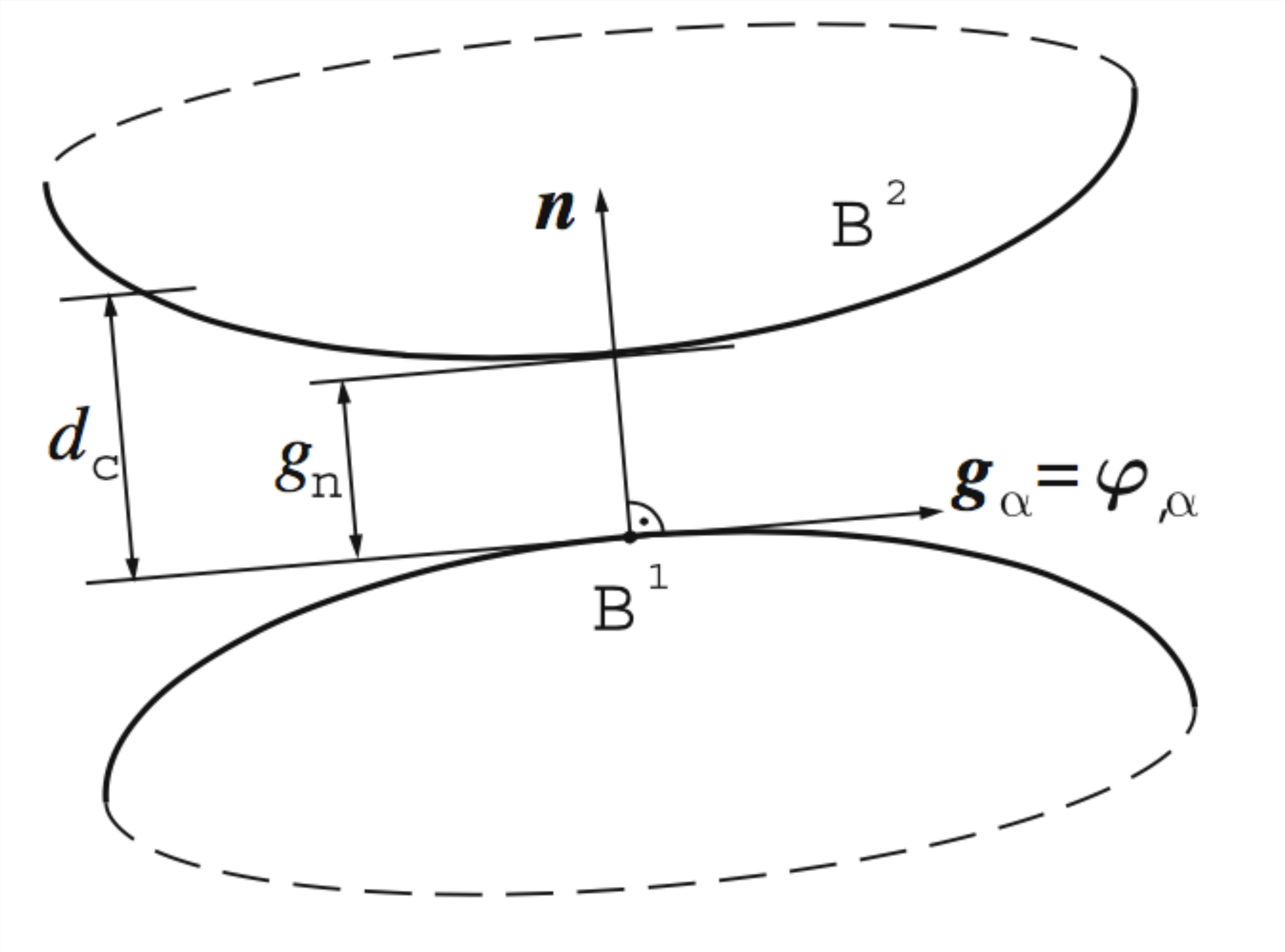

Contacts as interfaces

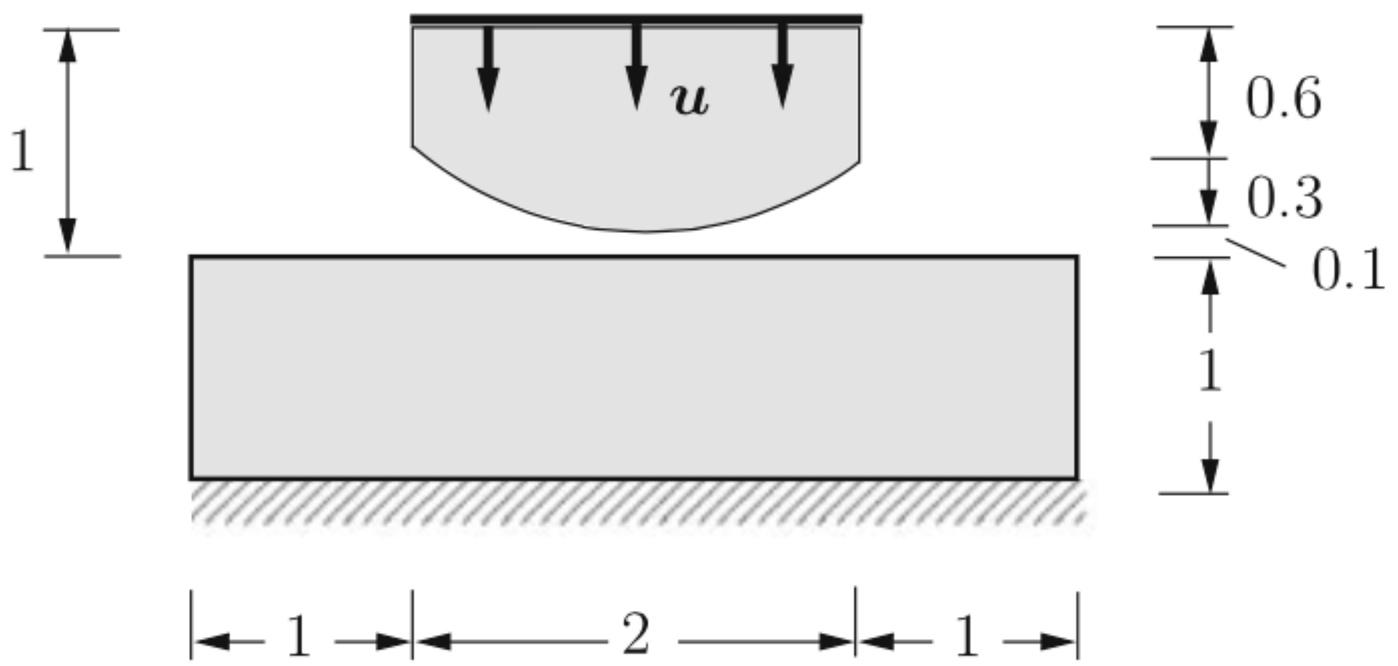

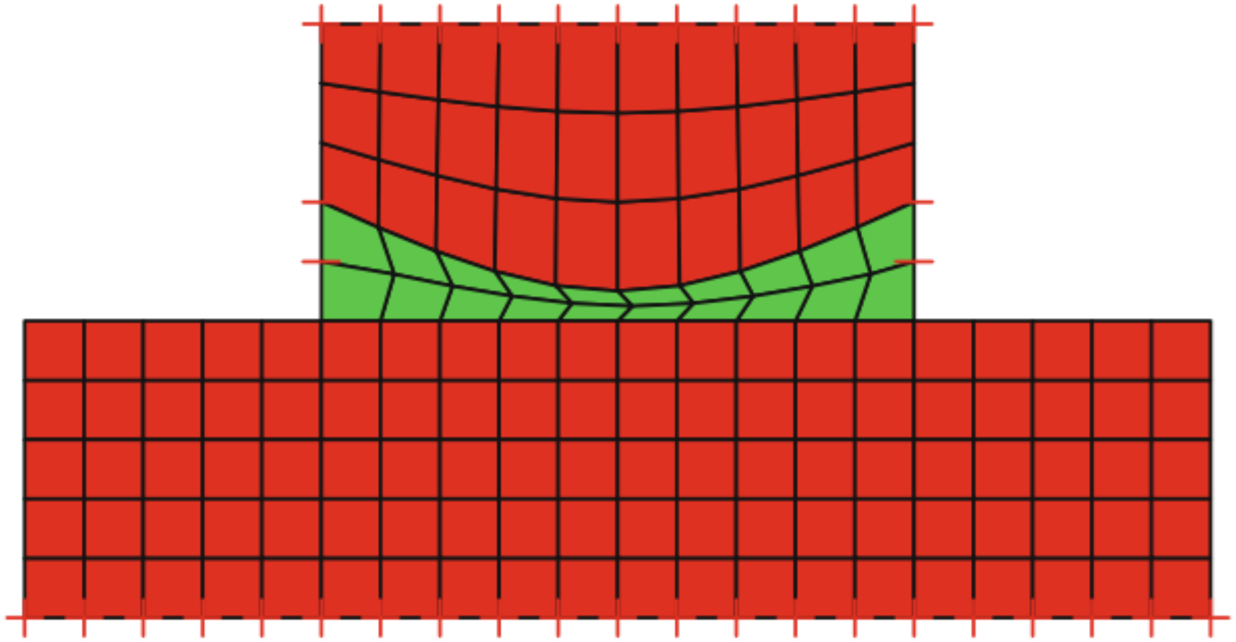

Future work: model selection (continuum, plate, beam, shell?)

Model selection

- Model with shells
- Identify “hot spots” - dual
- Couple with continuum
- Coarse-grain

- Nitsche coupling - NURBS-NURBS

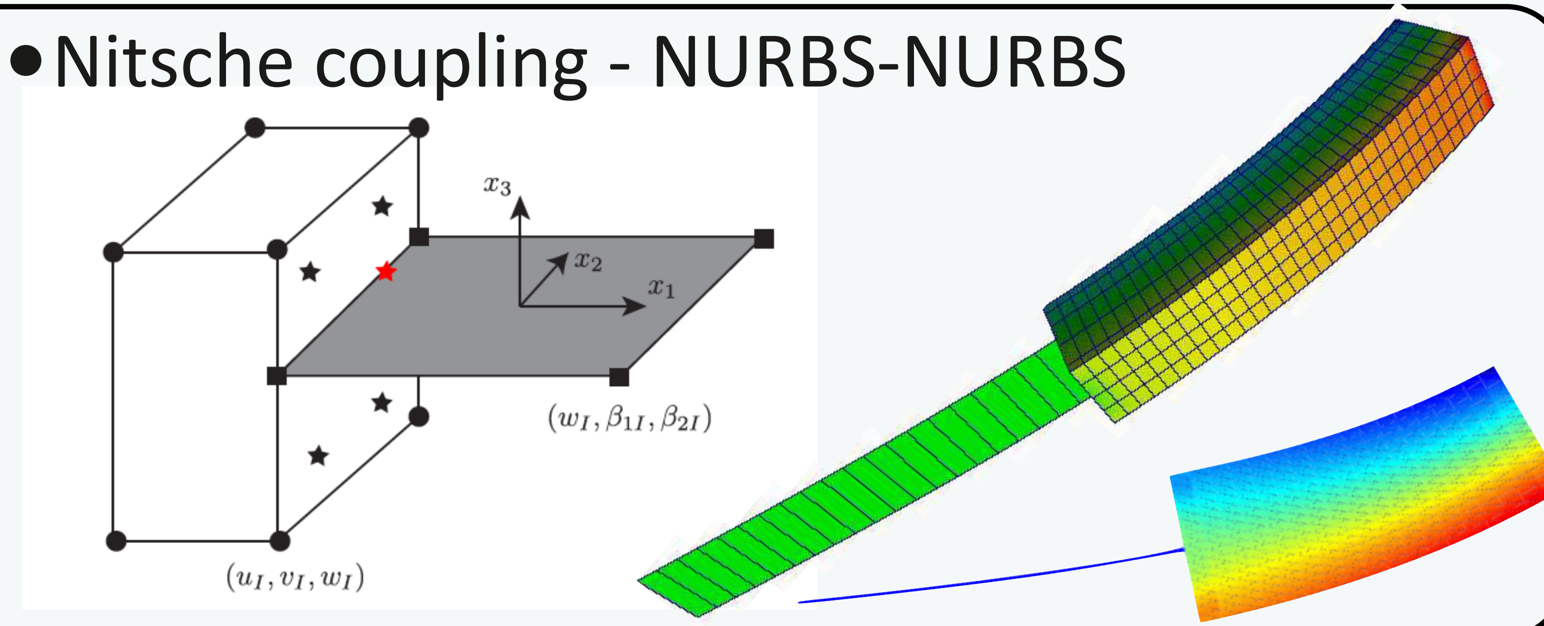

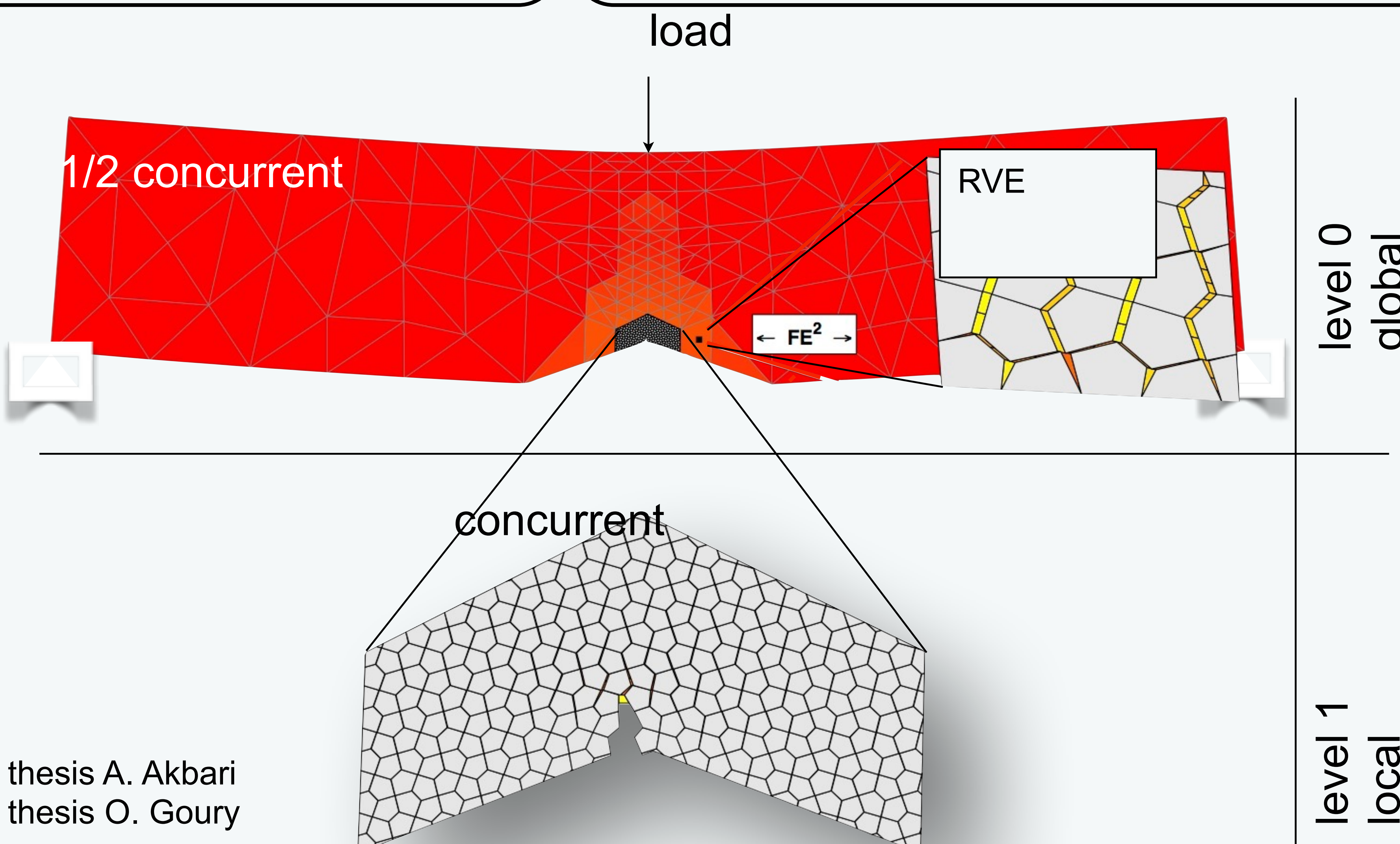

thesis A. Akbari
thesis O. Goury

Extended finite element method with smooth nodal stress for linear elastic crack growth

with Xuan Peng, PhD student

Institute of Mechanics & Advanced Materials

Double-interpolation finite element method (DFEM)

➢The construction of DFEM in 1D

Discretization

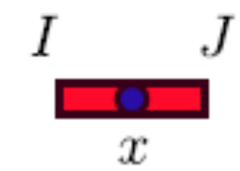

Support domain of FEM

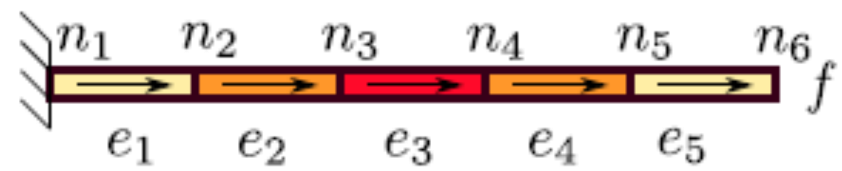

The ***first stage*** of interpolation: traditional FEM

$$u^h(x) = N_I(x_I)u^I + N_J(x_I)u^J$$

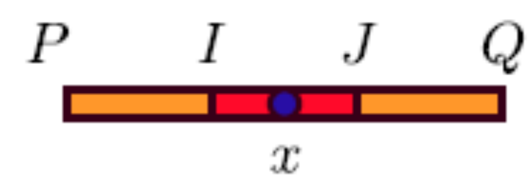

Support domain of DFEM

Provide $u, \bar{u}_{,x}$ at each node

The ***second stage*** of interpolation: reproducing from previous result

$$u^h(x) = \phi_I(x)u^I + \psi_I(x)\bar{u}^I_{,x} + \phi_J(x)u^J + \psi_J(x)\bar{u}^J_{,x}$$

$\phi_I, \psi_I, \phi_J, \psi_J$ are Hermitian basis functions

➢Calculation of average nodal derivatives

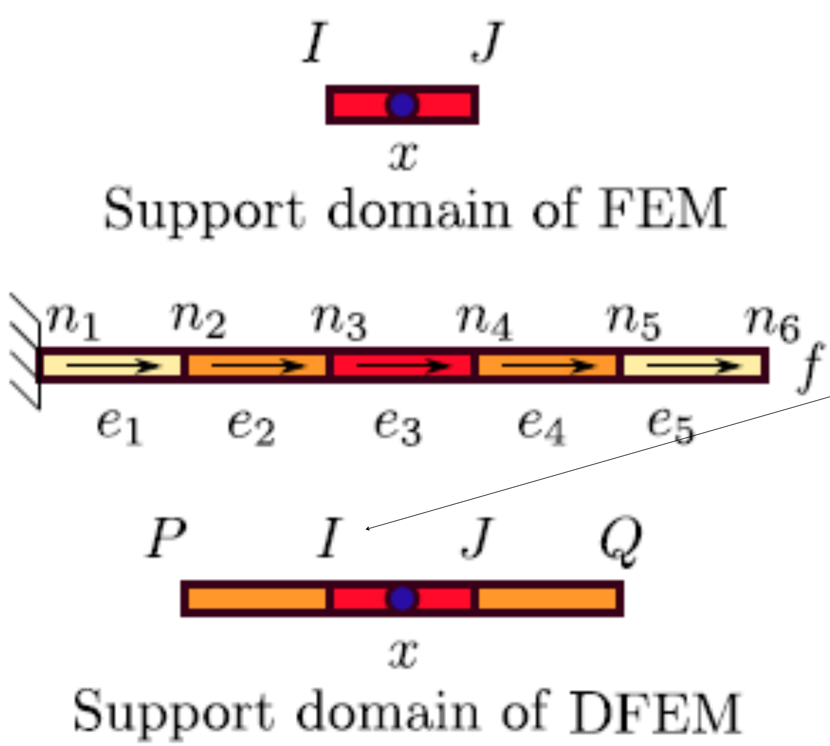

For node I, the support elements are: e_2, e_3

In element 2, we use linear Lagrange interpolation:

$$u_{,x}^{e_2}(x_I) = N_{P,x}^{e_2}(x_I)u^P + N_{I,x}^{e_2}(x_I)u^I$$

Weight function of e_2:

$$\omega_{e_{2,I}} = \frac{meas(e_{2,I})}{meas(e_{2,I}) + meas(e_{3,I})}$$

Element length

$$\bar{u}_{,x}^I = \bar{u}_{,x}(x_I) = \omega_{e_{2,I}} u_{,x}^{e_2}(x_I) + \omega_{e_{3,I}} u_{,x}^{e_3}(x_I)$$

Double-interpolation finite element method (DFEM)

The $\bar{u}^I_{,x}$ can be further rewritten as:

$$\bar{u}^I_{,x} = \left[\begin{array}{ccc} \omega_{e_{2,I}} N^{e2}_{P,x} & \omega_{e_{2,I}} N^{e2}_{I,x} + \omega_{e_{3,I}} N^{e3}_{I,x} & \omega_{e_{3,I}} N^{e3}_{J,x} \end{array} \right] \begin{bmatrix} u^P \\ u^I \\ u^J \end{bmatrix}$$

$$= \bar{N}_{P,x}(x_I)u^P + \bar{N}_{I,x}(x_I)u^I + \bar{N}_{J,x}(x_I)u^J$$

Substituting $\bar{u}^I_{,x}$ and $\bar{u}^J_{,x}$ into the second stage of interpolation leads to:

$$u^h(x) = \sum_{L \in N_S} \hat{N}_L(x) u^L$$

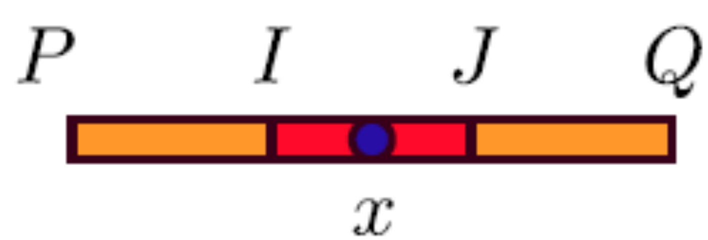

Support domain of DFEM

$$\hat{N}_L(x) = \phi_I(x) N_L(x_I) + \psi_I(x) \bar{N}_{L,x}(x_I) + \phi_J(x) N_L(x_J) + \psi_J(x) \bar{N}_{L,x}(x_J)$$

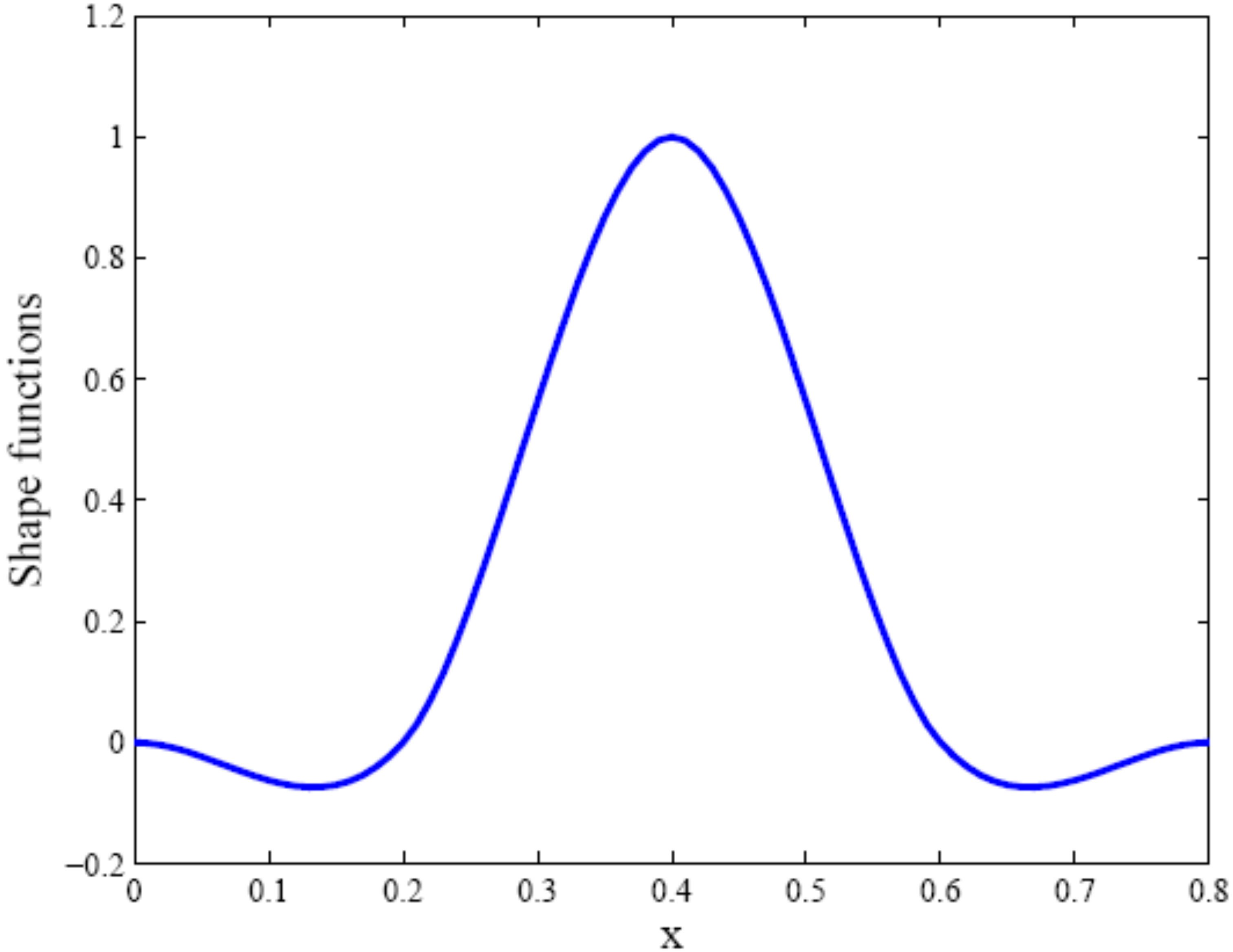

Shape function of DFEM 1D

Derivative of Shape function

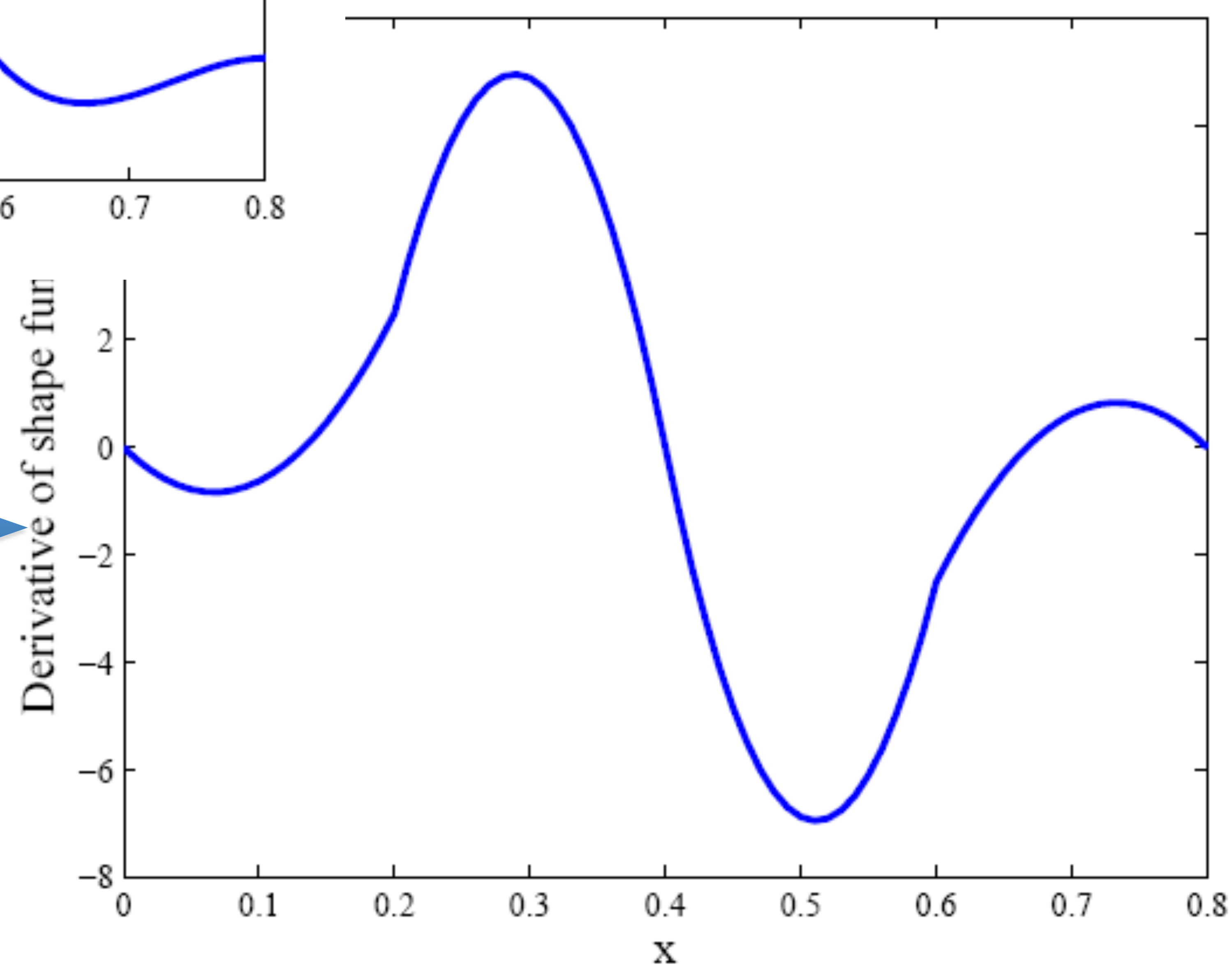

Double-interpolation finite element method (DFEM)

Same procedure for 2D ***triangular*** elements

First stage of interpolation (traditional FEM):

$$u^h(\mathbf{x}) = L_I(\mathbf{x})u^I + L_J(\mathbf{x})u^J + L_K(\mathbf{x})u^K$$

Second stage of interpolation :

$$\begin{aligned} u^h(\mathbf{x}) = &\phi_I(\mathbf{x})u^I + \psi_I(\mathbf{x})\bar{u}^I_{,x} + \varphi_I(\mathbf{x})\bar{u}^I_{,y} + \\ &\phi_J(\mathbf{x})\bar{u}^J + \psi_J(\mathbf{x})\bar{u}^J_{,x} + \varphi_J(\mathbf{x})\bar{u}^J_{,y} + \\ &\phi_K(\mathbf{x})\bar{u}^K + \psi_K(\mathbf{x})\bar{u}^K_{,x} + \varphi_K(\mathbf{x})\bar{u}^K_{,y} \end{aligned}$$

$\phi_I, \psi_I, \varphi_I, \phi_J, \psi_J, \varphi_J, \phi_K, \psi_K, \varphi_K$ are the basis functions with regard to $L_I(\mathbf{x}), L_J(\mathbf{x}), L_K(\mathbf{x})$

Calculation of Nodal derivatives:

$$\bar{N}_{L,x}(\mathbf{x}_I) = \sum_{e_{i,I} \in \Lambda_I} \omega_{e_{i,I}} N^{e_i}_{L,x}(\mathbf{x}_I)$$

$$\bar{N}_{L,y}(\mathbf{x}_I) = \sum_{e_{i,I} \in \Lambda_I} \omega_{e_{i,I}} N^{e_i}_{L,y}(\mathbf{x}_I)$$

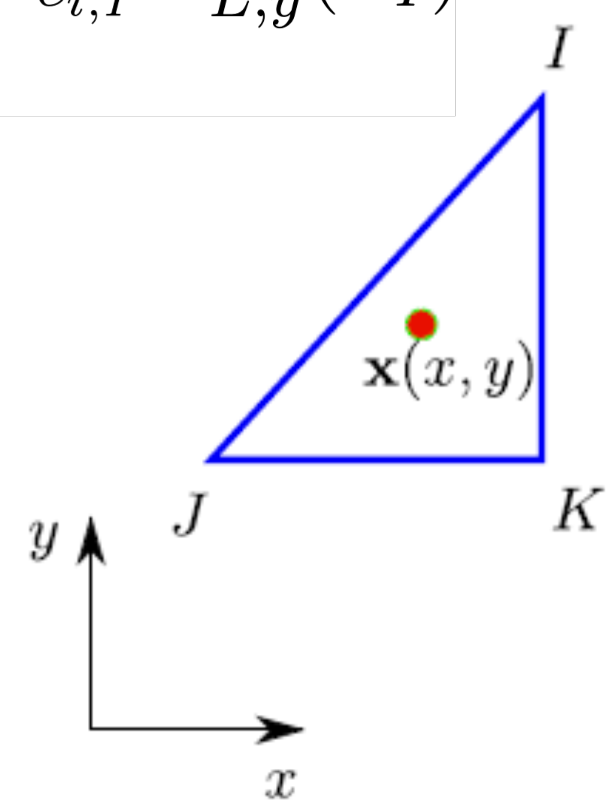

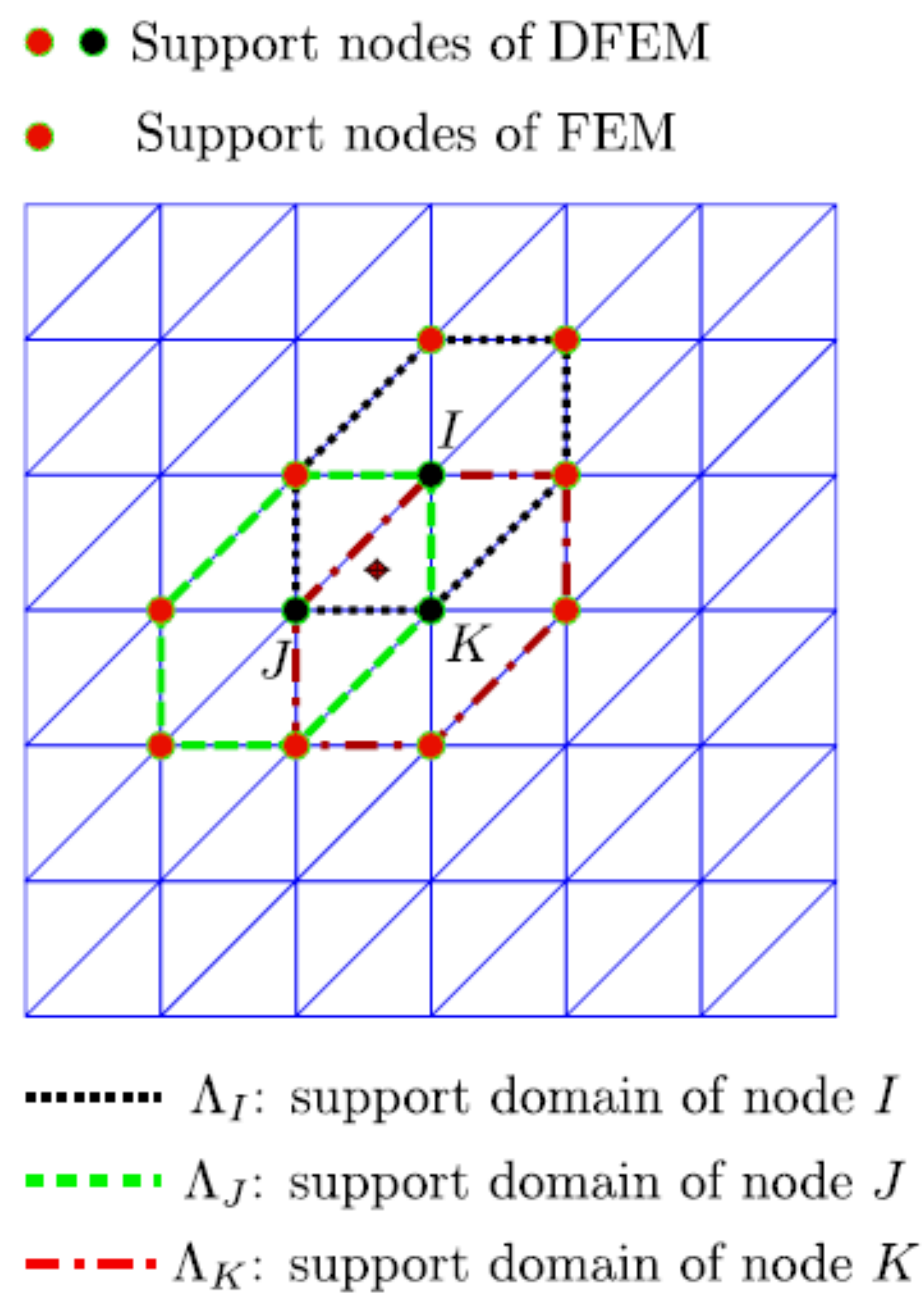

Double-interpolation finite element method (DFEM)

Calculation of weights:

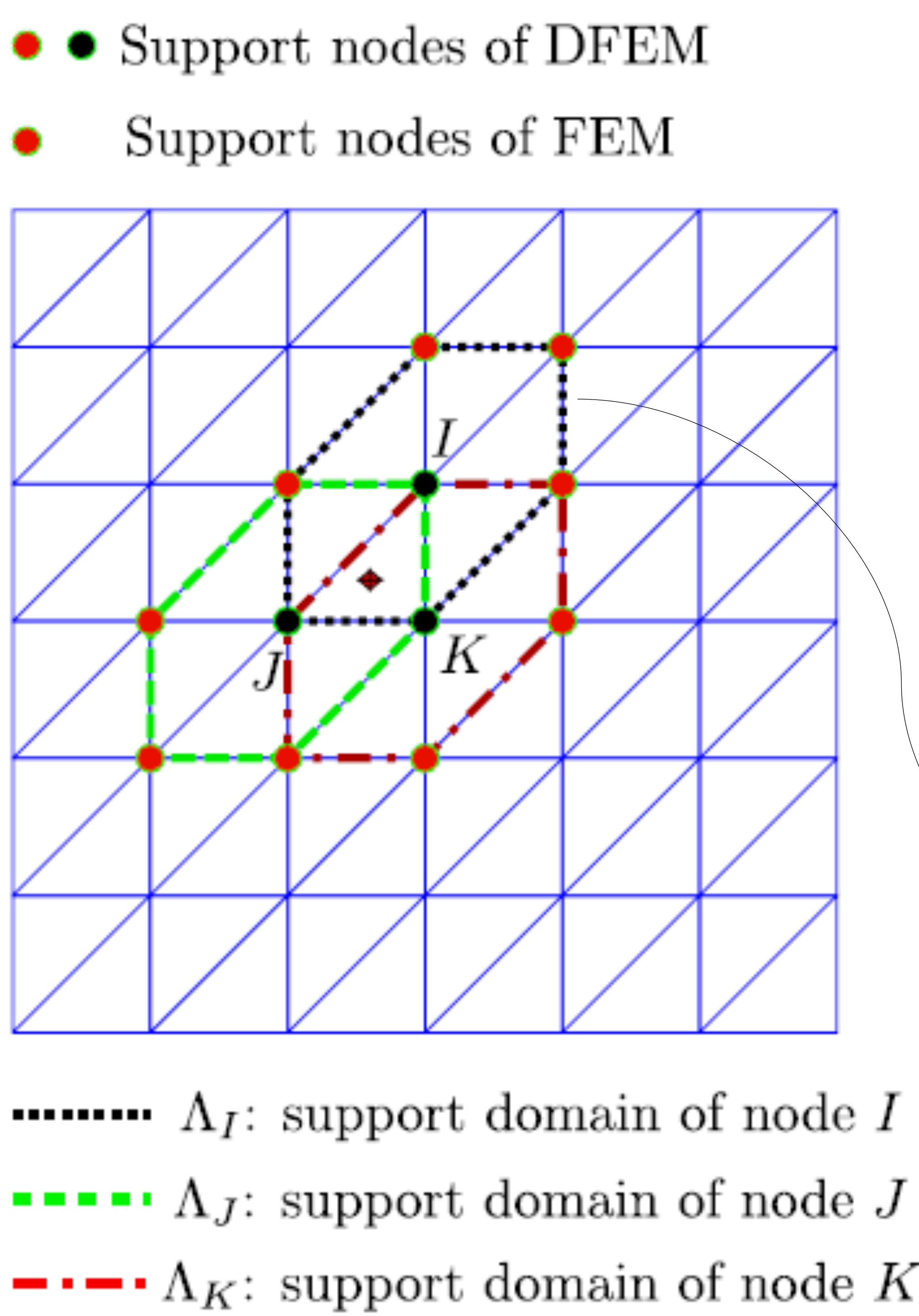

The weight of triangle *i* in support domain of *I* is:

$$\omega_{e_{i,I}} = \frac{\triangle_{e_{i,I}}}{\sum_{e_{j,I} \in \Lambda_I} \triangle_{e_{j,I}}}$$

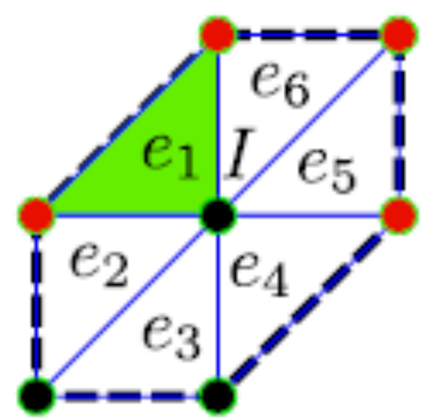

$$\omega_{e_1} = S_{e_1} / (\textstyle\sum_{e_i \in \Lambda_I} S_{e_i})$$

Double-interpolation finite element method (DFEM)

The basis functions are given as (node I):

$$\phi_I(\mathbf{x}) = L_I + L_I^2 L_J + L_I^2 L_K - L_I L_J^2 - L_I L_K^2$$

$$\psi_I(\mathbf{x}) = -c_J \left(L_K L_I^2 + \frac{1}{2} L_I L_J L_K \right) + c_K \left(L_I^2 L_J + \frac{1}{2} L_I L_J L_K \right)$$

$$\varphi_I(\mathbf{x}) = b_J \left(L_K L_I^2 + \frac{1}{2} L_I L_J L_K \right) - b_K \left(L_I^2 L_J + \frac{1}{2} L_I L_J L_K \right)$$

L_I, L_J, L_K are functions w.r.t $\mathbf{x}$

$$L_I(\mathbf{x}) = \frac{1}{2\triangle}(a_I + b_I x + c_I y)$$

Area of triangle

$$a_I = x_J y_K - x_K y_J$$
$$b_I = y_J - y_K$$
$$c_I = x_K - x_J$$

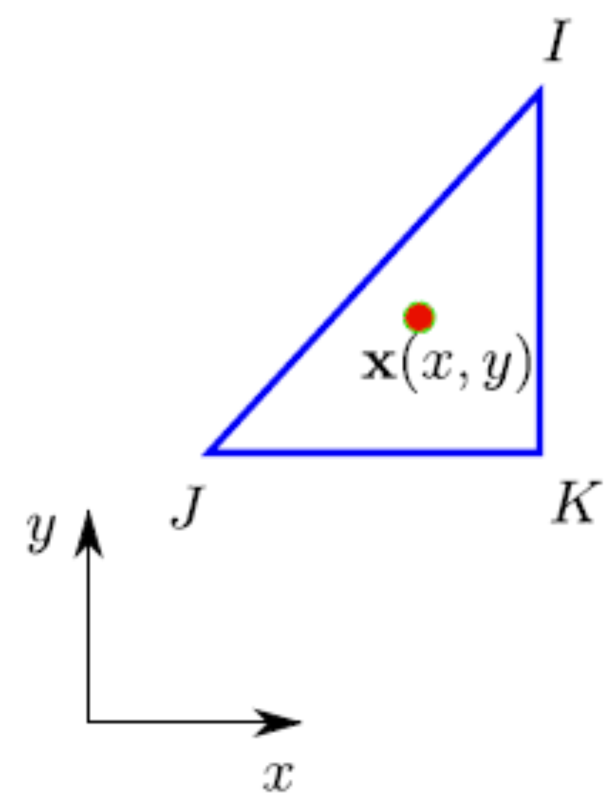

Shape functions

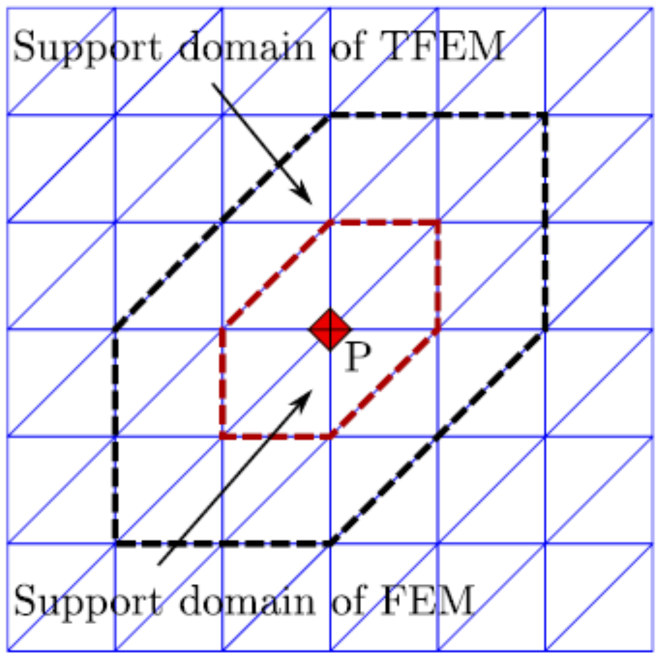

(a) Interior of the 2D domain

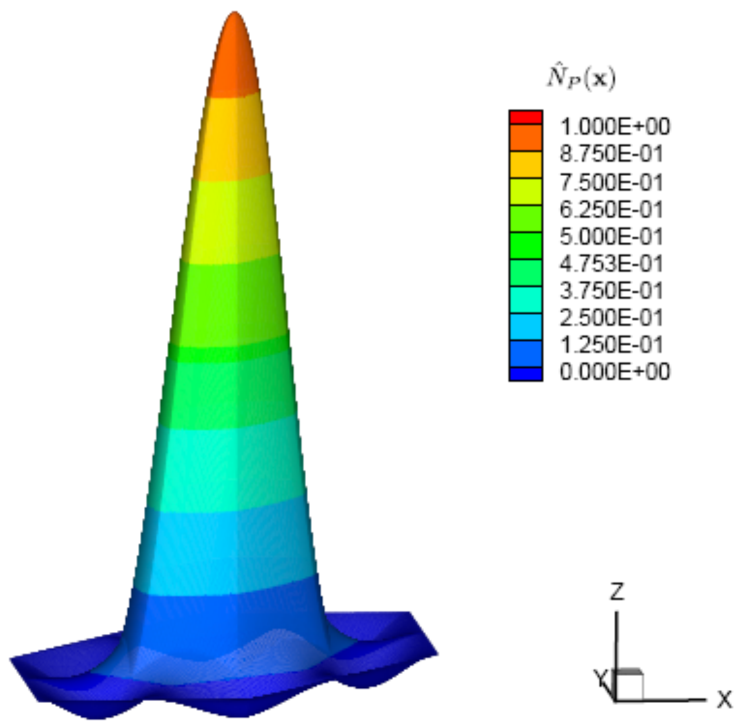

(b) 3D plot

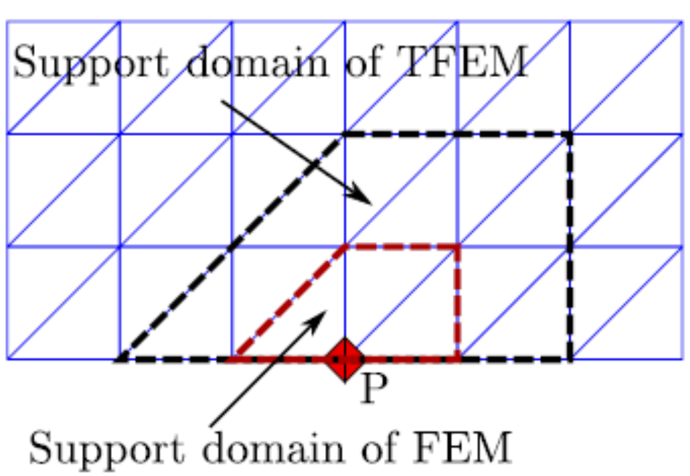

(c) Boundary of the 2D domain

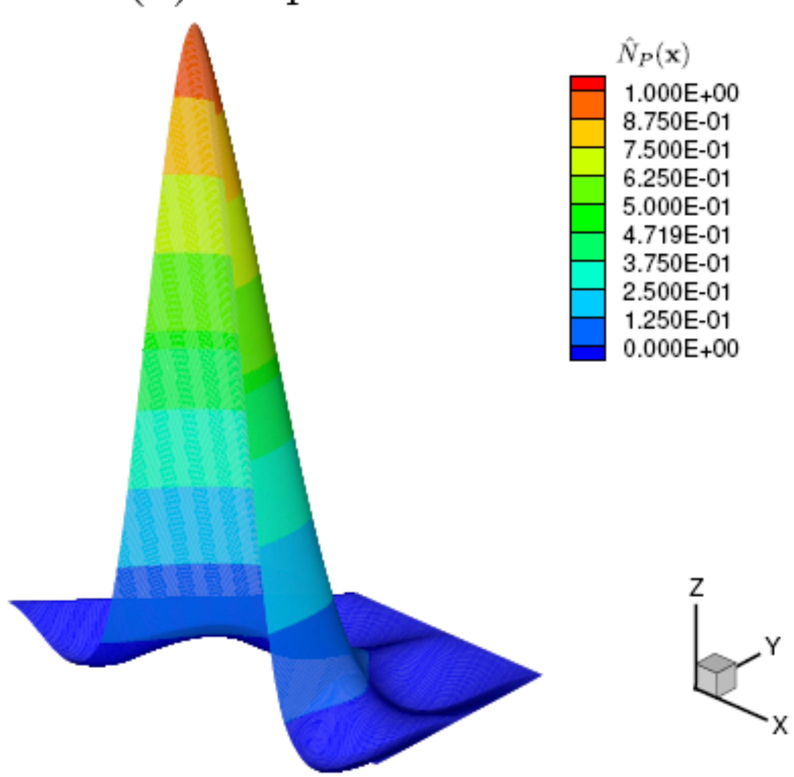

(d) 3D plot

The enriched DFEM for crack simulation

DFEM shape function

$$\mathbf{u}^h(\mathbf{x}) = \sum_{I\in\mathcal{N}_I} \hat{N}_I(\mathbf{x})\mathbf{u}^I + \sum_{J\in\mathcal{N}_J} \hat{N}_J(\mathbf{x})H(\mathbf{x})\mathbf{a}^J + \sum_{K\in\mathcal{N}_K} \hat{N}_K(\mathbf{x})\sum_{\alpha=1}^{4} f_\alpha(\mathbf{x})\mathbf{b}^{K\alpha}$$

$$\{f_\alpha(r,\theta), \alpha = 1,4\} = \left\{\sqrt{r}\sin\frac{\theta}{2}, \sqrt{r}\cos\frac{\theta}{2}, \sqrt{r}\sin\frac{\theta}{2}\sin\theta, \sqrt{r}\cos\frac{\theta}{2}\sin\theta\right\}$$

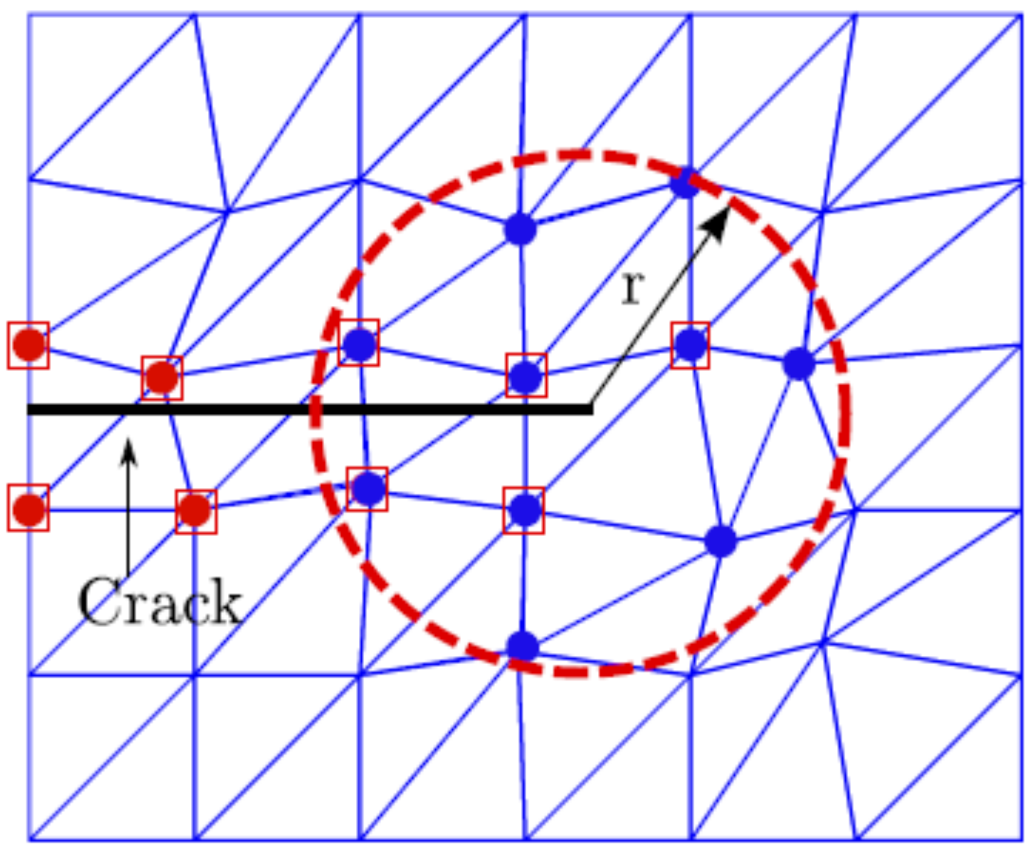

● Crack tip enriched node

● Heaviside enriched node

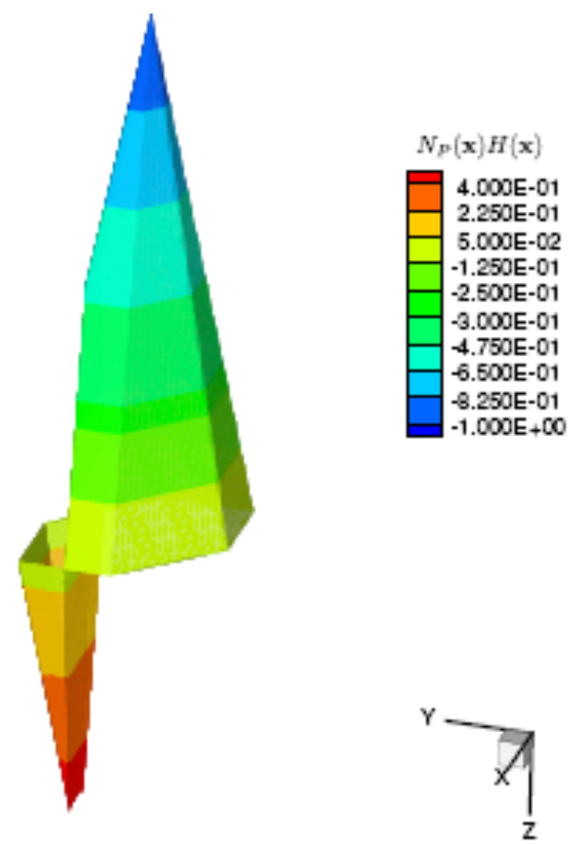

(d) XFEM

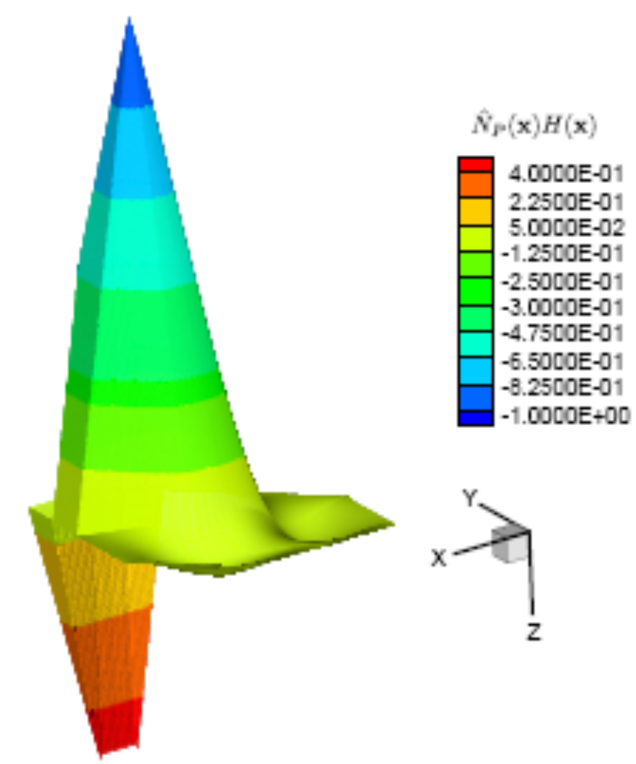

(b) XDFEM

Numerical example of 1D bar

Problem definition:

$$EA\frac{\mathrm{d}^2u}{\mathrm{d}x^2}+f=0$$

$$u|_{x=0}=0$$

Analytical solutions:

$$u(x)=\frac{fL^2}{EA}\left(\frac{x}{L}-\frac{1}{2}\left(\frac{x}{L}\right)^2\right)$$

$$\sigma(x)=\frac{fL}{A}\left(1-\frac{x}{L}\right)$$

E: Young's Modulus

A: Area of cross section

L:Length

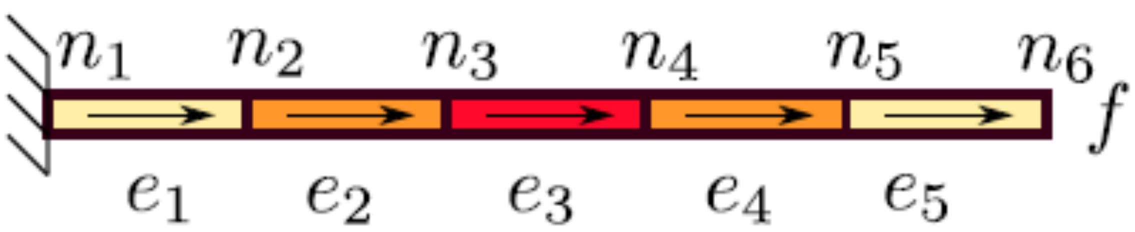

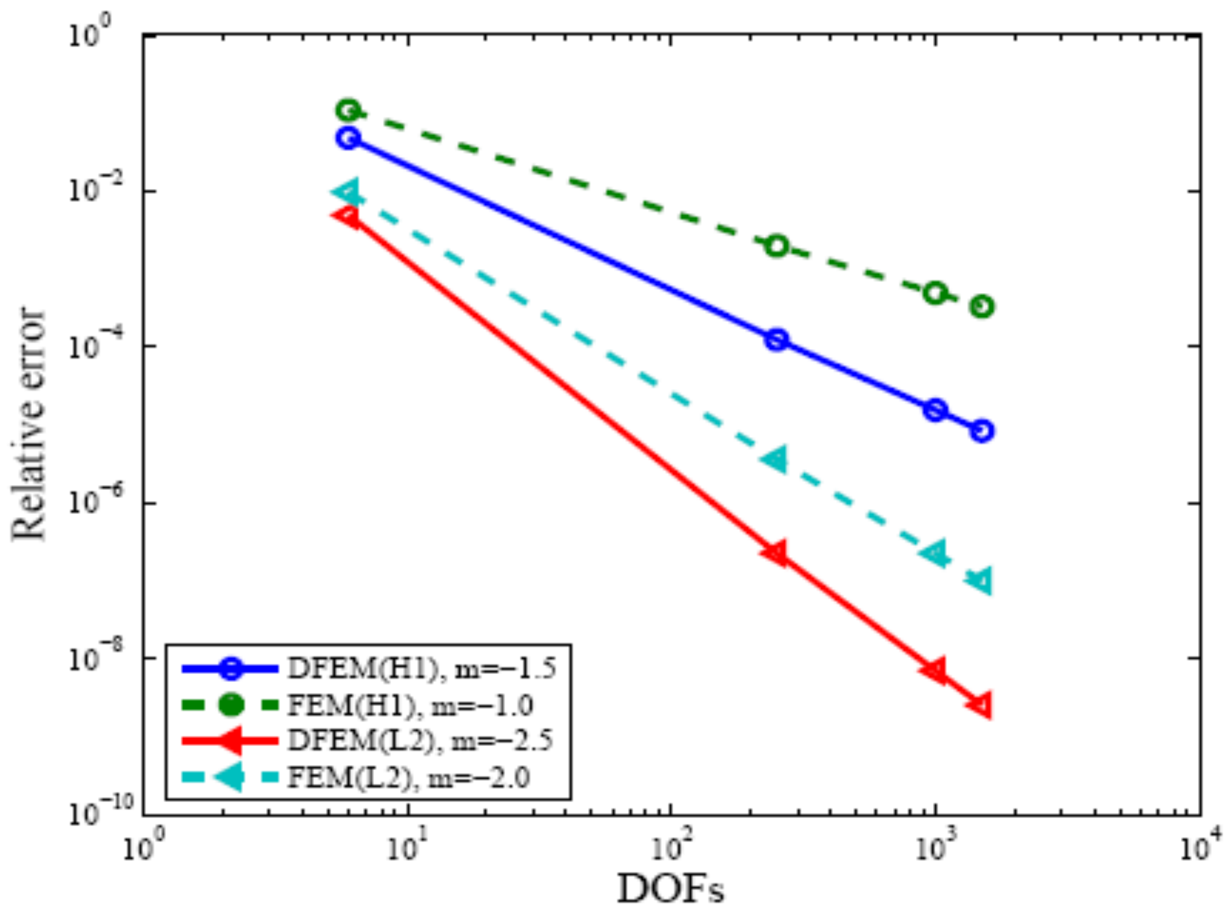

Displacement(L2) and energy(H1) norm

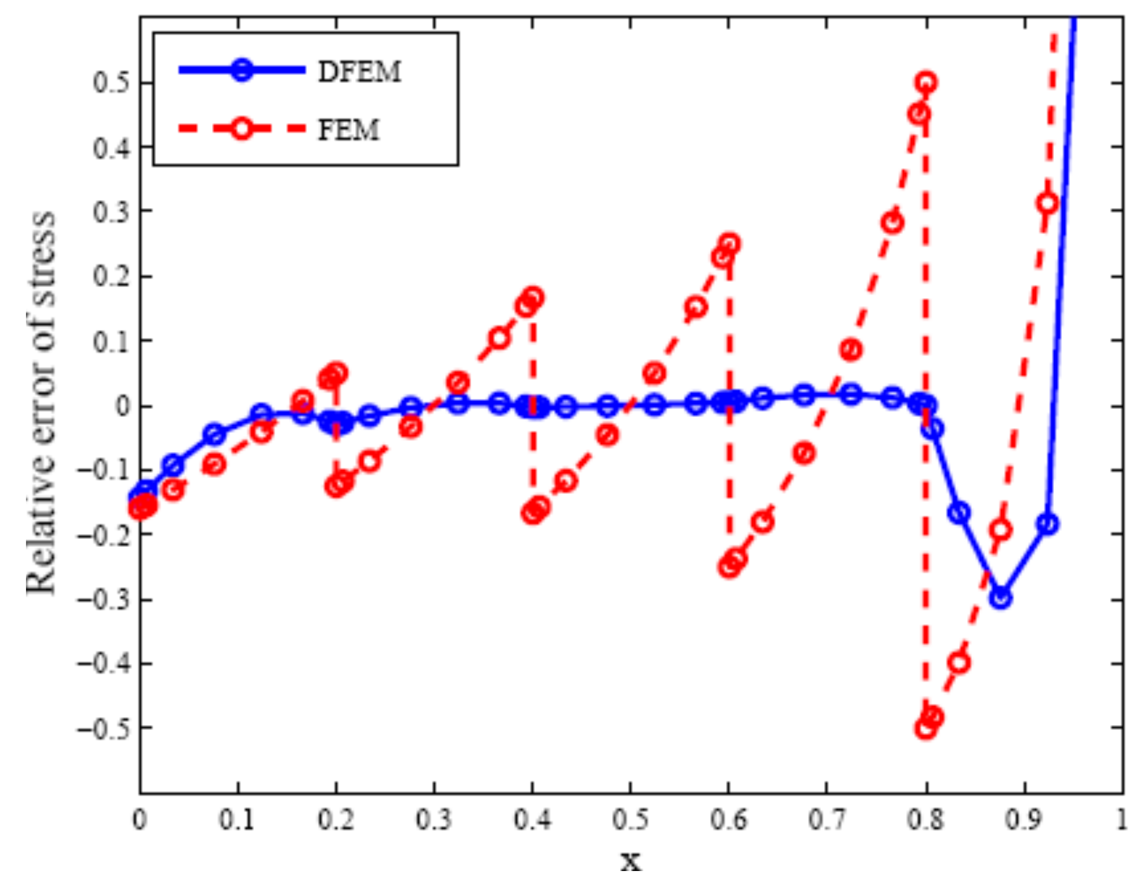

Relative error of stress distribution

Numerical example of Cantilever beam

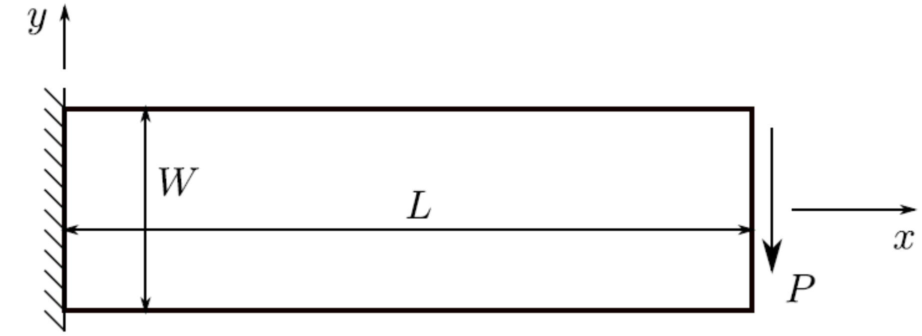

Analytical solutions

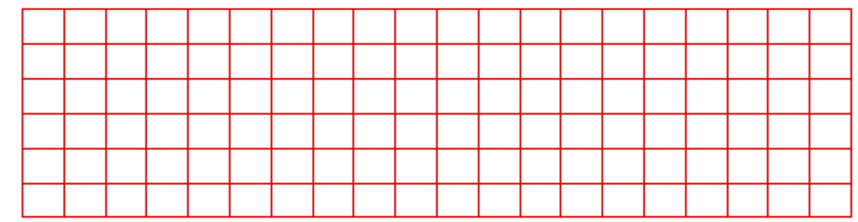

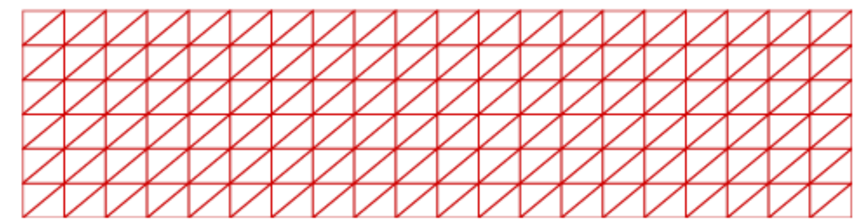

$$u_x(x,y) = \frac{Py}{6EI}\left[(6L-3x)x + (2+\nu)(y^2 - \frac{W^2}{4})\right]$$

$$u_y(x,y) = -\frac{P}{6EI}\left[3\nu y^2(L-x) + (4+5\nu)\frac{W^2 x}{4} + (3L-x)x\right.$$

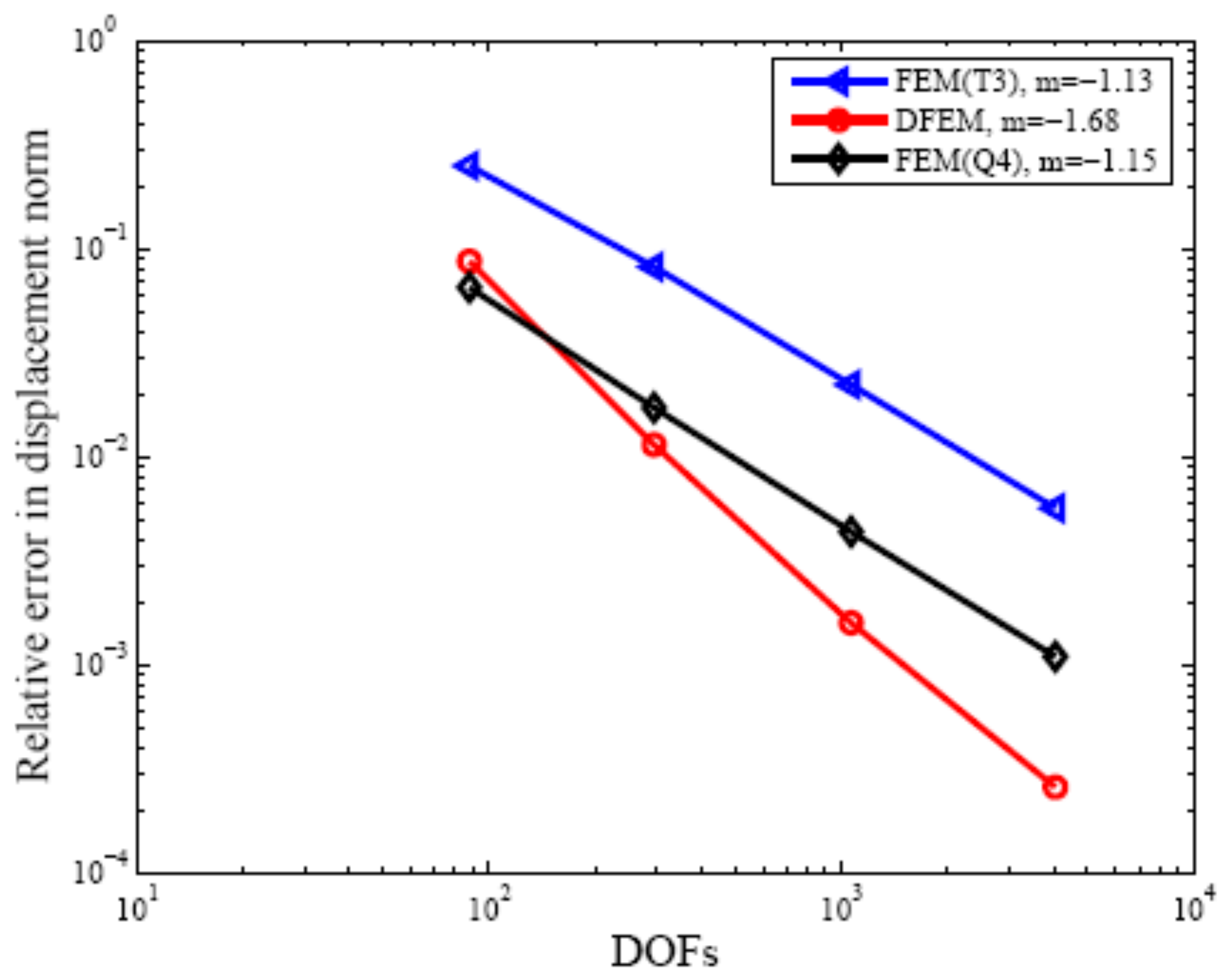

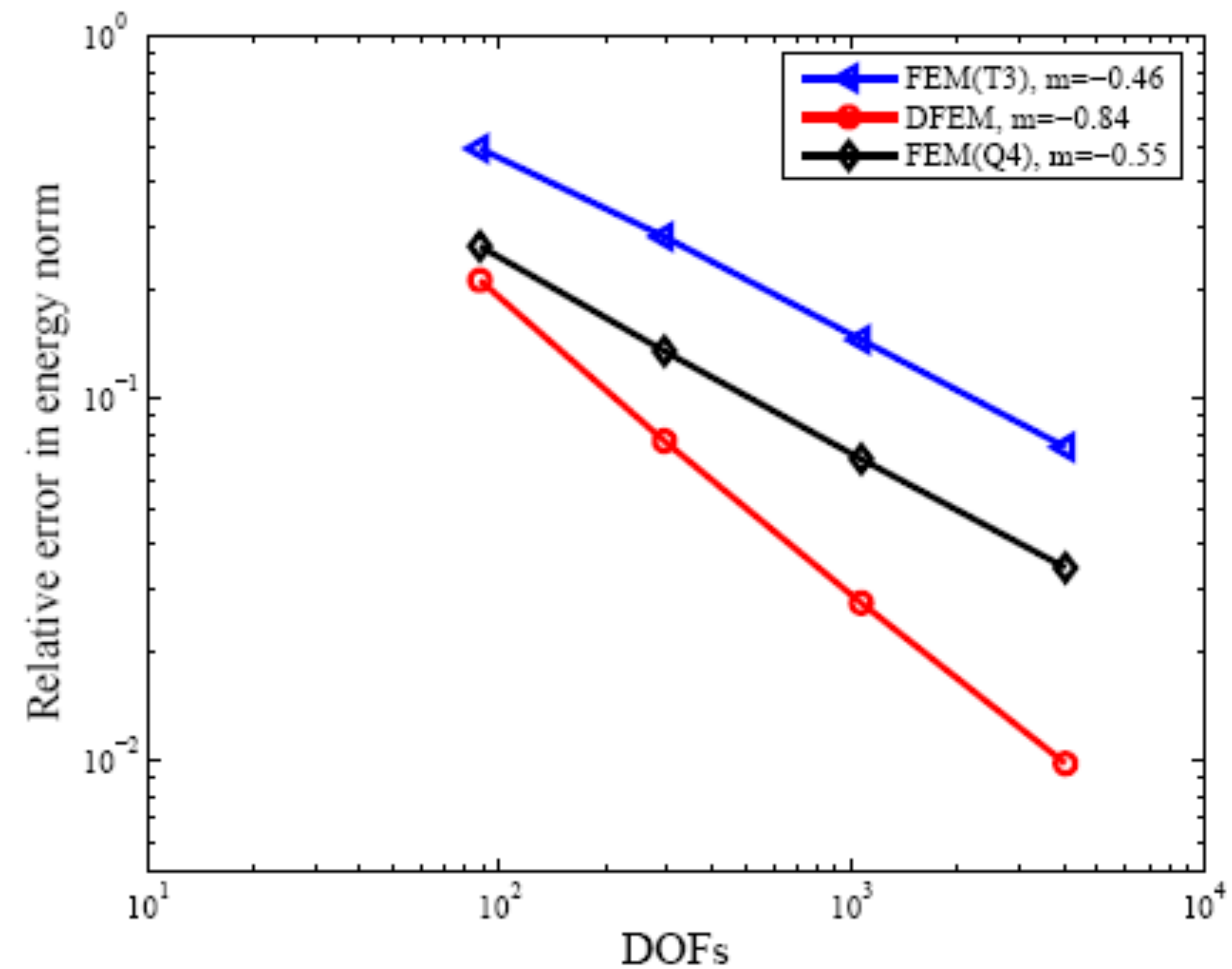

Numerical example of Cantilever beam

Mode-I crack results:

a) explicit crack (FEM);
b) only Heaviside enrichment;
c) full enrichment

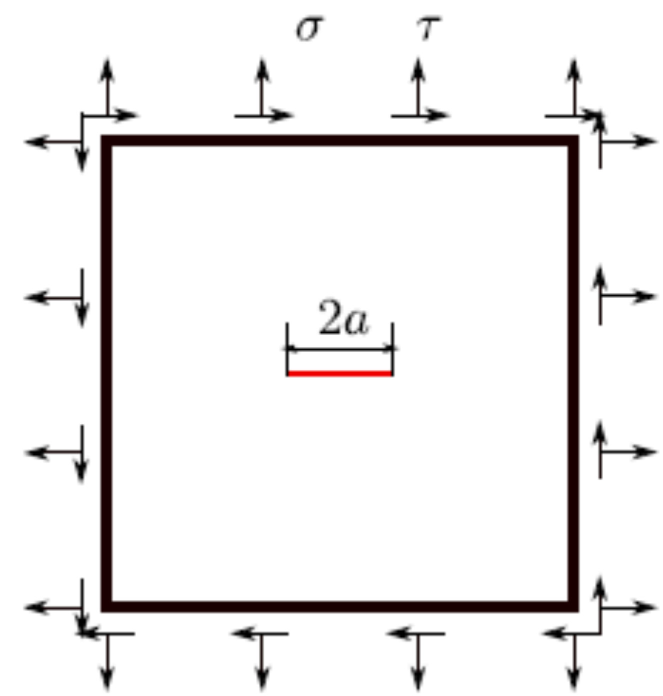

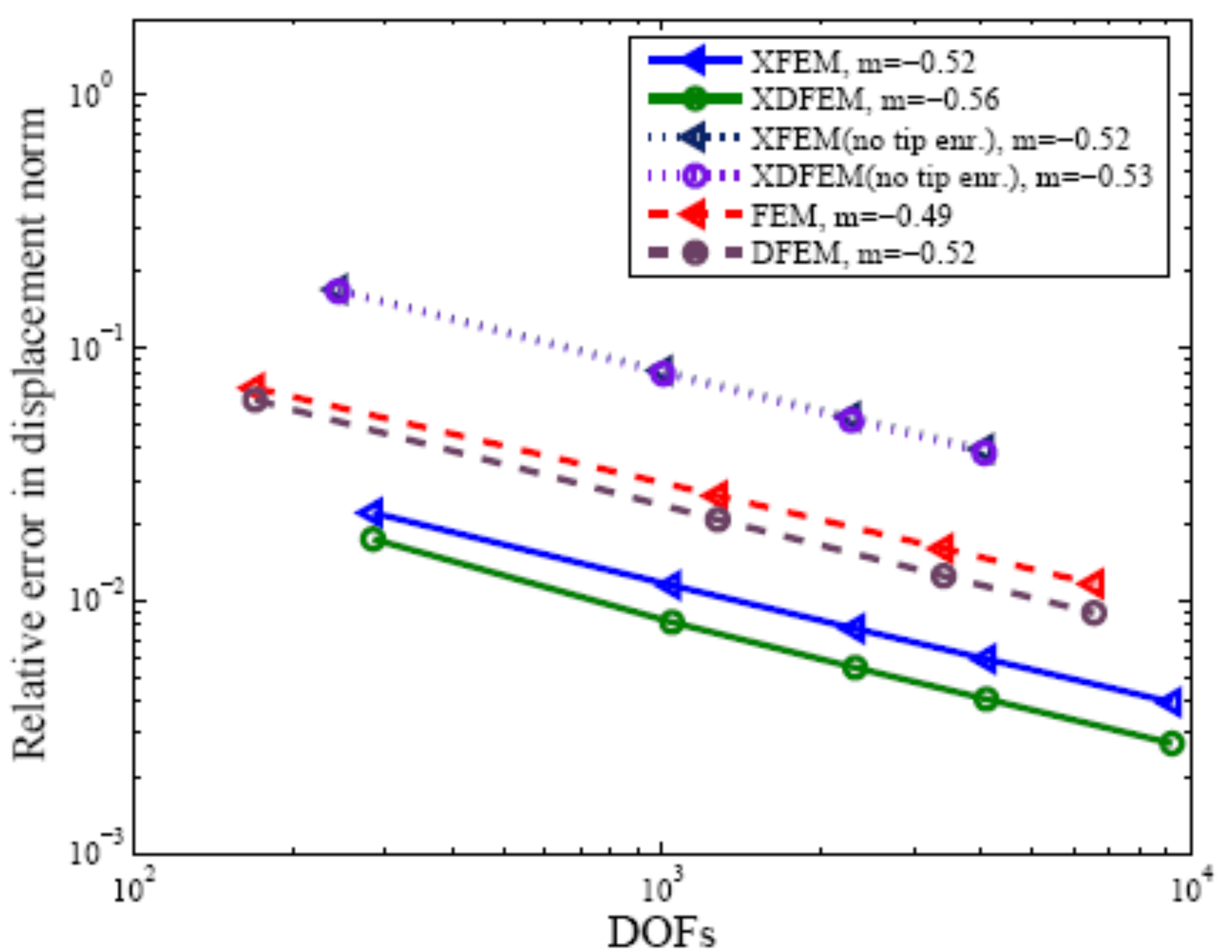

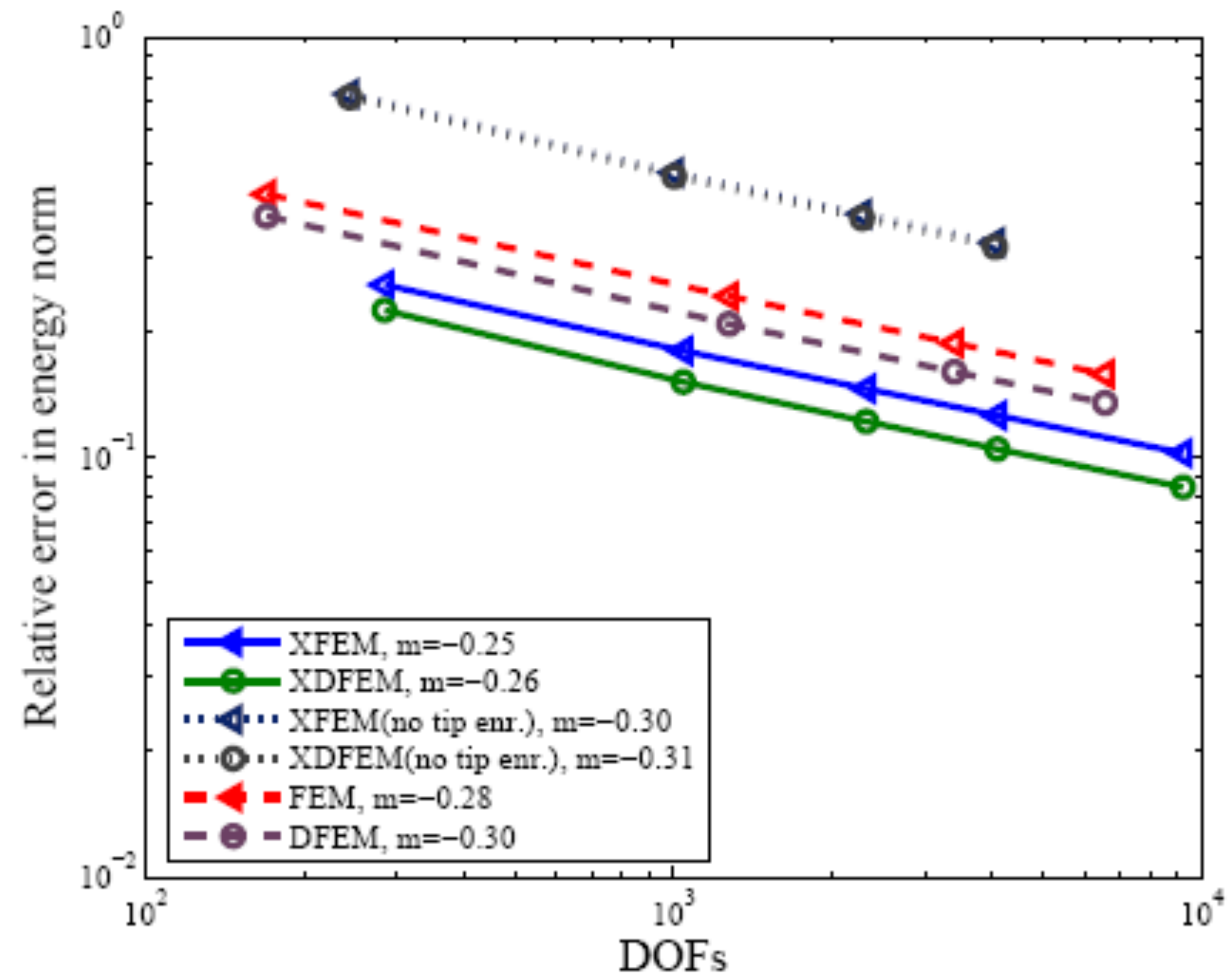

Numerical example of crack propagation

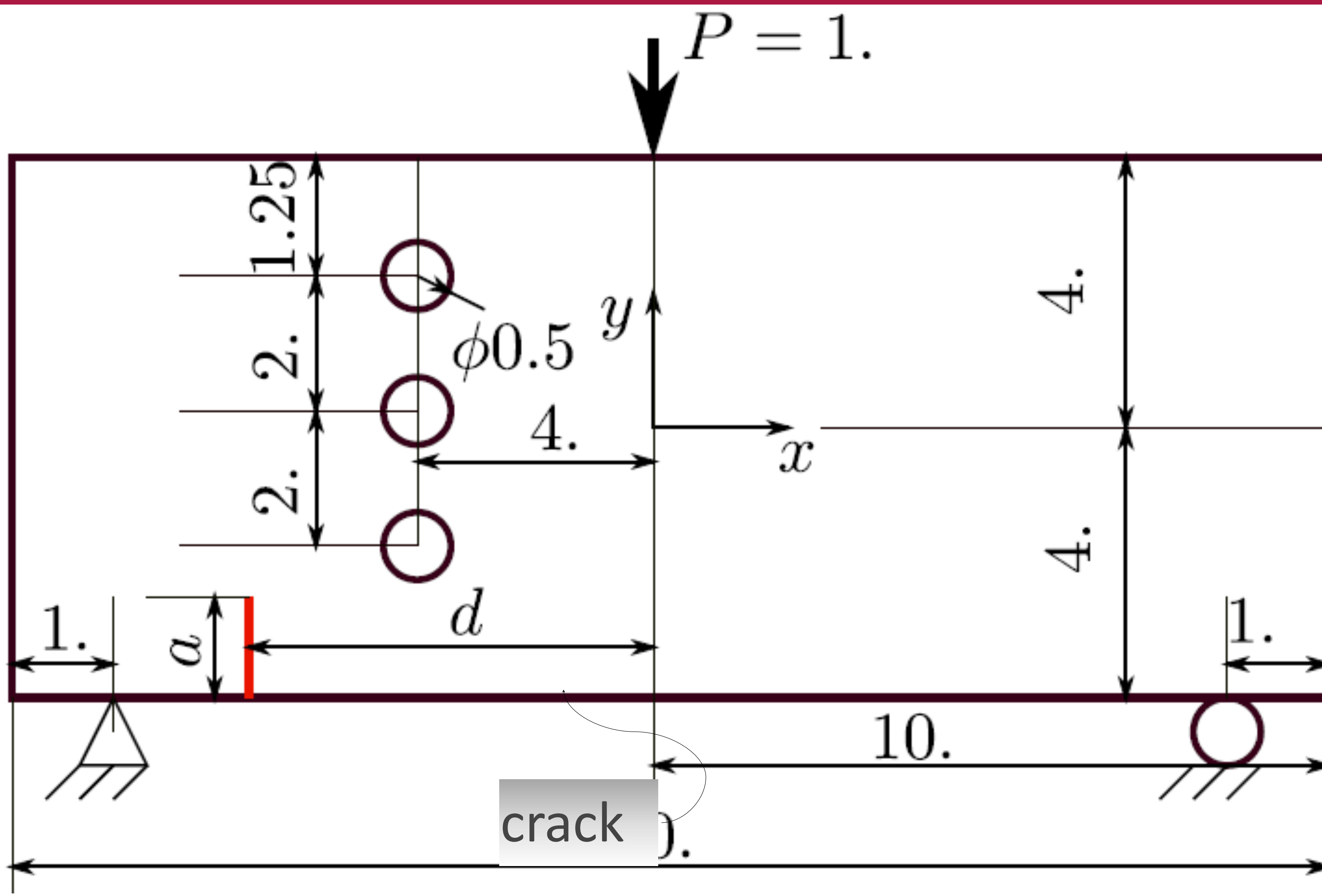

	d	a	crack increment	number of propagation
case 1	5	1.5	0.052	67
case 2	6	1.0	0.060	69
case 3	6	2.5	0.048	97

Numerical example of crack propagation

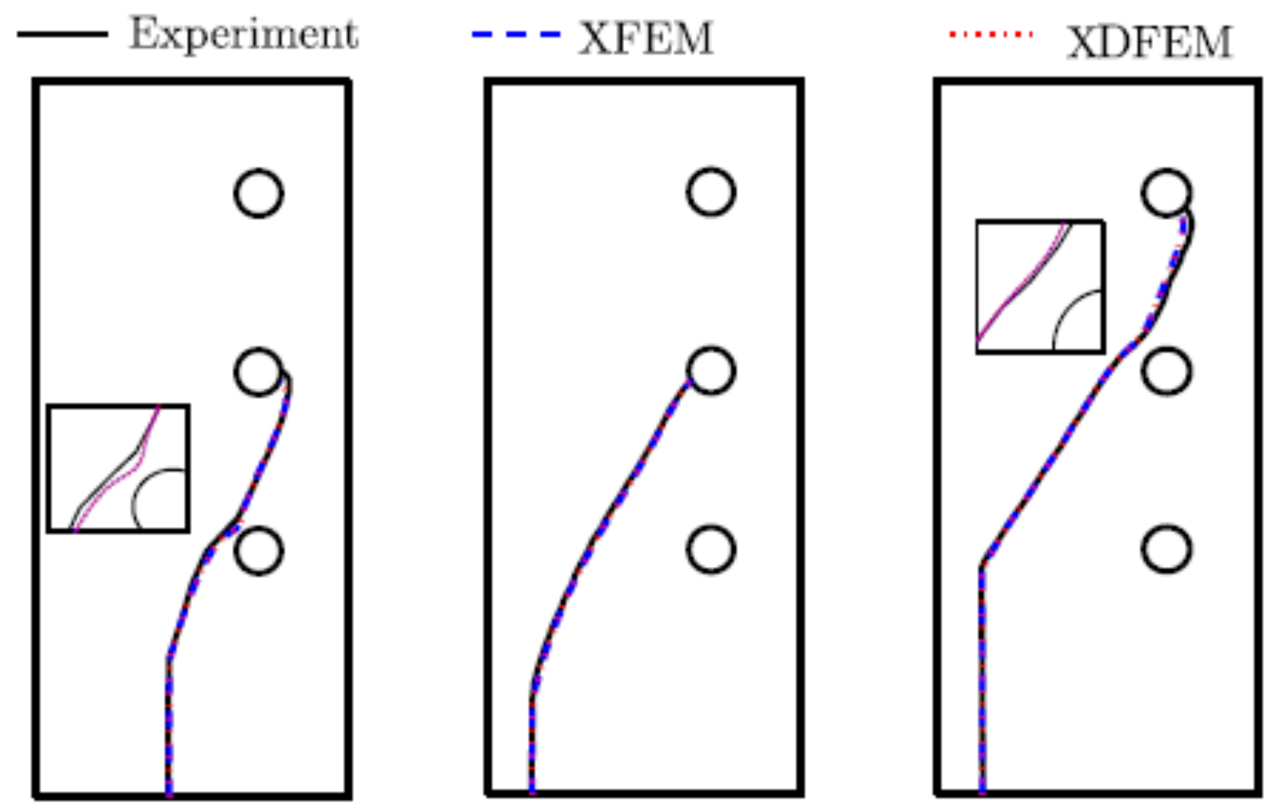

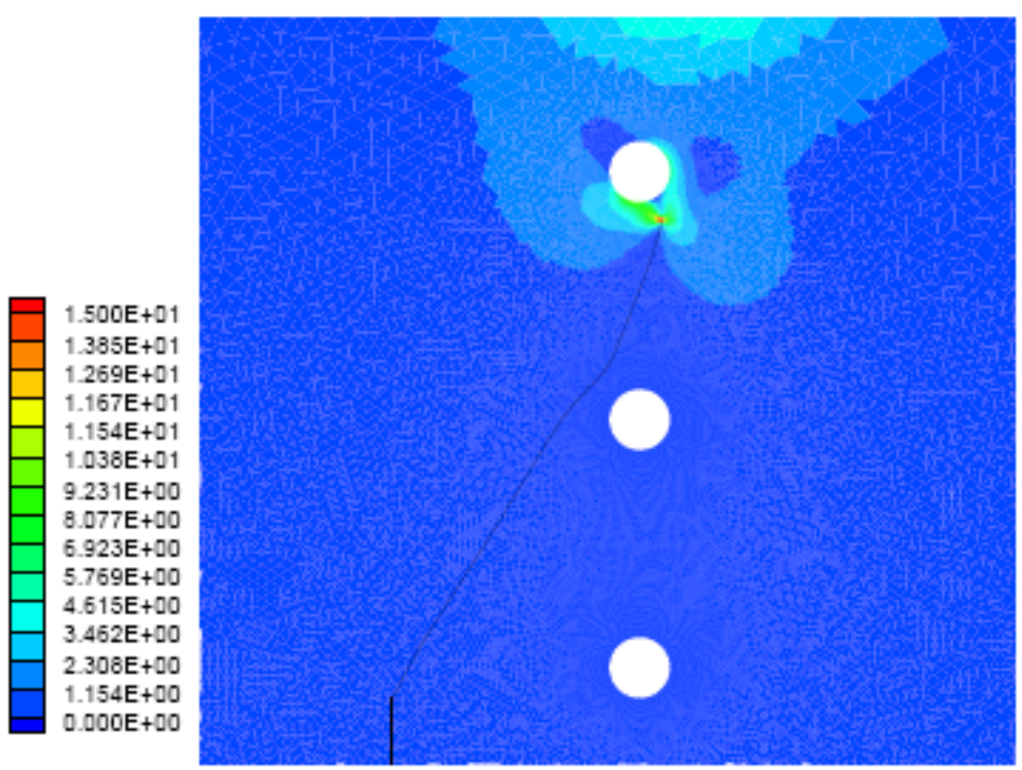

(c) XFEM, the 94th step

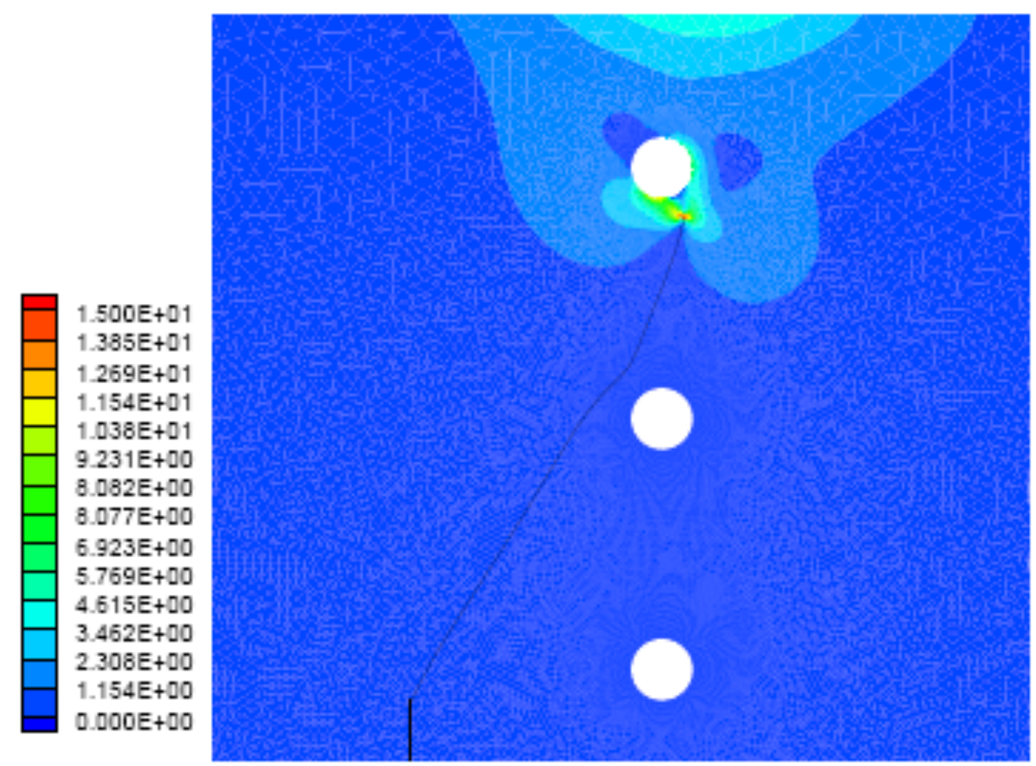

(d) XDFEM, the 94th step

Conclusions

- ✓Superconvergence in elasticity problems
- ✓Higher accuracy than XFEM in fracture problems
- ✓Consistent with XFEM in terms of crack evolution
- ✓Smooth nodal stress without post-processing

References

- Moës, N., Dolbow, J., & Belytschko, T. (1999). A finite element method for crack growth without remeshing. *IJNME*, *46*(1), 131–150.
- Melenk, J. M., & Babuška, I. (1996). The partition of unity finite element method: Basic theory and applications. *CMAME*, *139*(1-4), 289–314.
- Laborde, P., Pommier, J., Renard, Y., & Salaün, M. (2005). High-order extended finite element method for cracked domains. *IJNME*, *64*(3), 354–381.
- Wu, S. C., Zhang, W. H., Peng, X., & Miao, B. R. (2012). A twice-interpolation finite element method (TFEM) for crack propagation problems. IJCM, *09*(04), 1250055.
- Peng, X., Kulasegaram, S., Bordas, S. P.A., Wu, S. C. (2013). An extended finite element method with smooth nodal stress. http://arxiv.org/abs/1306.0536

Stabilised generalised/extended FEM

with Daniel Paladim, Marie Curie Fellow

Problem: In XFEM/GFEM, the enrichment function is not correctly reproduced in the elements that have enriched and non-enriched nodes (blending).

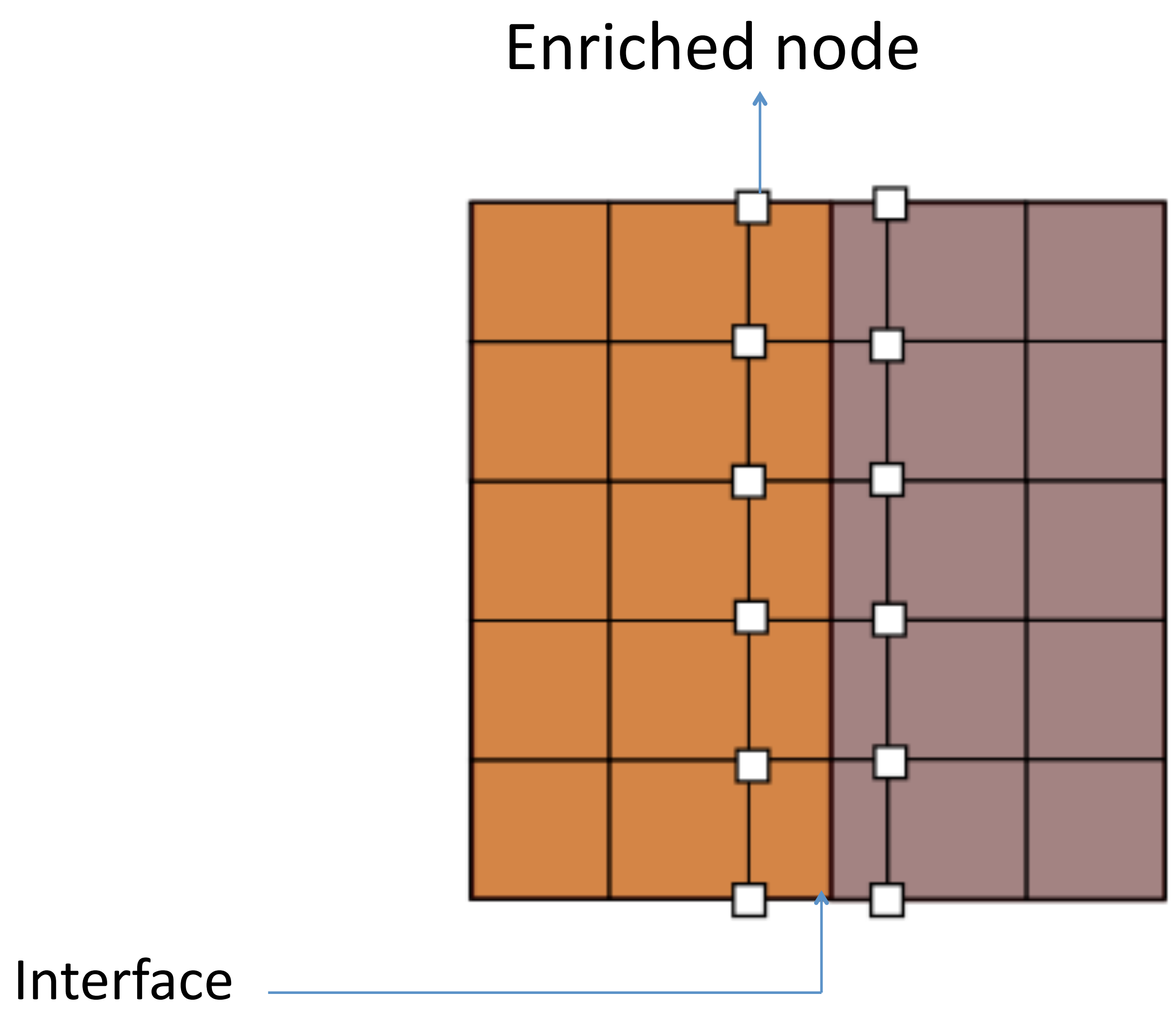

Solution: Corrected-XFEM by Fries (2008). Corrected XFEM, substitutes f(x) by R(x)f(x), where R(x) is the ramp function. A continuous function whose value is 1 in the enriched elements, 0 in the non-enriched elements and it varies continuously between 0 and 1.

Ramp function

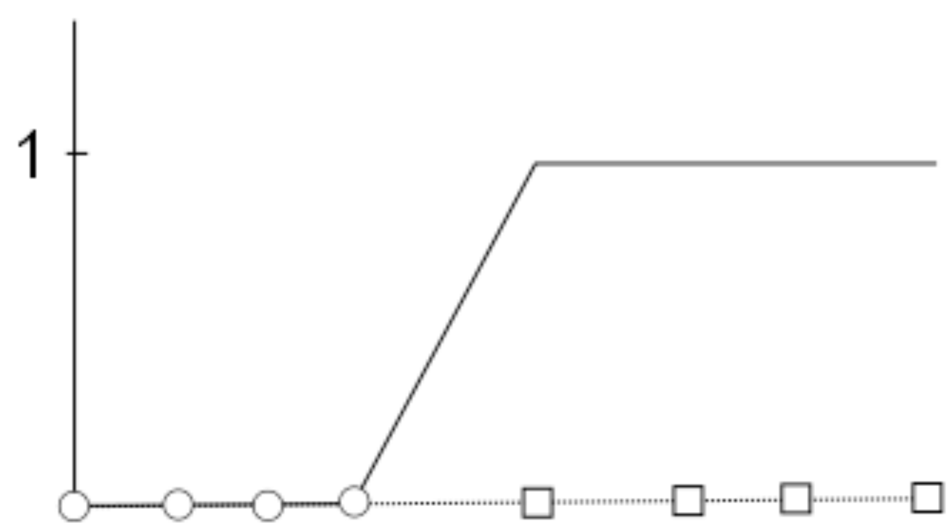

○ Non-enriched nodes

□ Enriched nodes

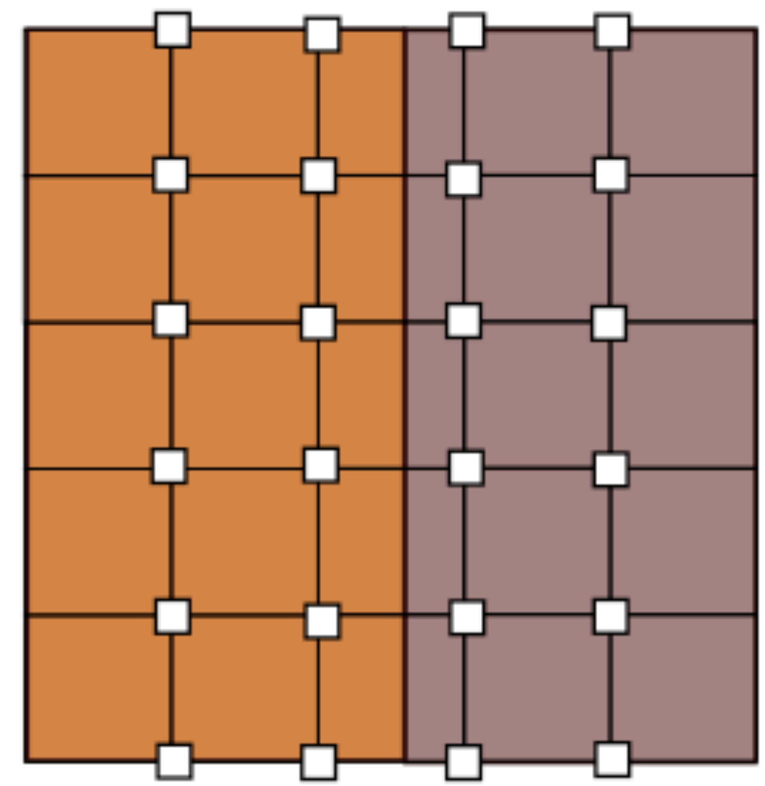

More solutions

•Suppressing blending elements by coupling enriched and standard regions. *Laborde et al. (2005) Gracie et al(2008)*

•Hierarchical shape functions in blending elements. *Chessa et al (2003) Tarancón et al. (2009)*

•Assumed strain blending elements. *Chessa et al. (2003) Gracie et al.*

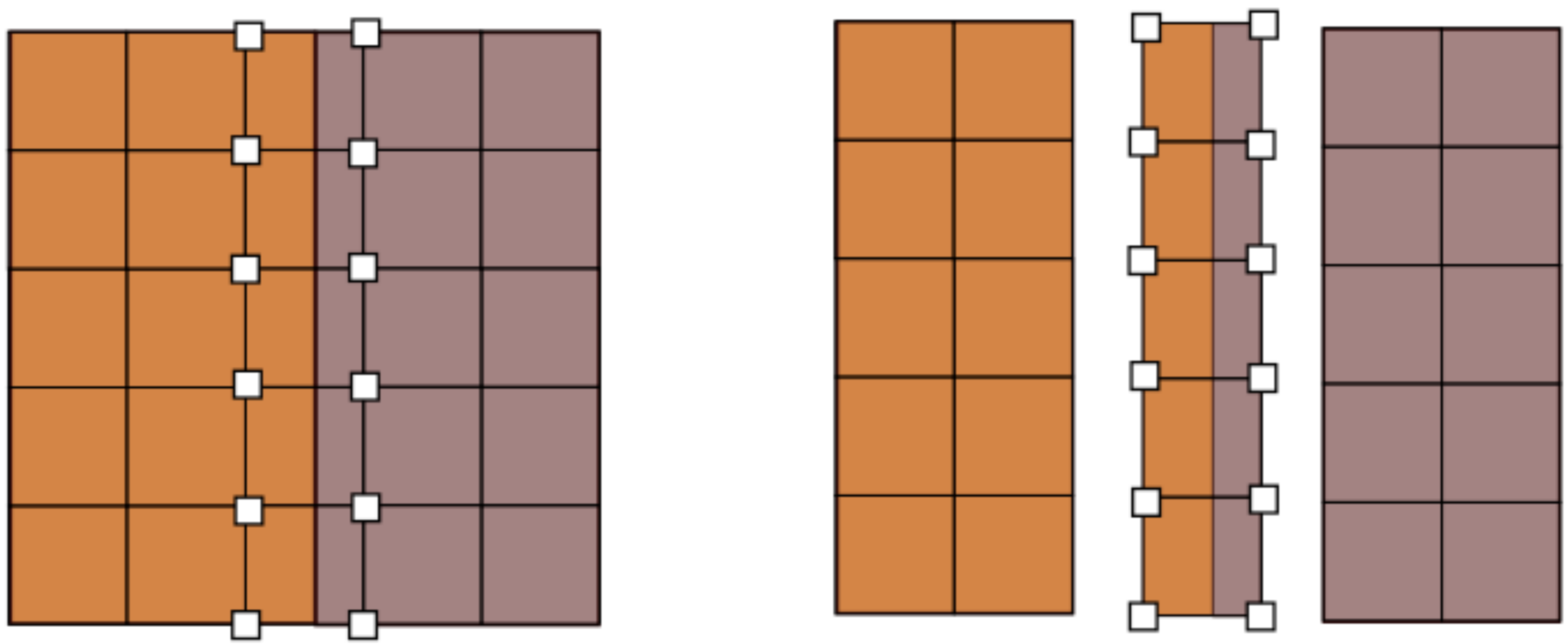

Another solution: Stable GFEM by Babuška and Banerjee (2012).

In SGFEM, the enrichment function f(x) is substituted by the following function $f(x)-\Sigma N_i(x)f(x_i)$. It is to say f minus its nodal interpolation.

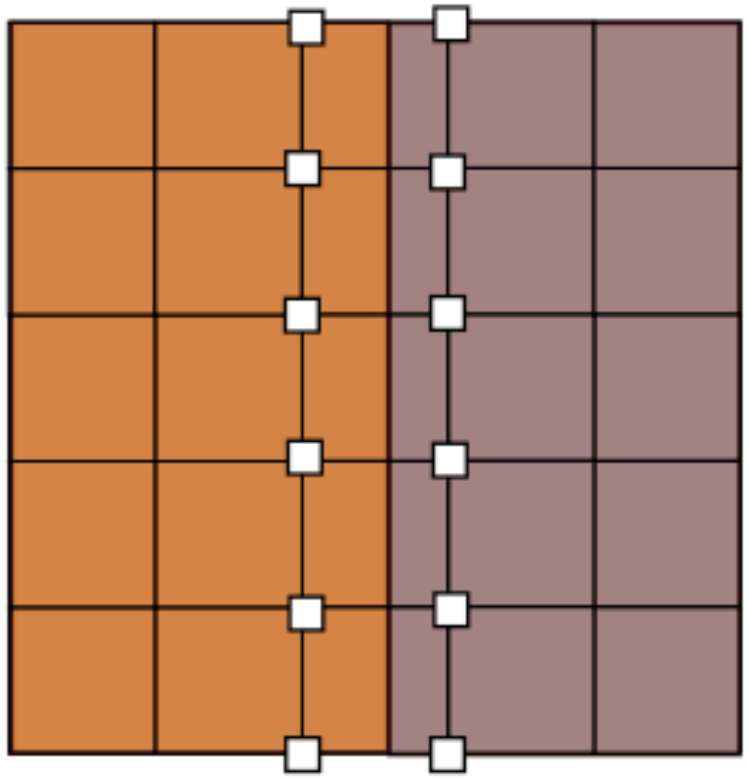

In the case that $f(x)=|\phi(x)|$, where ϕ is the level set of the interface we are trying to represent, we obtain the function introduced by Moës in 2003.

Problem: The stiffness matrix of GFEM/XFEM could be ill-conditioned. This is usually the case when the interface is very close to a node.

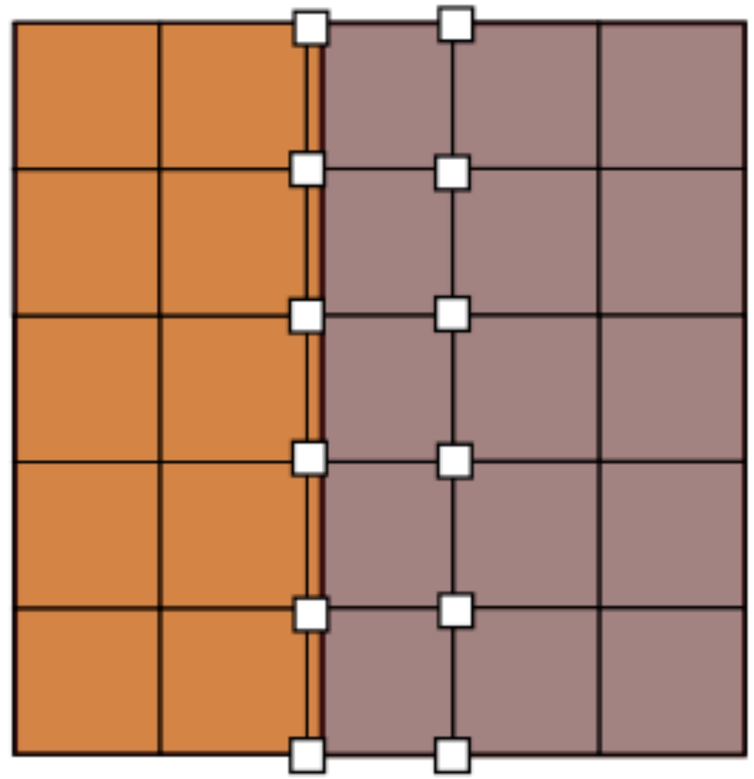

- Ill-conditioning reduces the accuracy when direct solvers are used (due to round-off errors).
- In iterative solvers, more iterations are required to bring the error

Solution: A preconditioner. Menk and Bordas (2011) proposed a preconditioner for GFEM/XFEM.

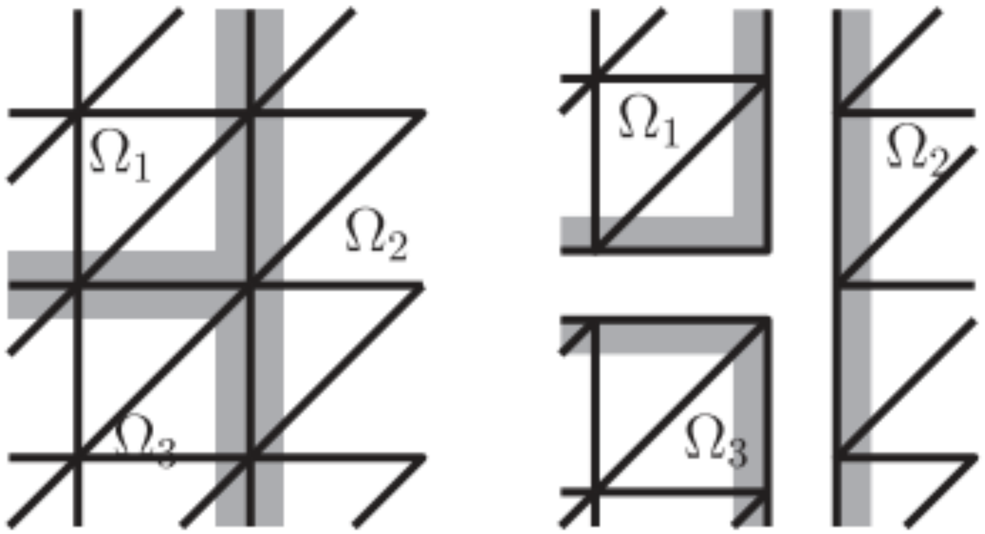

Standard DOFs

Enriched DOFs

$$\boldsymbol{K} = \begin{bmatrix} \boldsymbol{K}_{\mathrm{FEM,FEM}} & \boldsymbol{K}_{X,\mathrm{FEM}} \\ \boldsymbol{K}_{\mathrm{FEM},X} & \boldsymbol{K}_{X,X} \end{bmatrix}$$

$$\boldsymbol{P} = \begin{bmatrix} \boldsymbol{P}_{\mathrm{FEM}} & \boldsymbol{0} & \\ \boldsymbol{0} & \boldsymbol{P}_X & \boldsymbol{0} \\ & \boldsymbol{0} & \boldsymbol{L}^{-1} \end{bmatrix}$$

- Very robust to interfaces passing close to nodes.
- Can be parallelized.
- Not very easy to implement. Tuning is needed.

Basic idea The domain is divided only for the enriched DOFs.

$$\boldsymbol{K} = \begin{bmatrix} \boldsymbol{K}_{\mathrm{FEM,FEM}} & \boldsymbol{K}_{X,\mathrm{FEM}} \\ \boldsymbol{K}_{\mathrm{FEM},X} & \boldsymbol{K}_{X,X} \end{bmatrix}$$

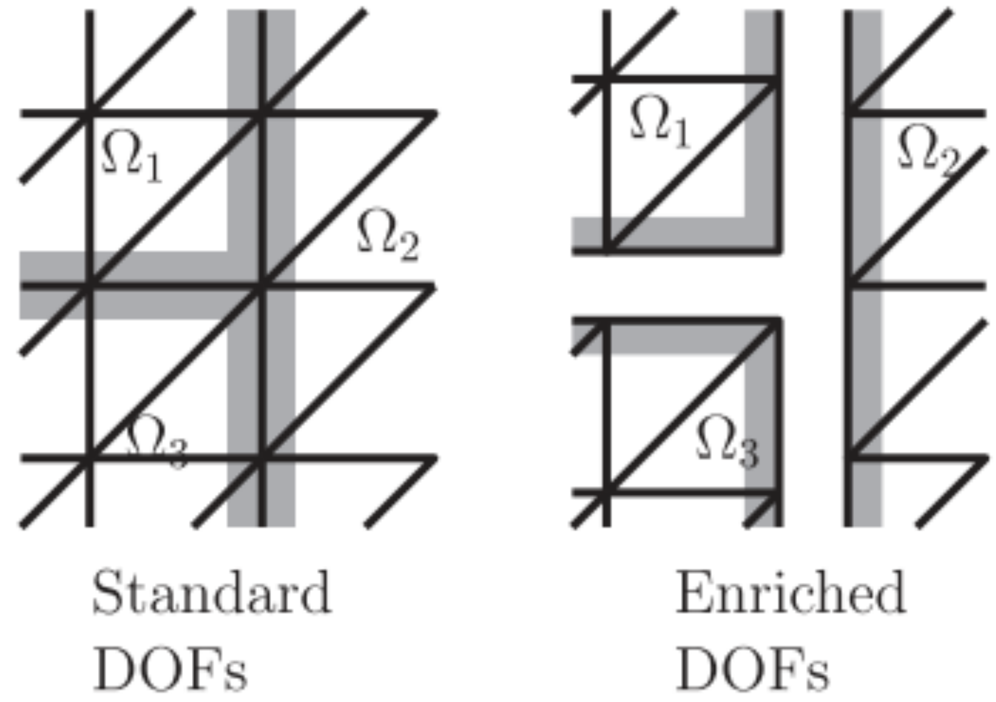

$$\boldsymbol{K} = \begin{bmatrix} \boldsymbol{K}_{\mathrm{FEM,FEM}} & \boldsymbol{K}_{X,\mathrm{FEM}} & \boldsymbol{0} \\ \boldsymbol{K}_{\mathrm{FEM},X} & \boldsymbol{K}_{X,X} & \boldsymbol{B}^{\mathrm{T}} \\ \boldsymbol{0} & \boldsymbol{B} & \boldsymbol{0} \end{bmatrix}$$

$$\boldsymbol{P} = \begin{bmatrix} \boldsymbol{P}_{\mathrm{FEM}} & \boldsymbol{0} & \\ \boldsymbol{0} & \boldsymbol{P}_X & \boldsymbol{0} \\ & \boldsymbol{0} & \boldsymbol{L}^{-1} \end{bmatrix}$$

$$\boldsymbol{P}_X = \begin{bmatrix} \boldsymbol{C}_1^{-1} & \boldsymbol{0} & \\ \boldsymbol{0} & \boldsymbol{C}_2^{-1} & \\ & & \ddots \end{bmatrix}$$

$$\tilde{\boldsymbol{K}} = \begin{bmatrix} \tilde{\boldsymbol{K}}_{\mathrm{FEM,FEM}} & \tilde{\boldsymbol{K}}_{X,\mathrm{FEM}} & \boldsymbol{0} \\ \tilde{\boldsymbol{K}}_{\mathrm{FEM},X} & \boldsymbol{I} & \boldsymbol{Q}^{\mathrm{T}} \\ \boldsymbol{0} & \boldsymbol{Q} & \boldsymbol{0} \end{bmatrix}$$

Another solution

- *SGFEM, if 2 assumptions hold, a stiffness matrix with condition a number similar to FEM is generated*

- *Node clustering*

One 1-D bimaterial bar. The exact solution is in the finite domain

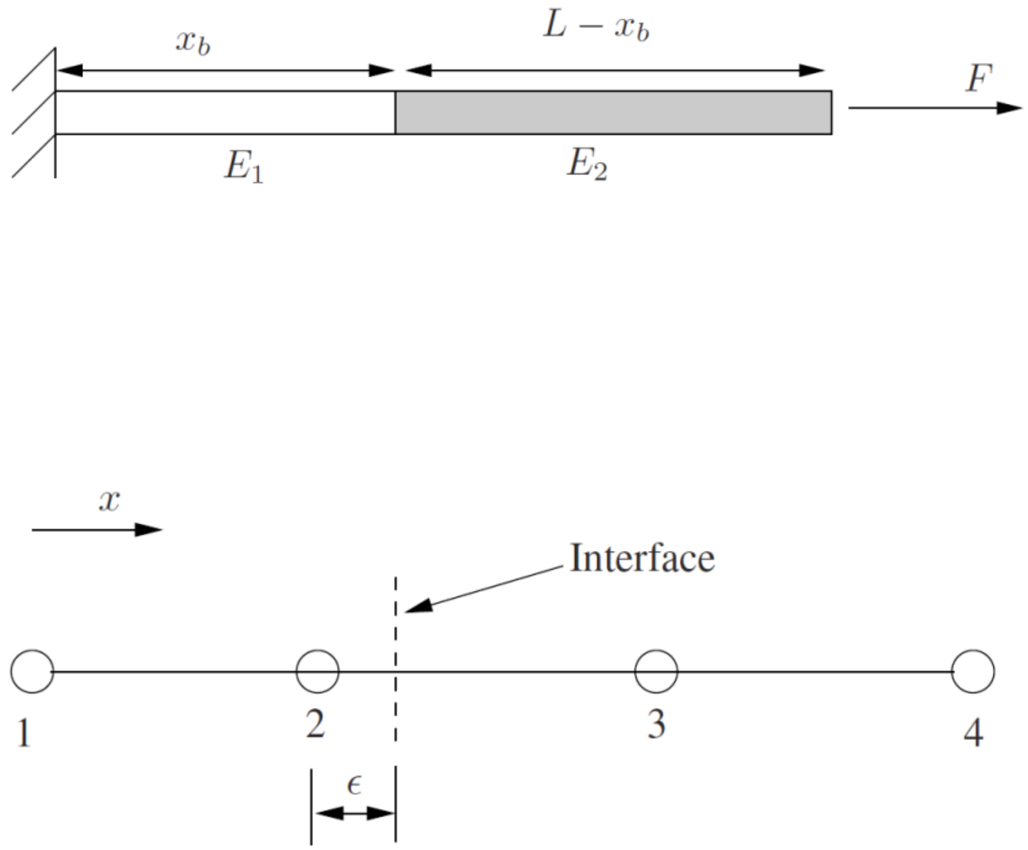

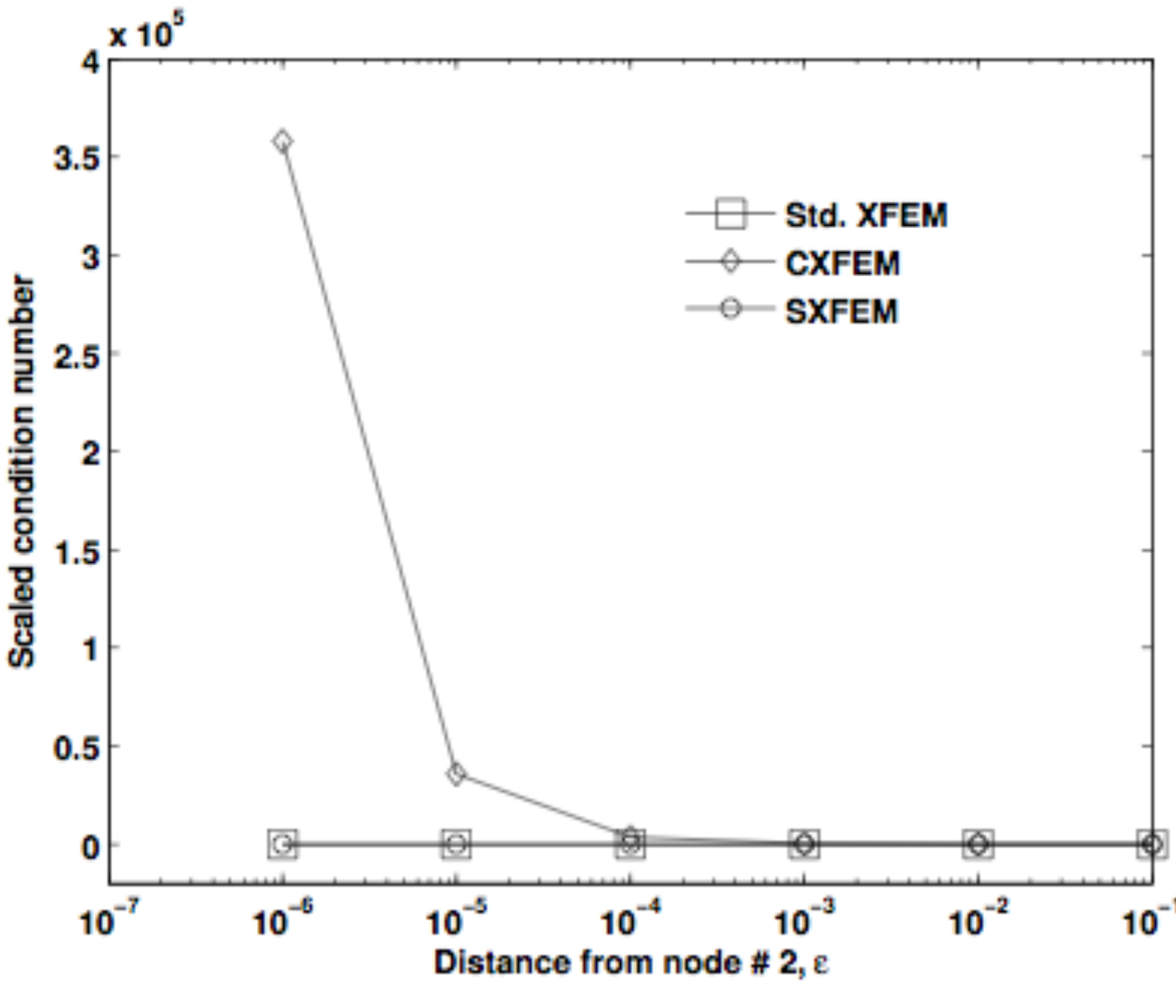

Circular inclusion

$$\begin{aligned} u_r(r) &= \begin{cases} \left[\left(1-\frac{b^2}{a^2}\right)\beta + \frac{b^2}{a^2}\right] r, & 0 \le r \le a, \\ \left(r - \frac{b^2}{r}\right)\beta + \frac{b^2}{r}, & a \le r \le b, \end{cases} \\ u_\theta(r) &= 0, \end{aligned}$$

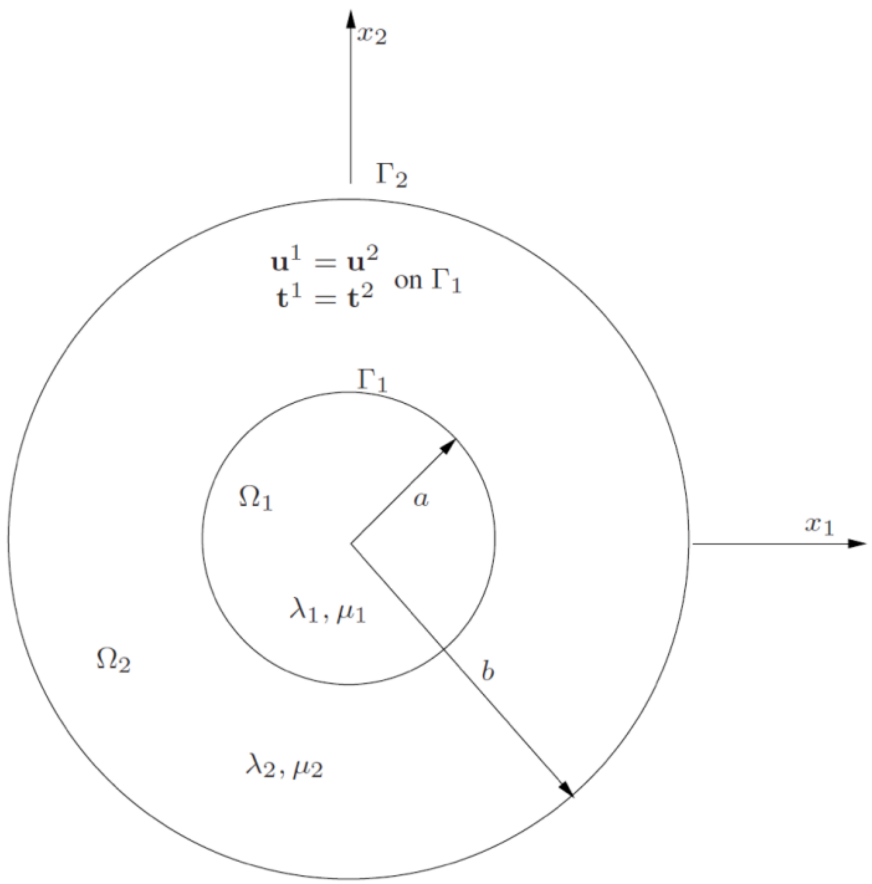

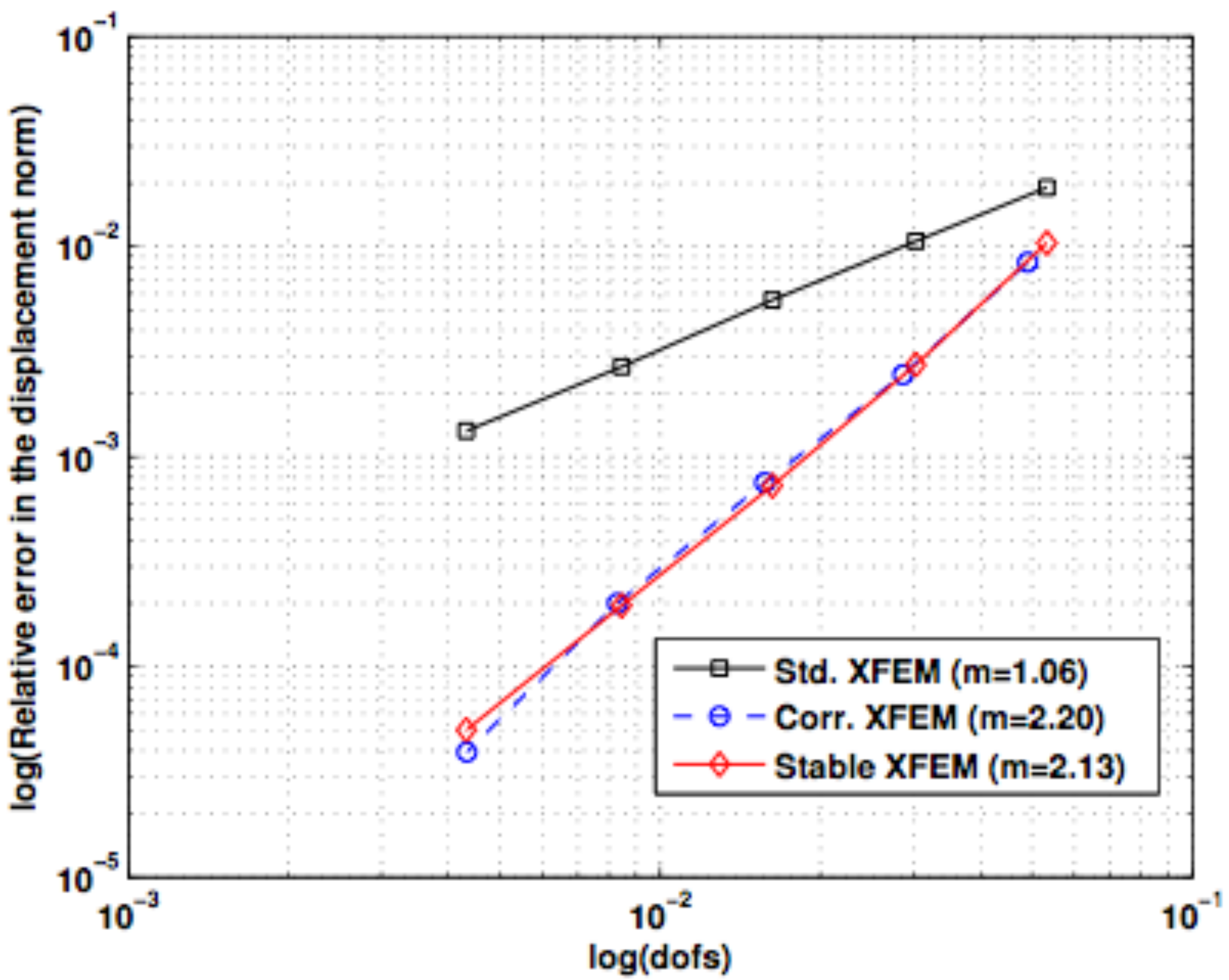

Infinite plate with crack in tension. Displacements prescribed along

$$u_x(r,\theta) = \frac{2(1+\nu)}{\sqrt{2\pi}}\frac{K_I}{E}\sqrt{r}\cos\frac{\theta}{2}\left(2-2\nu-\cos^2\frac{\theta}{2}\right)$$

$$u_y(r,\theta) = \frac{2(1+\nu)}{\sqrt{2\pi}}\frac{K_I}{E}\sqrt{r}\sin\frac{\theta}{2}\left(2-2\nu-\cos^2\frac{\theta}{2}\right)$$

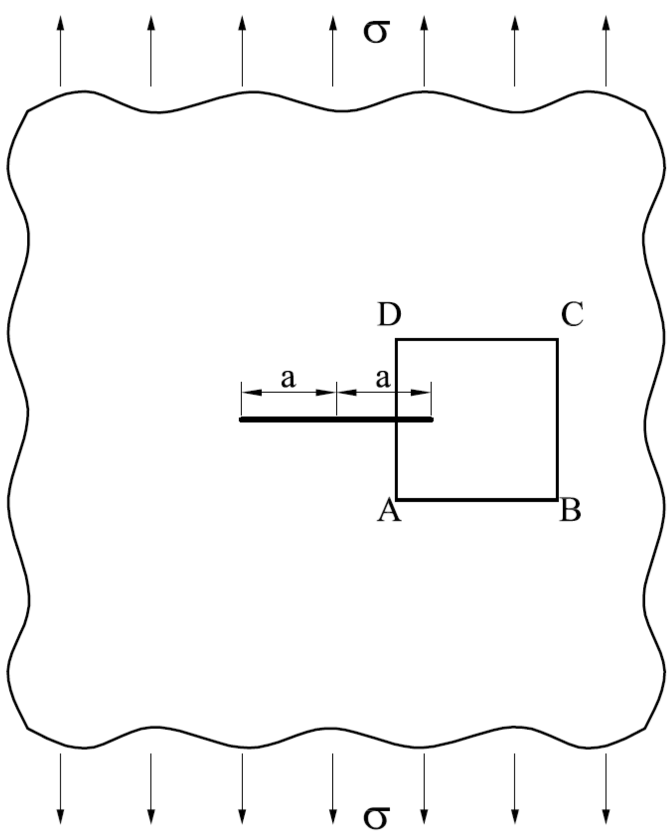

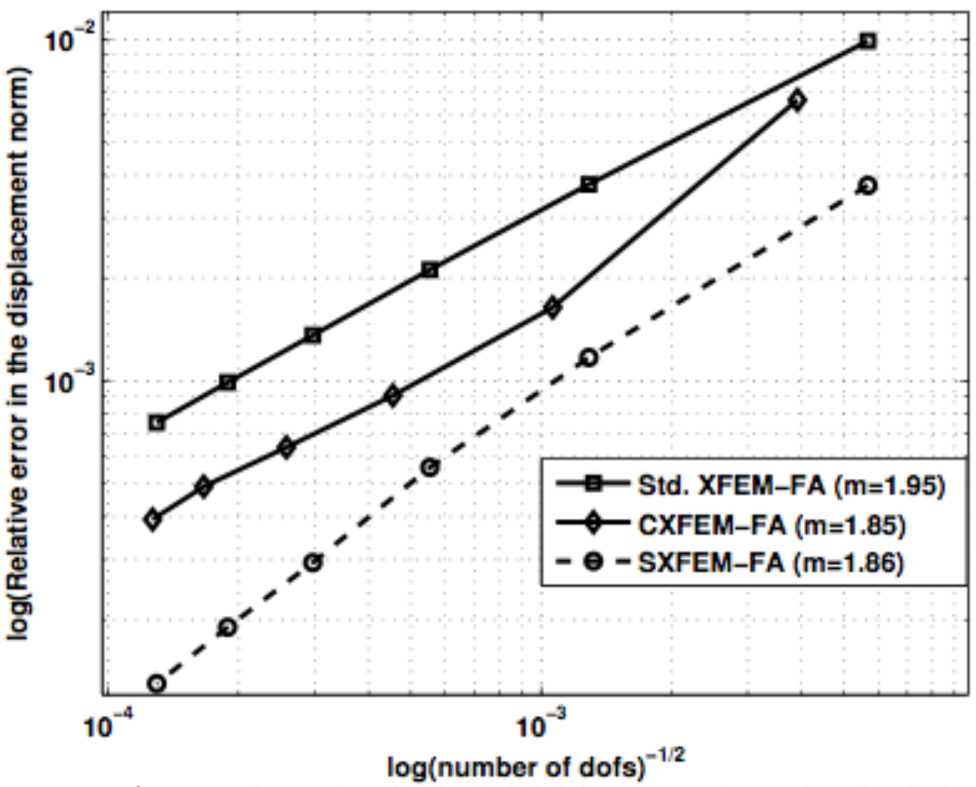

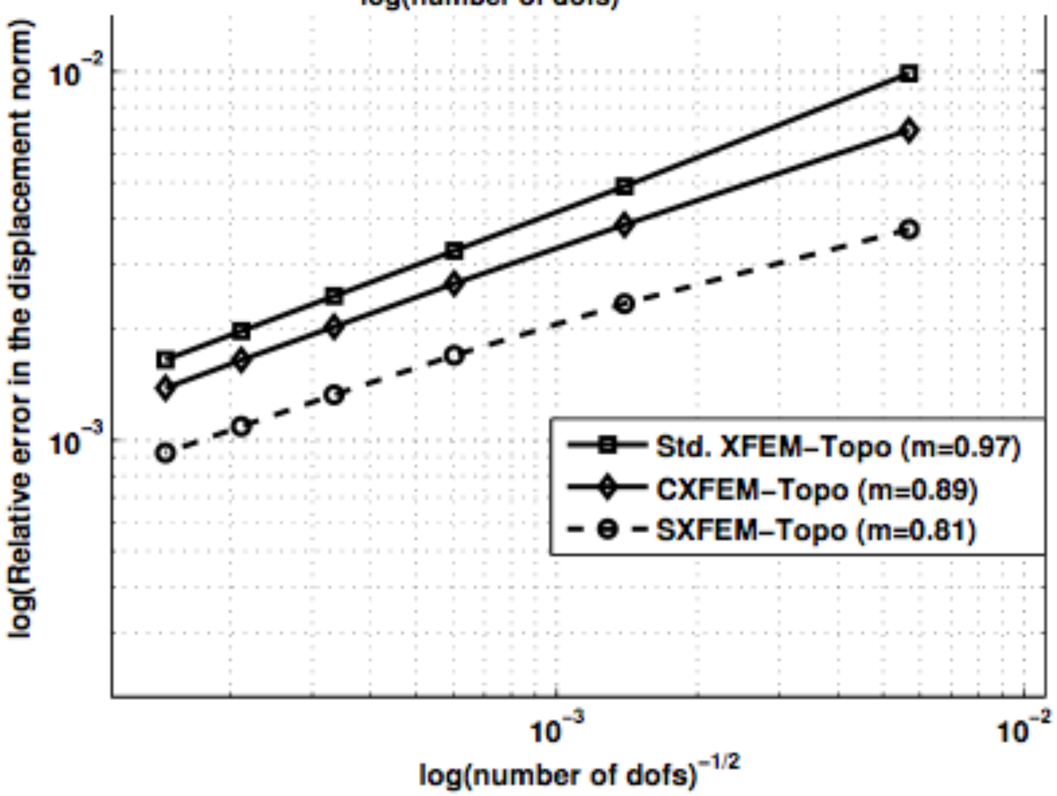

Edge crack in tension

$$K_I = F\left(\frac{a}{H}\right)\sigma\sqrt{\pi a}$$

$$F\left(\frac{a}{H}\right) = 1.12 - 0.231\left(\frac{a}{H}\right) + 10.55\left(\frac{a}{H}\right)^2 - 21.72\left(\frac{a}{H}\right)^3 + 30.39\left(\frac{a}{H}\right)^4$$

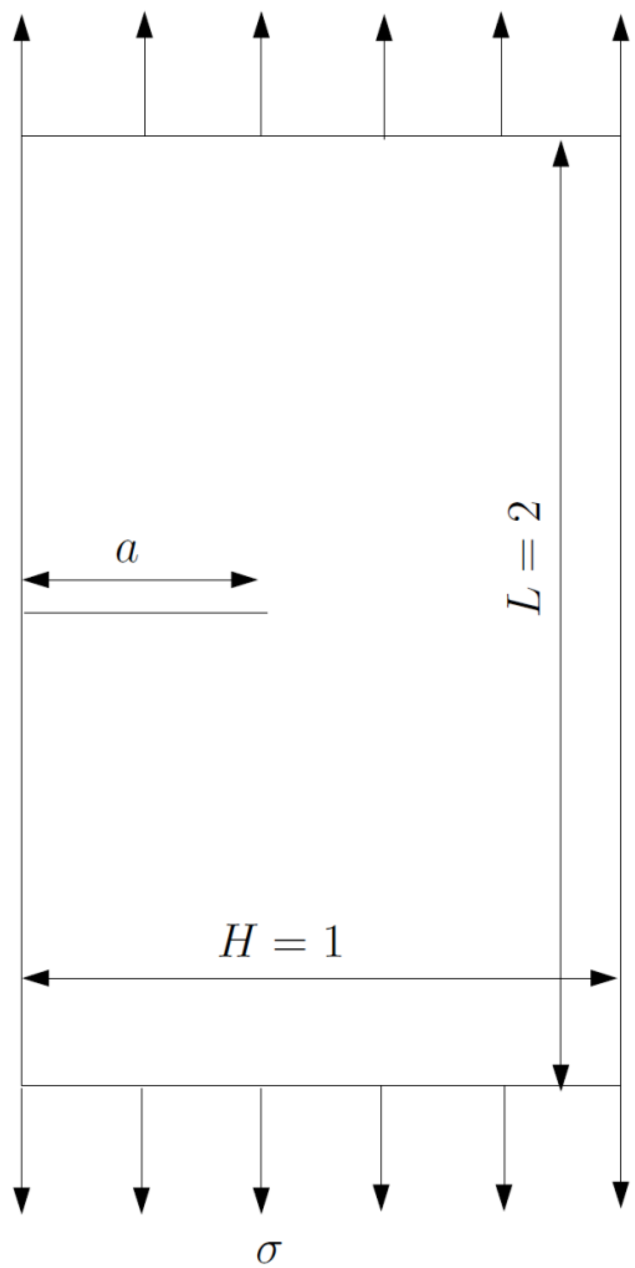

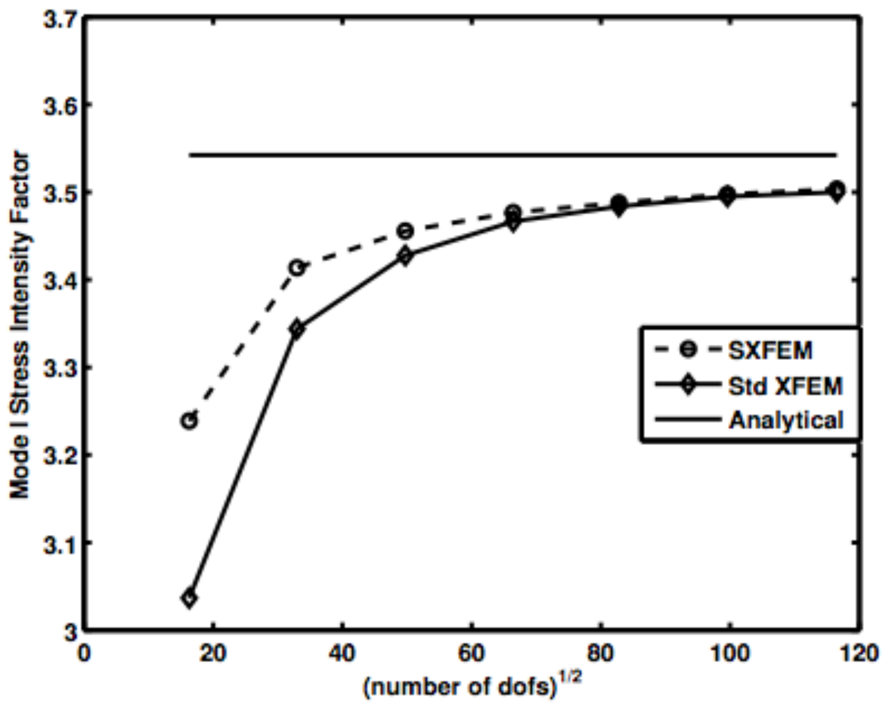

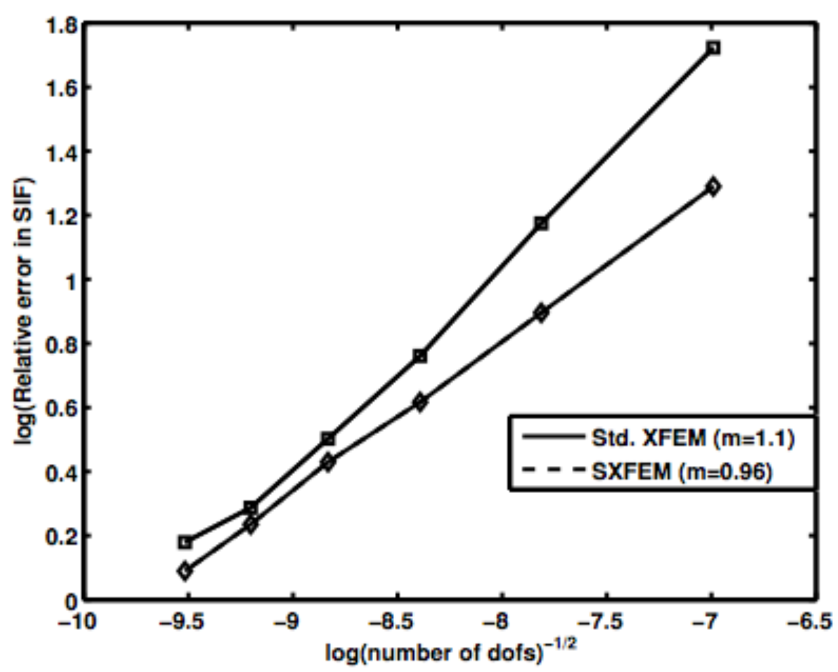

Work in progress

Development of 3D examples

- Spherical inclusion
- Several spherical inclusions
- Cracks in 3D

Stable generalized FEM

All those examples were implemented within Diffpack. Diffpack is a commercial software library used for the development numerical software, with main emphasis on numerical solutions of partial differential equations. It was developed in C++ following the object oriented paradigm.

The library is mostly oriented to the implementation of the finite element method, however it has tools for other methods, such as

Stable generalized FEM

•I. Babuška, U. Banerjee, Stable Generalized Finite Element Method (SGFEM), Computer Methods in Applied Mechanics and Engineering, Volumes 201–204, 1 January 2012, Pages 91-111, ISSN 0045-7825, 10.1016/j.cma.20

•Fries, T.-P. (2008), A corrected XFEM approximation without problems in blending elements. Int. J. Numer. Meth. Engng., 75: 503–532.

•Gracie, R., Wang, H. and Belytschko, T. (2008), Blending in the extended finite element method by discontinuous Galerkin and assumed strain methods. Int. J. Numer. Meth. Engng., 74: 1645–1669.

•Laborde, P., Pommier, J., Renard, Y. and Salaün, M. (2005), High-order extended finite element method for cracked domains. Int. J. Numer. Meth. Engng., 64: 354–381.

•Chessa, J., Wang, H. and Belytschko, T. (2003), On the construction of blending elements for local partition of unity enriched finite elements. Int. J. Numer. Meth. Engng., 57: 1015–1038.

•Tarancón, J. E., Vercher, A., Giner, E. and Fuenmayor, F. J. (2009), Enhanced blending elements for XFEM applied to linear elastic fracture mechanics. IJNME, 77: 126–148.